Identification of the Molecular Features that Facilitate the Thermal Adaptation of Aminoglycoside *O*-Nucleotidlytransferase 4' and a Novel Kinetic Mechanism for Nucleotidyl Transfer

A Dissertation Presented for the
Doctor of Philosophy
Degree
The University of Tennessee, Knoxville

Seda Kocaman
December 2019

DEDICATION

I dedicate this thesis to my parents Sema and Hakan Kocaman and my sister Selin Kocaman. They are my biggest luck and blessings. I will forever be grateful for them as they have loved, raised, guided, supported and encouraged me my entire life in the most cheerful way possible. I also dedicate this thesis to my grandparents Naile and Husnu Kilic and, Elmas and Sabit Kocaman, as well as my uncles and aunts. They are my favorite people, who have gladly taken care of me and raised me with love, joy and responsibility. A shout out to my cousins as well, for the most magical childhood we had together and our sisterhood! A very heartfelt gratitude to Gazi Mustafa Kemal Ataturk, the father of our nation, and the founder and the leader of Turkey. He has stated that, “science is the most genuine guide in life” and empowered Turkish women in all aspects of life. Perhaps, he is the main person to inspire and enable me to pursue science. None of my achievements would have been possible without any of these wonderful people. Thus, this thesis is sincerely dedicated to them.

ACKNOWLEDGEMENTS

I would like to convey my heartfelt gratitude to my PhD Advisor and mentor Dr Engin Serpersu, who has always been supportive and encouraging. I truly think that he is an excellent mentor. I have always felt a hundred percent positive that Dr Serpersu is a true mentor, who sincerely cares for the scientific development and the well being of his students. Even though we could not interact on a daily basis due to his appointment in NSF, he has guided me, trained me and supported me wonderfully during my PhD. I believe I have received the best training from him in the fields of biochemistry and biophysics. Thus, I feel fully confident and competitive as I graduate with my PhD and continue my scientific career. Dr Serpersu, it was an honor, a pleasure and a true blessing for me to be your student. I will always appreciate your time and effort that you have put in training me as a scientist and your positive and empowering approach.

I would like to extend my warmest gratitude to Dr Liz Howell. Dr Howell has been the best co-supervisor to me. She took me under her wing while Dr Serpersu was away and cared for me as if I was her own student. I joined her lab meetings in which, she has carefully monitored my progress, guided and supported me. She invited me to every single social event of her lab, and they all made me feel so welcome that I consider myself a member of both the Serpersu and the Howell labs. She was the only person who was thrilled about Halloween as much as I am! Dr Howell was an excellent scientist, had the best work ethic, was very supportive and had a very positive attitude towards life. She has been and continues to be an inspiration to everyone but especially to women scientists. Dr Howell, thank you for all you have done for me, I will always remember and appreciate you. I would like to thank Dr Pratul Agarwal as well, whom I met through Dr Howell's lab meetings. He has been very supportive and friendly as he guided me in my research. I would also like to thank my dissertation committee members Drs Gladys Alexandre, Francisco Barrera, Jaan Mannik and Kristina Kintziger. They have monitored my progress, guided me and have been very supportive and friendly over the years.

My deepest gratitude to Dr Mike Duff and Dr Ed Wright. They have helped me so much in my PhD with their great scientific knowledge. They were the first people that I went to

when I had troubles in my experiments or when I prepared for my prelim, committee meetings, thesis and job talks. Every single time, they did their best to help me and they were always friendly and approachable. Ed and Mike, you have helped me so much, I cannot thank you enough!

A shout out to my friends Dr Mike Duff, Gabriel Fuente, Dr Khushboo Bafna, Shantanu Shukla, Eshita and Ishan Gaud, Riddhi Shah, Dr Deepika Nambiar and Mustafa Murat Arat. You have been great friends to me, you supported and guided me. You are my family in Knoxville and my friends for life! Thank you all, I had the time of my youth with you! A special thanks to Deepika and Murat for watching over me and enjoying life together!

Last but not least, I would like to thank my family for their continuous love and support. I have been proud of you my entire life and I know you have always been proud of me too but admit it, a PhD thesis probably took things to a whole new level!

Finally, whoever reads this thesis thank you for your time and interest! I appreciate it.

ABSTRACT

The aminoglycoside nucleotidyltransferase 4' (ANT) is a homodimeric enzyme that detoxifies many aminoglycoside antibiotics by nucleotidylating them at the C4'-OH site. Two variants with increased thermostability (T130K, D80Y), which differed from the mesophilic wild type ANT (WT) only by a single residue, showed contrasting ligand binding thermodynamics properties. While T130K showed identical properties to WT, D80Y had stark differences. Our thermodynamics studies demonstrated that solvent reorganization becomes the major contributor to ligand binding as the temperature increases for WT and T130K, while changes in protein dynamics is the main contributor for D80Y. Our structural studies have shown that, in the T130K variant, there is an additional H-bond formed between the side chain of K130 and the backbone oxygen of S90, which explains the increased structural stability of the T130K. Despite having the highest melting temperature, an obvious additional stabilizing interaction is not identified in the D80Y structure. These observations have led us to further distinguish T130K from D80Y. We have concluded that T130K is the “thermostable variant”, since it has an increased structural stability yet mimics the ligand binding and protein dynamics behaviors of the mesophilic WT. Furthermore, we refer to D80Y as the “thermophilic variant”, since it behaves very differently from the WT in order to adapt to a harsher environment with elevated temperatures compared to that of the WT. Overall, we have shown that global thermodynamics of ligand-protein interactions and solvent effects may be among the molecular parameters that define true thermophilic enzyme behavior. The applicability of these findings to other systems remains to be seen and can be helpful in understanding if there is a general strategy that enzymes use to adapt to hot environments. We have also identified the catalytic mechanism of ANT. We propose a low barrier hydrogen bond (LBHB) formed between E52 and the ligand which enables the enzyme to bind to the ligand tightly. This LBHB is disrupted after the cofactor ATP is bound and the catalysis takes place, leading to the release of the modified aminoglycoside. LBHB thereby serves a novel “catch and release” mechanism for nucleotidyl transfer.

TABLE OF CONTENTS

LIST OF TABLES

LIST OF FIGURES

1 INTRODUCTION

1.1 Use of thermostable enzymes in industry

Thermostable enzymes are valuable for industrial use because, unlike most of the other enzymes, they can catalyze their chemical reactions under harsh industrial conditions which involve elevated temperatures *(1, 2)*. Most industries prefer to operate at high temperatures due to various beneficial reasons *(3)*. One of the most important reasons is that, as the temperature increases, rate of the chemical reaction also increases which decreases the amount of enzyme needed to be used *(4)*. Using higher temperatures (above 60°C) is also useful in preventing the microbial growth which could lead to microbial contamination *(3)*. Thus, discovering and/or designing new thermostable enzymes has significant biotechnology implications and is required to meet the ever growing needs of industries *(5)*.

Enzymes have multiple applications in many different industries *(6)*. Pectinases are heavily used in textile and paper industries due to their ability to remove pectin and hydrophobic materials, leading to a cleaner process with less raw material usage and waste production *(7)*. Cellulases are one of the enzyme families that are most heavily used in industry *(8)*. Cellulases convert cellulose to sugar which is useful in bioethanol, textile and detergent industries *(9)*. Xylanases produce sugars from lignocelluloses and are used in the paper and pulp industries to hydrolyze straw waste and produce biogas *(10-12)*. Amylases are used in starch processing, bakery, brewing, alcohol, textile, detergent, and bioethanol industries due to their ability to produce different maltooligosaccharides from starch *(13-16)*. Proteases are heavily used in the food industry, from the manufacturing of cheese to flavor enhancement *(17)*. Their ability to degrade proteins such as casein, gluten, gelatin and collagen make them an important source for nutrient utilization as well as a molecular tool for the analysis of protein sequence *(18, 19)*. Lipases can form fatty acids, glycerol, monoglycerides and diglycerides by hydrolyzing triglycerides *(20, 21)*. Due to this ability, lipases are commonly used in cosmetic, paper, textile, leather, detergent, pharmaceutical and food industries *(17, 22, 23)*. Laccases, which cleave aromatic compounds, are used in biotechnological processes like wastewater treatment and detoxification of the soil from

herbicides/pesticides. They are also used as medical diagnostic tools and biosensors *(24)*. Phytases are used in the diet of animals in order to increase their uptake of phosphorus from plant feeds *(25)*. Thermostable forms of these enzymes are particularly used in industries due to their thermal stabilities *(26)*. Some of these thermostable enzymes also confer pH stabilities, ability to function in the presence of detergents and high specificity towards certain substrates which further make them very valuable to industrial use *(6, 11, 13, 21, 22, 26-28)*. Thus, there is an ever growing need to use thermostable enzymes in different industries.

1.2 Natural sources of thermostable enzymes and their characteristics

In nature, thermostable enzymes are found in thermophilic and hyperthermophilic organisms which grow at 50-80 °C and 80-110 °C, respectively *(29)*. These enzymes are originated from archaea and bacteria that live in extreme environments, such as hot springs and volcanic pools *(29)*. Their mesophilic enzyme homologues are found in mesophilic organisms that grow at 20-40 °C *(30)*. Compared to their mesophilic homologues, thermophilic enzymes have a more stable protein structure both against heat and denaturants *(31)*, and they have a greater catalytic activity at high temperatures *(29)*. These characteristics define thermostability.

To identify the molecular features that govern thermostability, thermophilic enzymes were compared to their mesophilic homologues *(29, 32)*. These studies indicate that the homologues share 40-80% sequential identities *(33)*, superimposable crystal structures *(34)* and same catalytic mechanisms. Comparisons of the thermophilic and mesophilic enzyme homologues have shown that disulfide bridges, aromatic and hydrophobic interactions, hydrogen (H-) bonds, and ion pairs can be seen more in thermophilic enzymes. These interactions are believed to result in the thermostability of the thermophilic enzymes by creating a more stable protein structure *(35-37)*. Burial of each CH_2 group increased the stability of the globular proteins by 1.3 (±0.5) kcal/mol (on average), stating the importance of hydrophobic interactions in protein folding *(38)*. For T4 lysozyme, a single ion pair was able to create 3-5 kcal/mol of stabilization *(39)* while

for RNase T1, an individual H-bond contributed to stabilization by an average of 1.3 kcal/mol *(40)*. Tyr-Tyr and Phe-Phe aromatic pairs contributed approximately -1.3 kcal/mol towards the thermodynamic stabilization of *B. amyloliquefaciens* RNase *(41)*. Introduction of a disulfide bridge to the loop structure of *Cucurbita maxima* trypsin inhibitor-V, contributed to its stabilization by 4 kcal/mol *(42)*. An anion pi interaction (interaction between a negative charge and the aromatic ring of a residue) can contribute to stabilization by 2-9.5 kcal/mol *(43)*. Contributions of these interactions to protein stability were evaluated by creating mutations in the protein, which would abolish these interactions and then obtaining the ΔG (Gibbs free energy change) of folding values using CD (circular dichroism). It is important to note that these interactions do not always increase protein stability. In fact, they can sometimes destabilize the protein. The native structure of a protein is the result of precise intra- and inter- molecular interactions. Excessive chemical interactions can interfere with the protein structure and result in destabilization. Comparisons of numerous mesophilic and thermophilic homologues showed that there is not a single common chemical interaction that participates in the thermostabilities of all thermophilic enzymes, yet different chemical interactions can be found for different pairs.

Thermophilic enzymes have a more stable structure than their mesophilic counterparts both at moderate and high temperatures *(29)*. The optimum activity temperature of thermophilic enzymes is higher than that of their mesophilic homologues, and the activities of the enzyme homologues are very similar to each other at their own optimum temperatures *(44)*. Compared to their thermophilic homologues, mesophilic enzymes have a decreased activity, at the optimum temperature of their homologues, since they are not able to properly maintain their structure at high temperatures. Interestingly, compared to their mesophilic homologues, thermophilic enzymes also have a decreased activity, at the optimum temperature of their homologues, even though they can properly maintain their structure at these temperatures. This phenomenon has raised the perception that there is a structure-function tradeoff for the thermophilic proteins. This phenomenon is mainly explained by the reasoning that, due to the stable structure of the thermophilic enzymes, they are not flexible enough to undergo the conformational changes which would allow them to bind to their substrates and perform catalysis at

ambient temperatures *(44)*. This logic suggested that protein flexibility and dynamics can also be related to enzyme thermostability.

Proteins are folded and functional in their native states. In their native states, proteins have minimum energy and thus are structurally stable. The Gibbs free energy (ΔG) of protein folding depends on enthalpy (ΔH) and entropy ($T\Delta S$) according to the law of thermodynamics, $\Delta G = \Delta H - T\Delta S$. Thus, structural stability of proteins also depends on these thermodynamic parameters. Noncovalent interactions are driven by enthalpy *(45, 46)*. Noncovalent interactions lower the enthalpy and thereby result in a smaller ΔG *(46)*. Entropy is the measure of disorder in the system. Dynamics of proteins increase as the entropy increases *(47)*. Thus, dynamics is believed to be one of the molecular features that is related to thermostability via entropy. Dynamics of the thermophilic enzymes were compared to that of their mesophilic homologues at different time scales and temperatures by various experimental methods *(48)*. Hydrogen/deuterium (H/D) studies which determine motions in a millisecond to second time scale revealed that, for the enzymes tested, thermophilic enzymes were more rigid compared to their mesophilic counterparts *(49)*. On the other hand, molecular dynamics (MD) simulations conducted at nanosecond time scale revealed that thermophilic proteins had a larger number of conformational ensembles compared to their mesophilic counterparts *(50)*. Nuclear magnetic resonance (NMR) studies further suggested that, in picosecond to micro second time scale, thermophilic proteins had more atomic fluctuations than their mesophilic counterparts *(51)*. The results were not consistent. While some studies showed that there was not a significant difference between the dynamics of mesophilic/thermophilic enzyme pairs *(52)*, others showed that one of them was more dynamic than the other *(53)*. Overall, these studies suggest that one cannot come to a general, unifying conclusion as to how dynamics contribute to enzyme thermostability.

Oligomerization is also known to contribute to thermostability *(54)*. Some thermophilic enzymes have a larger number of subunits compared to their mesophilic counterparts *(55, 56)*. Disrupting the higher oligomeric state of thermophilic enzymes can result in the abolishment of thermostability by resulting in decreased catalytic activity at higher

temperatures *(29, 57-59)*. Oligomerization is believed to contribute to thermostability via stabilizing the protein structure by creating an enlarged buried surface area and an increased packing density *(29)*.

More stable loop, N and C termini structures were also seen in thermophilic enzymes compared to their mesophilic homologues. Stabilization of these regions via H-bonding, salt bridges or hydrophobic interactions were seen more in thermophilic proteins and is believed to contribute to thermostability *(29)*. Metal binding is also known to contribute to thermostability, both by stabilizing the protein structure and enhancing the catalytic activity. Some thermophilic enzymes are known to contain metal ions that are not present in their mesophilic homologues *(29)*. Posttranslational modifications (PTM) such as glycosylation are also known to contribute to thermostability since they can increase catalytic activity at high temperatures *(60)*.

Extrinsic factors, such as salt and substrate addition or pressure effects can also enhance thermostability. Salt addition can increase thermostability either by affecting the interaction of a metal ion with the protein, solvent-protein interactions or the interaction between the subunits of the protein *(61)*. Substrate addition stabilizes the active site *(62)*. Pressure favors the protein to have a smaller volume. Thus, pressure further stabilizes the proteins that are mainly stabilized by hydrophobic interactions but destabilizes the proteins that are mainly stabilized by ionic interactions *(63)*.

It is important to acknowledge that there is not a single common molecular feature that can make all proteins thermostable. In fact, it is shown that different molecular features are responsible for the thermostabilities of different thermostable proteins, and a protein can use a combination of these features to be thermostable *(29)*. Thus, it is crucial to further study if there might be other parameters that define the thermostability of proteins, perhaps in a more general manner. In this thesis as opposed to most of the studies in the literature which focused on the structural stability of apo (nonligand bound form) proteins, we studied the role of ligand binding thermodynamics on protein thermostability, using the mesophilic aminoglycoside nucleotidyltransferase(4') (ANT) and its two variants.

1.3 Strategies to create thermostable enzymes

Directed evolution is one of the strategies in protein engineering *(64, 65)*. Generation of thermostable enzymes for industrial needs also heavily relies on this approach. Directed evolution essentially consists of mutating the original protein through iterative rounds and then selecting the mutants under specific evolutionary pressure *(6)*. Random mutants of the original protein are created via DNA shuffling *(66)*, site saturation mutagenesis *(67)*, error prone mutagenesis *(68, 69)* or chemical mutagenesis *(70, 71)*. Enzyme mutants are screened via high-throughput techniques which involve multi-well plates and fluorescence assays. Usually, mutants with good catalytic efficiency or which enable good cell growth under the specific pressure are selected as successful candidates *(6)*. Specific evolutionary pressure is determined based on the qualities of the protein one likes to engineer. Catalytic activities of the mutants at elevated temperatures are assessed to identify the thermostable enzyme variants. Thermostabilities of the enzymes; galacto-N-biose/lacto-N-biose I phosphorylase (GLNBP) from *Bifidobacterium longum* JM1217 *(72)*, an amylase from *Thermus* sp. strain IM6501 (ThMA) *(73, 74)* and endo-β-1,4-xylanase (XynA) from *Thermomyces lanuginosus* were improved using directed evolution *(6)*.

Rational design is another approach to engineer proteins, including thermostable enzymes, and utilizes computational design. Even though more stable versions of proteins, such as cytokine, were developed with this strategy *(75)*, creating thermostable enzymes has been a bigger challenge since the structural stability of the enzyme should not abolish its catalytic activity. In this approach, geometry of the active site and enzyme dynamics is highly considered. Computational design tools, such as programs like Rosetta, are heavily used to analyze and design protein structures using a score system that is based on energy functions of the enzyme *(6)*. In order to create thermostable enzymes using the computational design, one aims to introduce additional structural stability to the enzyme by introducing new chemical interactions within the enzyme through mutations, as explained in section 1.2 in detail. The newly introduced interactions are desired to stabilize the protein without disrupting the active site and protein flexibility, and without creating drastic changes in the protein backbone. Rational design also takes

advantage of using the phylogenetic analysis and comparison of homologous proteins to figure out which mutations to introduce. This strategy still requires the visual inspection of the mutations by the scientist after the computational tools select the best mutants. Molecular Dynamics (MD) simulations are performed on the best mutant candidates and mutants with increased root mean square fluctuations are generally eliminated assuming that increased fluctuations might cause destabilization *(76)*. Finally, these mutants are experimentally tested. Mutants that are more structurally stable and more active (at high temperatures) compared to the original enzyme are the thermostable variants created using rational design approach. Although, this approach is more time consuming and challenging than the direct evolution method, it is very important to further understand the molecular features that govern the thermostabilities of enzymes.

1.4 Variants of aminoglycoside nucleotidyltransferase(4') (ANT) studied to understand enzyme thermostability

In this thesis, we investigated the molecular features that provide thermostability to enzymes by studying the aminoglycoside nucleotidyltransferase(4') (ANT) and its thermostable variants as a model system.

ANT is a member of the aminoglycoside modifying enzymes (AGMEs). Aminoglycosides are produced by *actinomycetes*, as a defense mechanism against mostly gram negative and aerobic bacteria which are also known to cause diseases like tuberculosis and hepatic coma *(77)*. Aminoglycosides are a group of antibiotics that bind to the 16S RNA of the 30S ribosome and thereby cause mistranslations and premature stops during translation in some prokaryotes *(78)*. Aminoglycosides are divided into two main families as kanamycins and neomycins. Neomycins have an extra ring structure compared to kanamycins. Substitution of the chemical groups of aminoglycosides yield many more new aminoglycosides (Figure 1.1). AGMEs inhibit the aminoglycosides by modifying them *(79, 80)*. There are more than 100 AGMEs. There are three different kinds of AGMEs; acetyltransferases, phosphotransferases and nucleotidyltransferases. AGMEs

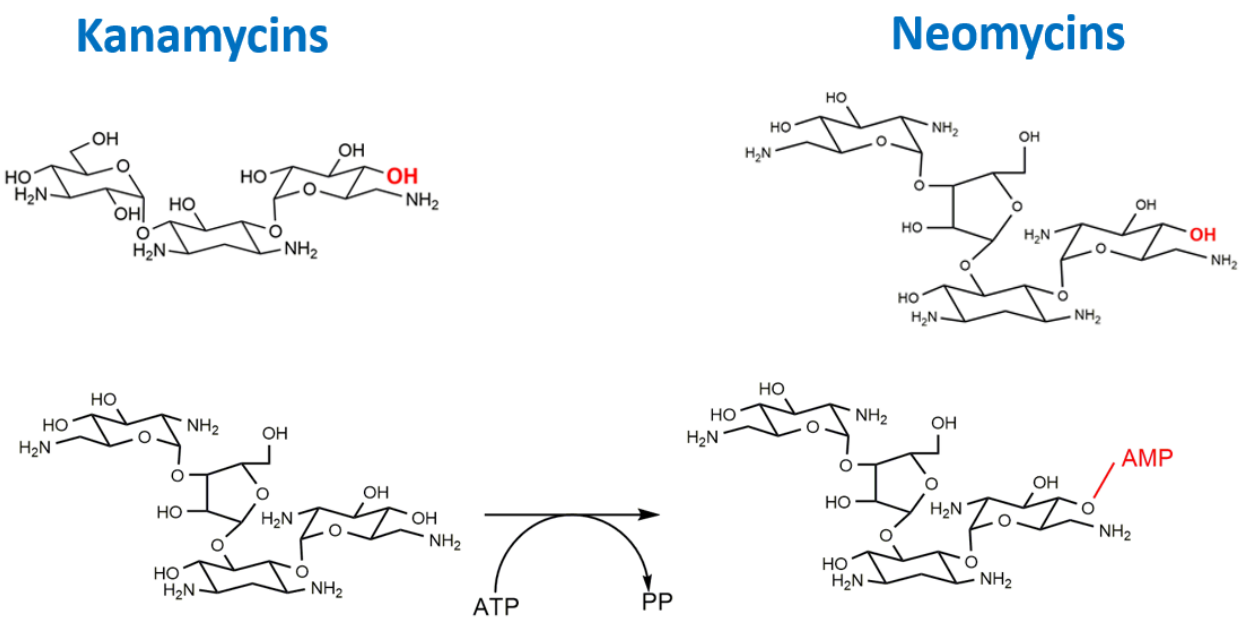

Figure 1.1: Aminoglycosides and aminoglycoside nucleotidyltransferase(4') (ANT) modification site. Aminoglycosides are divided into two main families as kanamycins and neomycins with neomycins having an extra ring structure compared to kanamycins. Substitution of the chemical groups on the aminoglycosides yield many more new aminoglycosides. ANT modifies the aminoglycosides by transferring an AMP group from Mg-ATP to the C4''--OH of aminoglycosides. The modification sites are shown in red.

use different donors such as acetyl coenzyme-A or ATP to modify the different groups of the aminoglycosides such as amino or hydroxyl moieties (Table 1.1). ANT modifies the aminoglycosides by transferring an AMP group from Mg-ATP to the C4''--OH of the aminoglycosides (Figure 1.1). Some bacterial species developed resistance against aminoglycosides by expressing AGMEs to eliminate their bactericidal activity. Aminoglycoside resistance has become a problem for the treatment of diseases caused by gram-negative, aerobic bacteria such as, tuberculosis and hepatic coma *(81)*.

T130K and D80Y are the two thermostable variants of the WT (wild type) ANT, which only differ from the WT by a single residue mutation as indicated in their names. Most studies compare mesophilic/thermophilic homologues, which can differ from each other up to 60% in their sequence, in order to study the molecular features that govern enzyme thermostability *(33)*. Even though this is a powerful approach, it is also prone to errors, since it is not easy to tell if the difference in the molecular features of the homologues are actually related to thermostability or to some other function of the protein. Thus, using ANT variants is an excellent system to study the molecular features that govern enzyme thermostability, since just one mutation can create a huge difference in their thermostabilities. This avoids the bias seen in enzyme homologues.

WT ANT, which may also be referred to as kanamycin nucleotidyltransferase in literature, was originally isolated from the mesophilic *Staphylococcus aureus (82)*. Thermostable versions of WT ANT were created via direct evolution. Plasmids harboring the gene which codes for ANT were treated with hydroxylamine using a phage system in order to create thermostable ANT mutants. Plasmids harboring the mutations were then transformed into *Bacillus stearothermophilus,* and colonies which conferred kanamycin resistance at nonpermissive temperatures for the WT were selected. Sequence analysis of the selected colonies revealed that T130K and D80Y mutations result in thermostable variants of WT *(83).* Compared to the WT, T130K and D80Y were more active at high temperatures (52 °C and 57°C), while they were less active at lower temperatures such as 37 °C *(83)*. T130K and D80Y were also more stable against the denaturants such as urea, detergent and proteinase K compared to WT *(84)*. Increased enzymatic activity at high

Table 1.1: Types of aminoglycoside modifying enzymes (AGMEs)

AGME	Donor	Affect
N-acetyltransferases	Acetyl coenzyme-A	Amino functions
O-phosphotransferases	ATP	Hydroxyl functions
O-nucleotidyltransferases	ATP	Hydroxyl functions

There are three different kinds of AGMEs; acetyltransferases, phosphotransferases and nucleotidyltransferases. AGMEs use different donors such as, acetyl coenzyme-A or ATP to modify the different groups on the aminoglycosides such as, amino or hydroxyl functions.

temperatures along with the increased structural stability concluded that T130K and D80Y were thermostable ANT variants *(83)*. Our lab has shown that the melting temperature (Tm) of WT ANT4 is (40.9±0.5ºC), T130K is (49.1±0.6 ºC) and D80Y is (56.2±0.2 ºC) *(85)*. The Tm, activity at high temperatures and the resistance against denaturants increase in the order of WT, T130K and D80Y, indicating that D80Y is more thermostable than T130K. We also have a double mutant named as T130KD80Y with a Tm of 62.6±0.1 ºC. The additivity in the Tm of the double mutant suggests that the T130K and the D80Y mutants achieve thermostability through different strategies. This observation has further led us to investigate how the ANT variants have achieved thermostability.

In this thesis, we have obtained the X-ray crystal structures of all three ANT variants. Our structures show that ANT is a homodimer enzyme, in which the T130K and D80Y mutation sites are both exposed to solvent and are not in direct contact with where the enzymatic reaction takes place (Figure 1.2). Superimposition of all three apo ANT variants returned a root mean square deviation (RMSD) value of 0.4 Å, which indicates that there are no global structural differences amongst these variants. These structures have also enabled us to study the chemical interactions in the mutation sites, which led us to conclude that T130K has an increased structural stability compared to the WT due to an extra H-bond between the side chain of Lys130 and the backbone oxygen of Ser 90. When we examined the D80Y mutation site, unlike the T130K, we did not find any obvious additional chemical interactions that could increase the stability of the structure. However, our earlier work has shown that, since D80Y is more dynamic compared to the WT and T130K, D80Y might have actually acquired a greater thermostability by acting as a node in the protein dynamics *(85)*. The same study from our lab also showed that T130K resembled the WT, while D80Y exhibited different ligand binding thermodynamics. This observation has led us to further study the ligand binging thermodynamics of these variants and how they are affected by the solvent in this thesis along with our structural analysis *(86)*. Taken together, we believe that T130K is just a structurally more stable version of the mesophilic WT enzyme, with very similar ligand binding and protein dynamics behavior, while D80Y displays very different behaviors from the others. Thermophilic enzymes behave differently than their mesophilic homologues since they need to accommodate a harsher

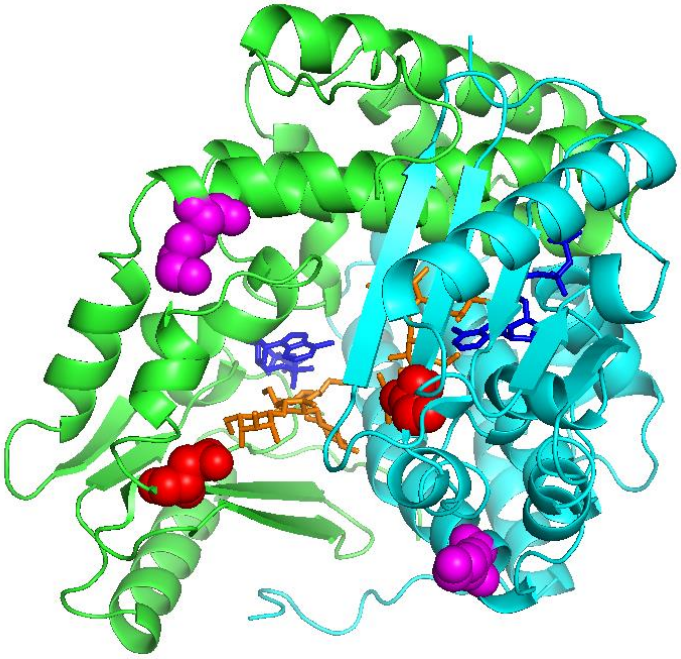

Figure 1.2: The crystal structure of aminoglycoside nucleotidyltransferase(4') (ANT). ANT is a homodimer enzyme. Each monomer is shown in cyan and green. T130K (pink) and D80Y (red) mutation sites are both exposed to solvent and are not in direct contact with where the enzymatic reaction takes place. Substrate neomycin is shown in orange while AMPCPP, an nonhydrolyzable analogue of the cofactor ATP, is shown in blue.

environment compared to their homologues *(29)*. This led us to conclude that, T130K is just a thermostable version of the WT, while D80Y is displaying distinct thermophilic enzyme behavior.

1.5 The role of solvent on the thermostability of enzymes

In nature, proteins are not found in a vacuum environment. In fact, they are surrounded by a solvent, which is typically water. Water is a polar molecule and tends to form H-bonds with the polar residues of proteins. Both the inter- and intra- molecular interactions contribute to the formation of the native structure of the proteins. Such inter-molecular interactions occur between the protein and the solvent. This suggest that solvent-protein interactions contribute to the folding and the stability of the proteins, as well as protein dynamics *(87)*. Hydrophobic amino acids tend to accumulate in the protein core to avoid being in contact with the water. Studies which compared the mesophilic proteins with their thermophilic and hyperthermophilic homologues have shown that thermostable proteins show an increased packing of the hydrophobic residues *(88)*. Most thermophilic enzymes tend to have a higher hydrophilic content compared to their mesophilic homologues *(30)*. When the enzyme homologues are compared, the presence of charged residues in the solvent exposed protein surface increase in the order of psychrophile (organisms that live in extremely cold environments), mesophile and thermophile *(89)*. Increased ionic interactions in the solvent exposed regions of the protein is believed to be one of the features that confer thermostability in the thermophilic homologues *(90, 91)*. Calorimetric methods enable one to study the solvation of different types of chemical groups in the proteins and how they are related to thermostability. Positive heat capacity signs the solvation of the hydrophobic groups, while negative heat capacity signs the solvation of the polar groups *(92, 93)*. Thus, polar character of thermophilic proteins decrease the heat capacity *(30)*.

A study which aimed to understand the thermal behavior of the guanosine triphosphate region of the EF-Tu using its mesophilic and thermophilic protein homologues has shown that the homologues were similar in their packing, but the thermophilic variant had a

greater solvent exposed area and displayed increased protein fluctuations due to its interaction with the solvent *(94-97)*. This study also included the hyperthermophilic variant. The main conclusion of this study was that behavior of the hydration water and the protein surface area (exposed to solvent) were the two factors that differed the most amongst the three variants upon increasing the temperature and that internal packing was not as important in thermostability *(30)*.

Compared to their homologues, thermophilic protein variants display more flexibility and increased fluctuations at the time scale of the protein-water H-bond life time, and they also exhibit more hydrophilic moieties exposed to water *(52)*. This phenomenon has led to the understanding that thermophilic proteins are able to form a more stable hydration shell surrounding themselves, due to the creation of H-bonds between the hydrophilic residues on their surface and the solvent. This stronger hydration shell protects the thermophilic proteins from the penetration of water, resulting in a more stable structure compared to their homologues *(30)*.

The structured organization of the water molecules in the surface of the thermophilic proteins is believed to cause conformational changes in the protein and thereby increase their thermostability *(30)*. This is a global feature explaining protein thermostability rather than most studies which focused on the specific structural differences. Our own studies also state that global properties play a great role in the thermostability of ANT variants. Earlier we have shown that, rather than the specific structural differences between the T130K and D80Y, the differences in their global dynamics manifest the differences in their thermostabilities *(85)*. In this thesis, as another global feature, we examined the role of solvent on the ligand binding thermodynamics of the ANT variants. We have shown that this phenomenon is very different for D80Y compared to other ANT variants. This led us to further distinguish the T130K and D80Y from each other and claim D80Y as the variant with thermophilic enzyme properties, while we referred to T130K as just a more thermostable version of the WT since it was mimicking the WT *(86)*.

1.6 References

1. Bauer, M. W.; Driskill, L. E.; Callen, W.; Snead, M. A.; Mathur, E. J.; Kelly, R. M., An endoglucanase, EglA, from the hyperthermophilic archaeon *Pyrococcus furiosus* hydrolyzes β-1, 4 bonds in mixed-linkage (1→ 3),(1→ 4)-β-D-glucans and cellulose. *Journal of Bacteriology* **1999,** *181* (1), 284-290.
2. Liebl, W.; Wagner, B.; Schellhase, J., Properties of an α-galactosidase, and structure of its gene galA, within an α-and β-galactoside utilization gene cluster of the hyperthermophilic bacterium *Thermotoga maritima*. *Systematic Applied Microbiology* **1998,** *21* (1), 1-11.
3. Zamost, B. L.; Nielsen, H. K.; Starnes, R. L., Thermostable enzymes for industrial applications. *Journal of Industrial Microbiology* **1991,** *8* (2), 71-81.
4. Wasserman, B. P., Thermostable enzyme production. *Food Technology* **1984**.
5. Kumar, S.; Nussinov, R., How do thermophilic proteins deal with heat? *Cellular Molecular Life Sciences* **2001,** *58* (9), 1216-1233.
6. Rigoldi, F.; Donini, S.; Redaelli, A.; Parisini, E.; Gautieri, A., Engineering of thermostable enzymes for industrial applications. *APL Bioengineering* **2018,** *2* (1), 011501.
7. Solbak, A. I.; Richardson, T. H.; McCann, R. T.; Kline, K. A.; Bartnek, F.; Tomlinson, G.; Tan, X.; Parra-Gessert, L.; Frey, G. J.; Podar, M., Discovery of pectin-degrading enzymes and directed evolution of a novel pectate lyase for processing cotton fabric. *Journal of Biological Chemistry* **2005,** *280* (10), 9431-9438.
8. Sadhu, S.; Maiti, T. K., Cellulase production by bacteria: a review. *British Microbiology Research Journal* **2013,** *3* (3), 235-258.
9. Hill, J.; Nelson, E.; Tilman, D.; Polasky, S.; Tiffany, D., Environmental, economic, and energetic costs and benefits of biodiesel and ethanol biofuels. *Proceedings of the National Academy of Sciences* **2006,** *103* (30), 11206-11210.
10. Rifaat, H.; Nagieb, Z.; Ahmed, Y., Production of xylanases by Streptomyces species and their bleaching effect on rice straw pulp. *Applied Ecology Environmental Research* **2006,** *4* (1), 151-160.

11. Haltrich, D.; Nidetzky, B.; Kulbe, K. D.; Steiner, W.; Župančič, S., Production of fungal xylanases. *Bioresource Technology* **1996,** *58* (2), 137-161.

12. Priya, B. S.; Stalin, T.; Selvam, K., Efficient utilization of xylanase and lipase producing thermophilic marine actinomycetes (Streptomyces albus and Streptomyces hygroscopicus) in the production of ecofriendly alternative energy from waste. *African Journal of Biotechnology* **2012,** *11* (78), 14320-14325.

13. Stamford, T.; Stamford, N.; Coelho, L.; Araujo, J., Production and characterization of a thermostable α-amylase from *Nocardiopsis sp.* endophyte of yam bean. *Bioresource Technology* **2001,** *76* (2), 137-141.

14. Yang, C.-H.; Liu, W.-H., Purification and properties of a maltotriose-producing α-amylase from *Thermobifida fusca*. *Enzyme Microbial Technology* **2004,** *35* (2-3), 254-260.

15. Kikani, B.; Singh, S., Single step purification and characterization of a thermostable and calcium independent α-amylase from *Bacillus amyloliquifaciens* TSWK1-1 isolated from Tulsi Shyam hot spring reservoir, Gujarat (India). *International Journal of Biological Macromolecules* **2011,** *48* (4), 676-681.

16. Kuddus, M.; Roohi, A. J.; Ramteke, P. W., An overview of cold-active microbial α-amylase: adaptation strategies and biotechnological potentials. *Biotechnology* **2011,** *10* (3), 246-258.

17. Jaeger, K.-E.; Eggert, T., Lipases for biotechnology. *Current Opinion in Biotechnology* **2002,** *13* (4), 390-397.

18. Wu, Y. T.; Zhou, N. D.; Zhou, Z. M.; Gao, X. X.; Tian, Y. P., A thermo-stable lysine aminopeptidase from *Pseudomonas aeruginosa*: isolation, purification, characterization, and sequence analysis. *Journal of Basic Microbiology* **2014,** *54* (10), 1110-1119.

19. Méndez, Y.; Pérez-Labrada, K.; González-Bacerio, J.; Valdés, G.; de los Chavez, M. A.; Osuna, J.; Charli, J. L.; Pascual, I.; Rivera, D. G., Combinatorial multicomponent access to natural products inspired peptidomimetics: discovery of selective inhibitors of microbial metallo-aminopeptidases. *ChemMedChem* **2014,** *9* (10), 2351-2359.

20. Houde, A.; Kademi, A.; Leblanc, D., Lipases and their industrial applications. *Applied Biochemistry Biotechnology* **2004,** *118* (1-3), 155-170.

21. Haefner, S.; Knietsch, A.; Scholten, E.; Braun, J.; Lohscheidt, M.; Zelder, O., Biotechnological production and applications of phytases. *Applied Microbiology Biotechnology* **2005,** *68* (5), 588-597.

22. Hasan, F.; Shah, A. A.; Hameed, A., Industrial applications of microbial lipases. *Enzyme Microbial Technology* **2006,** *39* (2), 235-251.

23. Pervez, S.; Aman, A.; Iqbal, S.; Siddiqui, N. N.; Qader, S. A. U., Saccharification and liquefaction of cassava starch: an alternative source for the production of bioethanol using amylolytic enzymes by double fermentation process. *BMC Biotechnology* **2014,** *14* (1), 49.

24. Couto, S. R.; Herrera, J. L. T., Industrial and biotechnological applications of laccases: a review. *Biotechnology Advances* **2006,** *24* (5), 500-513.

25. Vohra, A.; Satyanarayana, T., Phytases: microbial sources, production, purification, and potential biotechnological applications. *Critical Reviews in Biotechnology* **2003,** *23* (1), 29-60.

26. Zhang, J.; Siika-aho, M.; Puranen, T.; Tang, M.; Tenkanen, M.; Viikari, L., Thermostable recombinant xylanases from *Nonomuraea flexuosa* and *Thermoascus aurantiacus* show distinct properties in the hydrolysis of xylans and pretreated wheat straw. *Biotechnology for Biofuels* **2011,** *4* (1), 12.

27. Ammar, Y. B.; Matsubara, T.; Ito, K.; Iizuka, M.; Limpaseni, T.; Pongsawasdi, P.; Minamiura, N., New action pattern of a maltose-forming alpha-amylase from *Streptomyces sp.* and its possible application in bakery. *Journal of Biochemistry Molecular Biology* **2002,** *35* (6), 568-575.

28. Kar, S.; Ray, R. C., Statistical optimization of á-amylase production by *Streptomyces erumpens* MTCC 7317 cells in calcium alginate beads using response surface methodology. *Polish Journal of Microbiology* **2008,** *57*, 49-57.

29. Vieille, C.; Zeikus, G. J., Hyperthermophilic enzymes: sources, uses, and molecular mechanisms for thermostability. *Microbiology Molecular Biology Review* **2001,** *65* (1), 1-43.

30. Sterpone, F.; Bertonati, C.; Briganti, G.; Melchionna, S., Key role of proximal water in regulating thermostable proteins. *The Journal of Physical Chemistry B* **2008,** *113* (1), 131-137.

31. Liang, Z. X.; Tsigos, I.; Lee, T.; Bouriotis, V.; Resing, K. A.; Ahn, N. G.; Klinman, J. P., Evidence for increased local flexibility in psychrophilic alcohol dehydrogenase relative to its thermophilic homologue. *Biochemistry* **2004,** *43* (46), 14676-14683.

32. Böhm, G.; Jaenicke, R., Relevance of sequence statistics for the properties of extremophilic proteins. *International Journal of Peptide Protein Research* **1994,** *43* (1), 97-106.

33. Davies, G. J.; Gamblin, S. J.; Littlechild, J. A.; Watson, H. C., The structure of a thermally stable 3-phosphoglycerate kinase and a comparison with its mesophilic equivalent. *Proteins: Structure, Function, Bioinformatics* **1993,** *15* (3), 283-289.

34. Auerbach, G.; Ostendorp, R.; Prade, L.; Korndörfer, I.; Dams, T.; Huber, R.; Jaenicke, R., Lactate dehydrogenase from the hyperthermophilic bacterium *Thermotoga maritima*: the crystal structure at 2.1 Å resolution reveals strategies for intrinsic protein stabilization. *Structure* **1998,** *6* (6), 769-781.

35. Elcock, A. H., The stability of salt bridges at high temperatures: implications for hyperthermophilic proteins. *Journal of Molecular Biology* **1998,** *284* (2), 489-502.

36. Gromiha, M. M.; Oobatake, M.; Sarai, A., Important amino acid properties for enhanced thermostability from mesophilic to thermophilic proteins. *Biophysical Chemistry* **1999,** *82* (1), 51-67.

37. Zhou, P.; Tian, F.; Lv, F.; Shang, Z., Geometric characteristics of hydrogen bonds involving sulfur atoms in proteins. *Proteins: Structure, Function, Bioinformatics* **2009,** *76* (1), 151-163.

38. Pace, C. N., Contribution of the hydrophobic effect to globular protein stability. *Journal of Molecular Biology* **1992,** *226* (1), 29-35.

39. Anderson, D. E.; Becktel, W. J.; Dahlquist, F. W., pH-induced denaturation of proteins: a single salt bridge contributes 3-5 kcal/mol to the free energy of folding of T4 lysozyme. *Biochemistry* **1990,** *29* (9), 2403-2408.

40. Shirley, B. A.; Stanssens, P.; Hahn, U.; Pace, C. N., Contribution of hydrogen bonding to the conformational stability of ribonuclease T1. *Biochemistry* **1992,** *31* (3), 725-732.

41. Serrano, L.; Bycroft, M.; Fersht, A. R., Aromatic-aromatic interactions and protein stability: investigation by double-mutant cycles. *Journal of Molecular Biology* **1991,** *218* (2), 465-475.

42. Zavodszky, M.; Chen, C. W.; Huang, J. K.; Zolkiewski, M.; Wen, L.; Krishnamoorthi, R., Disulfide bond effects on protein stability: designed variants of *Cucurbita maxima* trypsin inhibitor-V. *Protein Science* **2001,** *10* (1), 149-160.

43. Kapoor, K.; Duff, M. R.; Upadhyay, A.; Bucci, J. C.; Saxton, A. M.; Hinde, R. J.; Howell, E. E.; Baudry, J., Highly dynamic anion–quadrupole networks in proteins. *Biochemistry* **2016,** *55* (43), 6056-6069.

44. Danson, M. J.; Hough, D. W.; Russell, R. J.; Taylor, G. L.; Pearl, L., Enzyme thermostability and thermoactivity. *Protein Engineering, Design Selection* **1996,** *9* (8), 629-630.

45. Howard, D. L.; Kjaergaard, H. G., Hydrogen bonding to divalent sulfur. *Physical Chemistry Chemical Physics* **2008,** *10* (28), 4113-4118.

46. Curtiss, L.; Blander, M., Thermodynamic properties of gas-phase hydrogen-bonded complexes. *Chemical Reviews* **1988,** *88* (6), 827-841.

47. Zanotti, J.; Gibrat, G.; Bellissent-Funel, M., Hydration water rotational motion as a source of configurational entropy driving protein dynamics. Crossovers at 150 and 220 K. *Physical Chemistry Chemical Physics* **2008,** *10* (32), 4865-4870.

48. Wintrode, P. L.; Zhang, D.; Vaidehi, N.; Arnold, F. H.; Goddard III, W. A., Protein dynamics in a family of laboratory evolved thermophilic enzymes. *Journal of Molecular Biology* **2003,** *327* (3), 745-757.

49. Zavodszky, P.; Kardos, J.; Svingor, Á.; Petsko, G. A., Adjustment of conformational flexibility is a key event in the thermal adaptation of proteins. *Proceedings of the National Academy of Sciences* **1998,** *95* (13), 7406-7411.

50. Szilágyi, A.; Závodszky, P., Structural differences between mesophilic, moderately thermophilic and extremely thermophilic protein subunits: results of a comprehensive survey. *Structure* **2000,** *8* (5), 493-504.

51. Liu, Z.; Lemmonds, S.; Huang, J.; Tyagi, M.; Hong, L.; Jain, N., Entropic contribution to enhanced thermal stability in the thermostable P450 CYP119. *Proceedings of the National Academy of Sciences* **2018,** *115* (43), E10049-E10058.

52. Hernández, G.; Jenney, F. E.; Adams, M. W.; LeMaster, D. M., Millisecond time scale conformational flexibility in a hyperthermophile protein at ambient temperature. *Proceedings of the National Academy of Sciences* **2000,** *97* (7), 3166-3170.

53. Meinhold, L.; Clement, D.; Tehei, M.; Daniel, R.; Finney, J. L.; Smith, J. C., Protein dynamics and stability: the distribution of atomic fluctuations in thermophilic and mesophilic dihydrofolate reductase derived using elastic incoherent neutron scattering. *Biophysical Journal* **2008,** *94* (12), 4812-4818.

54. Nesper, M.; Nock, S.; Sedlák, E.; Antalík, M.; Podhradský, D.; Sprinzl, M., Dimers of *Thermus thermophilus* elongation factor Ts are required for its function as a nucleotide exchange factor of elongation factor Tu. *European Journal of Biochemistry* **1998,** *255* (1), 81-86.

55. Hess, D.; Krüger, K.; Knappik, A.; Palm, P.; Hensel, R., Dimeric 3-phosphoglycerate kinases from hyperthermophilic archaea: cloning, sequencing and expression of the 3-phosphoglycerate kinase gene of *Pyrococcus woesei* in *Escherichia coli* and characterization of the protein. Structural and functional comparison with the 3-phosphoglycerate kinase of *Methanothermus fervidus*. *European Journal of Biochemistry* **1995,** *233* (1), 227-237.

56. Voorhorst, W.; Eggen, R.; Luesink, E. J.; De Vos, W., Characterization of the celB gene coding for beta-glucosidase from the hyperthermophilic archaeon *Pyrococcus furiosus* and its expression and site-directed mutation in *Escherichia coli*. *Journal of Bacteriology* **1995,** *177* (24), 7105-7111.

57. Thoma, R.; Hennig, M.; Sterner, R.; Kirschner, K., Structure and function of mutationally generated monomers of dimeric phosphoribosylanthranilate isomerase from *Thermotoga maritima*. *Structure* **2000,** *8* (3), 265-276.

58. Hashimoto, K.; Panchenko, A. R., Mechanisms of protein oligomerization, the critical role of insertions and deletions in maintaining different oligomeric states. *Proceedings of the National Academy of Sciences* **2010,** *107* (47), 20352-20357.

59. Tanaka, Y.; Tsumoto, K.; Yasutake, Y.; Umetsu, M.; Yao, M.; Fukada, H.; Tanaka, I.; Kumagai, I., How oligomerization contributes to the thermostability of an archaeon protein protein L-isoaspartyl-O-methyltransferase from *Sulfolobus tokodaii*. *Journal of Biological Chemistry* **2004,** *279* (31), 32957-32967.

60. Jaenicke, R., What ultrastable globular proteins teach us about protein stabilization. *Biochemistry New York English Translation of Biokhimiya* **1998,** *63* (3), 312-321.

61. Breitung, J.; Borner, G.; Scholz, S.; Linder, D.; Stetter, K. O.; Thauer, R. K., Salt dependence, kinetic properties and catalytic mechanism of N-formylmethanofuran: tetrahydromethanopterin formyltransferase from the extreme thermophile *Methanopyrus kandleri*. *European Journal of Biochemistry* **1992,** *210* (3), 971-981.

62. Andreotti, G.; Cubellis, M. V.; Nitti, G.; Sannia, G.; Mai, X.; Adams, M. W.; Marino, G., An extremely thermostable aromatic aminotransferase from the hyperthermophilic archaeon *Pyrococcus furiosus*. *Biochimica et Biophysica Acta -Protein Structure Molecular Enzymology* **1995,** *1247* (1), 90-96.

63. Michels, P. C.; Clark, D. S., Pressure-enhanced activity and stability of a hyperthermophilic protease from a deep-sea methanogen. *Applied Environmental Microbiology* **1997,** *63* (10), 3985-3991.

64. Packer, M. S.; Liu, D. R., Methods for the directed evolution of proteins. *Nature Reviews Genetics* **2015,** *16* (7), 379-394.

65. Tiwari, V., In vitro engineering of novel bioactivity in the natural enzymes. *Frontiers in Chemistry* **2016,** *4*, 39.

66. Axarli, I.; Muleta, A. W.; Chronopoulou, E. G.; Papageorgiou, A. C.; Labrou, N. E., Directed evolution of glutathione transferases towards a selective glutathione-binding site and improved oxidative stability. *Biochimica et Biophysica Acta -General Subjects* **2017,** *1861* (1), 3416-3428.

67. Belsare, K. D.; Horn, T.; Ruff, A. J.; Martinez, R.; Magnusson, A.; Holtmann, D.; Schrader, J.; Schwaneberg, U., Directed evolution of P450cin for mediated electron transfer. *Protein Engineering, Design Selection* **2017,** *30* (2), 119-127.

68. Yang, J.; Ruff, A. J.; Arlt, M.; Schwaneberg, U., Casting epPCR (cepPCR): A simple random mutagenesis method to generate high quality mutant libraries. *Biotechnology Bioengineering* **2017,** *114* (9), 1921-1927.

69. Shim, J. H.; Kim, Y. W.; Kim, T. J.; Chae, H. Y.; Park, J. H.; Cha, H.; Kim, J. W.; Kim, Y. R.; Schaefer, T.; Spendler, T., Improvement of cyclodextrin glucanotransferase as an antistaling enzyme by error-prone PCR. *Protein Engineering Design Selection* **2004,** *17* (3), 205-211.

70. Dutta, S.; Basak, B.; Bhunia, B.; Sinha, A.; Dey, A., Approaches towards the enhanced production of rapamycin by *Streptomyces hygroscopicus* MTCC 4003 through mutagenesis and optimization of process parameters by Taguchi orthogonal array methodology. *World Journal of Microbiology Biotechnology* **2017,** *33* (5), 90.

71. Windle, C. L.; Simmons, K. J.; Ault, J. R.; Trinh, C. H.; Nelson, A.; Pearson, A. R.; Berry, A., Extending enzyme molecular recognition with an expanded amino acid alphabet. *Proceedings of the National Academy of Sciences* **2017,** *114* (10), 2610-2615.

72. Kitaoka, M.; Tian, J.; Nishimoto, M., Novel putative galactose operon involving lacto-N-biose phosphorylase in *Bifidobacterium longum*. *Journal of Applilied Environmental Microbiology* **2005,** *71* (6), 3158-3162.

73. Arnold, F. H.; Volkov, A. A., Directed evolution of biocatalysts. *Current Opinion in Chemical Biology* **1999,** *3* (1), 54-59.

74. Shoichet, B. K.; Baase, W. A.; Kuroki, R.; Matthews, B. W., A relationship between protein stability and protein function. *Proceedings of the National Academy of Sciences* **1995,** *92* (2), 452-456.

75. Luo, P.; Hayes, R. J.; Chan, C.; Stark, D. M.; Hwang, M. Y.; Jacinto, J. M.; Juvvadi, P.; Chung, H. S.; Kundu, A.; Ary, M. L., Development of a cytokine analog with enhanced stability using computational ultrahigh throughput screening. *Protein Science* **2002,** *11* (5), 1218-1226.

76. Wijma, H. J.; Floor, R. J.; Jekel, P. A.; Baker, D.; Marrink, S. J.; Janssen, D. B.; Selection, Computationally designed libraries for rapid enzyme stabilization. *Protein Engineering, Design Selection* **2014,** *27* (2), 49-58.

77. Vakulenko, S. B.; Mobashery, S., Versatility of aminoglycosides and prospects for their future. *Clinical Microbiology Reviews* **2003,** *16* (3), 430-450.

78. Moazed, D.; Noller, H. F., Interaction of antibiotics with functional sites in 16S ribosomal RNA. *Nature Review Genetics* **1987,** *327* (6121), 389-394.

79. Umezawa, H., Biochemical mechanism of resistance to aminoglycoside antibiotics. In *Advances in Carbohydrate Chemistry and Biochemistry*, Elsevier: 1974; Vol. 30, pp 183-225.

80. Norris, A. L.; Özen, C.; Serpersu, E. H., Thermodynamics and kinetics of association of antibiotics with the aminoglycoside acetyltransferase (3)-IIIb, a resistance-causing enzyme. *Biochemistry* **2010,** *49* (19), 4027-4035.

81. Davies, J.; Wright, G. D., Bacterial resistance to aminoglycoside antibiotics. *Trends in Microbiology* **1997,** *5* (6), 234-240.

82. Matsumura, M.; Katakura, Y.; Imanaka, T.; Aiba, S., Enzymatic and nucleotide sequence studies of a kanamycin-inactivating enzyme encoded by a plasmid from thermophilic bacilli in comparison with that encoded by plasmid pUB110. *Journal of bacteriology* **1984,** *160* (1), 413-420.

83. Matsumura, M.; Aiba, S., Screening for thermostable mutant of kanamycin nucleotidyltransferase by the use of a transformation system for a thermophile, *Bacillus stearothermophilus*. *Journal of Biological Chemistry* **1985,** *260* (28), 15298-15303.

84. Liao, H. H., Thermostable mutants of kanamycin nucleotidyltransferase are also more stable to proteinase K, urea, detergents, and water-miscible organic solvents. *Enzyme Microbial Technology* **1993,** *15* (4), 286-292.

85. Jing, X.; Evangelista Falcon, W.; Baudry, J.; Serpersu, E. H., Thermophilic enzyme or mesophilic enzyme with enhanced thermostability: can we draw a line? *The Journal of Physical Chemistry B* **2017,** *121* (29), 7086-7094.

86. Kocaman, S.; Serpersu, E. H., The thermodynamics of ligand binding to the aminoglycoside O-nucleotidyltransferase(4') and variants yields clues about thermophilic properties. *Biochemistry* **2019,** *58* (12), 1579-1586.

87. Nemethy, G.; Peer, W. J.; Scheraga, H. A., Effect of protein-solvent interactions on protein conformation. *Annual Review of Biophysics Bioengineering* **1981,** *10* (1), 459-497.

88. Maes, D.; Zeelen, J. P.; Thanki, N.; Beaucamp, N.; Alvarez, M.; Thi, M. H. D.; Backmann, J.; Martial, J. A.; Wyns, L.; Jaenicke, R., The crystal structure of

triosephosphate isomerase (TIM) from *Thermotoga maritima*: a comparative thermostability structural analysis of ten different TIM structures. *Proteins: Structure, Function, Bioinformatics* **1999,** *37* (3), 441-453.

89. Georlette, D.; Damien, B.; Blaise, V.; Depiereux, E.; Uversky, V. N.; Gerday, C.; Feller, G., Structural and functional adaptations to extreme temperatures in psychrophilic, mesophilic, and thermophilic DNA ligases. *Journal of Biological Chemistry* **2003,** *278* (39), 37015-37023.

90. Kumar, S.; Nussinov, R., Fluctuations in ion pairs and their stabilities in proteins. *Proteins: Structure, Function, Bioinformatics* **2001,** *43* (4), 433-454.

91. Chakravarty, S.; Varadarajan, R., Elucidation of factors responsible for enhanced thermal stability of proteins: a structural genomics based study. *Biochemistry* **2002,** *41* (25), 8152-8161.

92. Makhatadze, G. I.; Privalov, P. L., Energetics of protein structure. In *Advances in protein chemistry*, Elsevier: 1995; Vol. 47, pp 307-425.

93. Privalov, P.; Makhatadze, G., Heat capacity of proteins: II. Partial molar heat capacity of the unfolded polypeptide chain of proteins: protein unfolding effects. *Journal of Molecular Biology* **1990,** *213* (2), 385-391.

94. Melchionna, S.; Briganti, G.; Londei, P.; Cammarano, P., Water induced effects on the thermal response of a protein. *Physical Review Letters* **2004,** *92* (15), 158101.

95. Melchionna, S.; Sinibaldi, R.; Briganti, G., Explanation of the stability of thermophilic proteins based on unique micromorphology. *Biophysical Journal* **2006,** *90* (11), 4204-4212.

96. Šanderová, H., EF-Tu protein domains functions and thermostability. **2008**.

97. Nock, S.; Grillenbeck, N.; Ahmadian, M. R.; Ribeiro, S.; Kreutzer, R.; Sprinzl, M., Properties of isolated domains of the elongation factor Tu from *Thermus thermophilus* HB8. *European Journal of Biochemistry* **1995,** *234* (1), 132-139.

2 THERMODYNAMICS OF LIGAND BINDING TO THE AMINOGLYCOSIDE *O*-NUCLEOTIDYLTRANSFERASE(4') AND VARIANTS YIELDS CLUES ON THERMOPHILIC PROPERTIES

This part is a slightly revised version of a manuscript with the same title published in the journal, Biochemistry.

Reprint (adapted) with permission from Seda Kocaman, Engin H. Serpersu*., “Thermodynamics of ligand binding to the aminoglycoside *O*-nucleotidyltransferase(4') and variants yields clues on thermophilic properties”, Biochemistry, Feb 2019, 58 (12), 1579-86.

(DOI: 10.1021/acs.biochem.8b01201)

Address correspondence to Engin H. Serpersu, eserpers@nsf.gov (or serpersu@utk.edu)

2.1 Abstract

The aminoglycoside nucleotidyltransferase(4') (ANT) is an enzyme with high substrate promiscuity and catalyzes the transfer of the AMP group from ATP to the 4'-OH site of many structurally diverse aminoglycosides, which results in the elimination of their effectiveness as antibiotics. Two thermostable variants carrying single site mutations are used to determine molecular properties associated with thermophilicity. Thermodynamics of enzyme-ligand interactions showed that one variant (T130K) has identical properties to the mesophilic WT while the other (D80Y) behaved differently. Differences between D80Y and T130K/WT pair include the change in heat capacity (ΔCp), which show temperature-dependence for D80Y but not for WT or T130K. The change of ΔCp with temperature ($\Delta\Delta Cp$) with D80Y is aminoglycoside-dependent only in H_2O and remains the same with all aminoglycosides in D_2O. Furthermore, the offset temperature (T_{off}), the temperature difference to yield identical enthalpies in H_2O and D_2O, become larger with increasing temperature for WT and T130K but remained mostly unchanged for D80Y. Studies in H_2O and D_2O revealed that solvent reorganization becomes the major contributor to ligand binding with increasing temperature for WT and T130K but changes in low frequency vibrational modes is the main contributor with D80Y. Data presented in

this paper suggest that global properties associated with the enzyme-ligand interactions, such as thermodynamics of ligand binding, may yield clues on thermophilicity and permit distinguishing those variants that are simply a more thermostable version of the mesophilic protein.

2.2 Introduction

Thermostable enzymes that are naturally found in thermophilic organisms and their ability to function at elevated temperatures are highly desirable for biotechnological and industrial applications. Thermophilic proteins may adopt various strategies to achieve thermal adaptation and yet they are structurally quite like their mesophilic variants. Therefore, understanding of molecular properties that render proteins thermophilic is necessary. Numerous studies made comparisons to identify the differences in various structural and dynamic features of thermophilic and mesophilic enzyme homologs. Although several molecular aspects such as the presence of more polar interactions or H-bonds or tighter packing of the hydrophobic core are suggested by earlier work *(1-6)*, more distributed effects and global dynamics of proteins playing a significant role was also suggested by other studies *(7, 8)*.

These efforts, however, are somewhat complicated by the fact that they included all thermostable enzymes, some of which may simply be enzymes with higher melting temperature (Tm) than mesophilic enzymes such as those with added stabilizing interactions in the form of disulfide bonds or ionic or hydrophobic interactions. Furthermore, these comparisons included proteins that have differences ranging from a few residues to tens of residues in their primary sequences as well as differences in their oligomeric state, which may introduce changes that are not necessarily specific for thermophilicity. In this work, we are separating the terms “thermostable” and “thermophilic” in the following manner; thermostable defines a variant of the mesophilic protein with increased thermostability achieved by either evolutionary-based or structure-based strategies leaving other properties of the protein like the mesophilic variant.

Contrary to this, thermophilic proteins may have significantly different dynamic and thermodynamic properties relative to the mesophilic variants.

To identify molecular properties associated with thermophilicity we used the wild-type (WT) and two thermostable, single amino acid mutants (D80Y and T130K) of the aminoglycoside nucleotidyltransferase(4') (ANT), which provides excellent opportunity to distinguish the thermophilic variant from the thermostable one. This is because, although both mutants are thermostable, only one (D80Y) appears to be a thermophilic protein while the other (T130K) is simply a more heat stable variant of WT. Earlier computational work with these three variants suggested that global dynamics of the mesophilic and thermophilic variants differ and T130K is similar to WT *(9)*. Thermodynamics of enzyme-ligand interactions and solvent effects on ligand binding, presented in this work, showed that while T130K shows identical behavior to WT, D80Y dramatically differs from both. Thus, data presented in this paper suggest that global properties associated with the enzyme-ligand interactions, such as thermodynamics of ligand binding, may also yield clues on thermophilicity.

2.3 Materials and methods

2.3.1 Chemicals and reagents

All chemicals including the aminoglycosides were purchased from Sigma-Aldrich (St. Louis, MO) at the highest purity available. Concentrated stock solutions of aminoglycosides were prepared after the removal of sulfate salt by ion exchange chromatography and then used in ITC experiments. Concentration of aminoglycoside solutions were determined by enzymatic assay as described earlier *(10)*. Isopropyl β-D-1-thiogalactopyranoside (IPTG) was purchased from Inalco SAS, Italy. Ni- Sepharose high performance and ion exchange matrix Macro Q, were purchased from GE Healthcare, (Sweden) and Bio-Rad Laboratories (Hercules, CA), respectively. Thrombin was obtained from EMD Millipore Corp., USA.

2.3.2 Overexpression and purification

WT ANT4 was originally isolated from the mesophilic *Staphylococcus aureus (11)*. Thermostable T130K and D80Y were from *Bacillus stearothermophilus (12) and were* codon optimized for *Thermosynechococcus elongatus (13).* T130K gene was transferred from *T. elongatus* to *E. coli* and D80Y, WT and the T130K/D80Y (double mutant is not used in this work) were generated via site directed mutations in T130K *(13)*. All three variants were overexpressed and purified as described earlier *(13-15)*. All three ANT4 variants were stable for three weeks at 4°C without a significant loss of activity (>90%). Protein concentration was determined by using the extinction coefficients of 50880 $M^{-1}cm^{-1}$ for D80Y and 49390 $M^{-1}cm^{-1}$ for both WT and T130K.

2.3.3 Isothermal titration calorimetry

ITC experiments were performed using VP-ITC microcalorimeter, GE Healthcare (Hercules, CA) over a temperature range of 10-40 ºC. Proteins were dialyzed in a buffer system composed of 50 mM MOPS, 100 mM NaCl (pH 7.5 at 25 ºC) in H_2O or D_2O (99.9%) prior to the ITC experiments. All aminoglycosides were diluted from concentrated stock solutions into the dialysate from enzyme preparations. Enzyme concentration in the calorimetry cell was 20 µM (monomer) while the aminoglycoside concentration in the syringe ranged from 400 to 800 µM. Enzyme and the ligand solutions were degassed for 10-15 minutes before they were loaded to the microcalorimeter. 10 µl of ligand was titrated into the enzyme in each injection. The experiments were composed of 27 injections separated by 240 seconds and the cell stirring speed was 307 rpm. Most ITC experiments were repeated 2-3 times and the data were fit using the global fit feature of SEDPHAT *(16)* considering the A+B ↔ AB hetero-association model to determine the binding enthalpy (ΔH) and the association constant (Ka). Gibbs energy (ΔG) and the entropy ($T\Delta S$) were determined from $\Delta G = -RT \ln Ka$ and $\Delta G = \Delta H - T\Delta S$ respectively. Data for T130K was taken from an earlier work *(14)*.

2.3.4 Analytical ultracentrifugation

Experiments were performed using Beckman XL-1 analytical ultracentrifuge and an An-50Ti rotor. Proteins were dialyzed in 50 mM MOPS buffer (pH 7.5 at 25 ºC) either with or without 100 mM NaCl to test the effect of salt on the monomer-dimer equilibrium. 400 µl of 1 µM enzyme and 390 µl of buffer were loaded into double-sector cells. 300 absorbance scans were collected at 230 nm, 50,000 rpm over a temperature range of 10-40 ºC. SEDNTERP *(17)* was used to calculate the buffer viscosity, buffer density and protein partial specific volume. SEDFIT *(18)* was used to fit the sedimentation data to a continuous [c(s)] distribution model.

2.4 Results

2.4.1 Thermodynamics of ligand binding distinguishes D80Y from T130K and WT

The thermodynamics of the ligand binding to the mesophilic (WT) and two thermostable variants (T130K and D80Y) of ANT was studied by ITC over a temperature range of 10°C to 40°C in H_2O and D_2O. Owing to the high substrate promiscuity of the enzyme, four aminoglycosides were used in this study. The aminoglycosides used were representatives of neomycin (neomycin B and paromomycin) and kanamycin (kanamycin A-henceforth kanamycin and tobramycin) groups (Figure 2.1). In all cases, the binding was enthalpically favored. An example data set is shown in Figure 2.2. Entropic contribution was aminoglycoside- and enzyme-dependent and always unfavorable for WT and T130K. Only exceptions were for the binding of kanamycin and tobramycin to WT and neomycin to T130K at 10°C. Contrary to this, favorable entropic contribution was more significant with D80Y and in some cases remained favorable up to 25°C. Exemplary data sets are presented in Tables 2.1-2.4. In all cases ΔG remained favorable ($\Delta G<0$). While the binding enthalpy was becoming more favorable with increasing temperature the entropic contribution became more unfavorable.

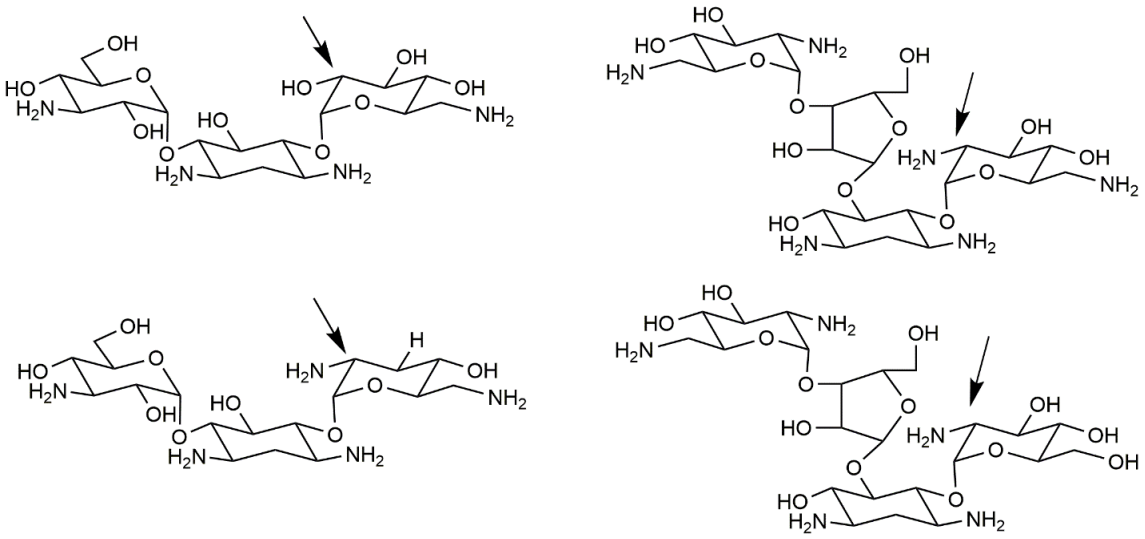

Figure 2.1: Aminoglycosides used in this work. Kanamycin A (left top), tobramycin (left bottom), neomycin (right top) and paromomycin (right bottom). Arrows mark the 2' site.

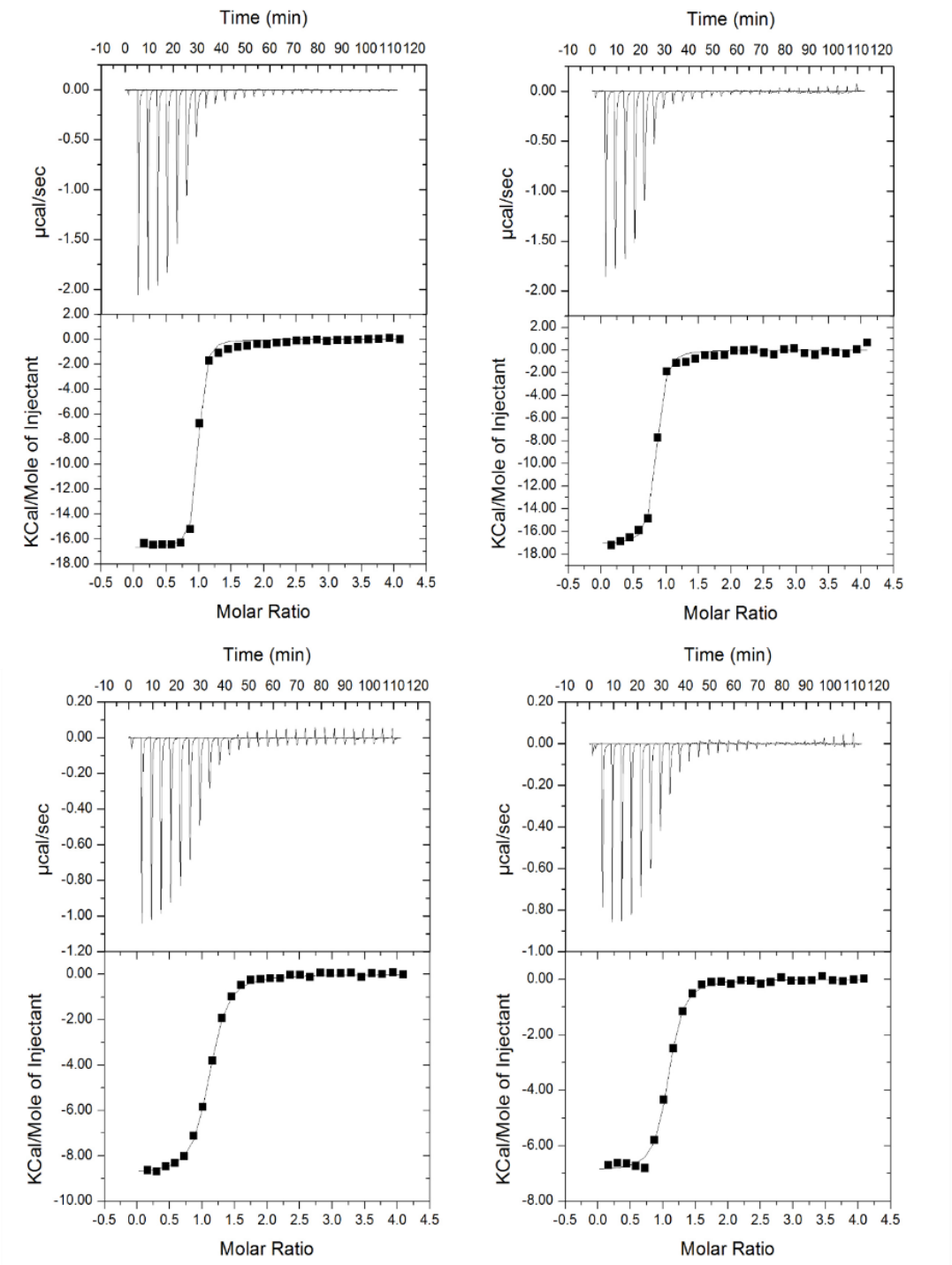

Figure 2.2: Examples of thermograms and isotherms.Titration of WT (top) and D80Y (bottom) with neomycin (20°C). Left and right panels represent titration in H_2O and D_2O respectively.

Table 2.1. Binding of neomycin to ANT and variants in H_2O

Temperature (°C)	WT		T130K		D80Y	
	ΔH	TΔS	ΔH	TΔS	ΔH	TΔS
10	-10.3	-1.4	-10.0	-0.2	-5.7	**3.1**
15	-12.9	-3.4	-14.1	-4.2	-7.5	**1.3**
20	-17.7	-7.7	-16.9	-6.8	-9.5	-0.8
25	-19.2	-9.5	-23.7	-12.4	-11.3	-2.6
30	-25.3	-9.9	-24.9	-14.8	-13.4	-4.9
35	ND	ND	-28.8	-18.8	-16.6	-8.2
40	ND	ND	-36.4	-26.6	-21.6	-13.2

All values are kcal/mol. Favorable entropic contributions are highlighted in bold red font.

Table 2.2: Binding of neomycin to ANT and variants in D_2O

Temperature (°C)	WT		T130K		D80Y	
	ΔH	TΔS	ΔH	TΔS	ΔH	TΔS
10	-10.0	-1.4	-9.0	**1.2**	-4.4	**4.8**
15	-11.0	-2.9	-11.1	-0.8	-6.1	**2.6**
20	-14.6	-5.0	-12.9	-2.7	-7.0	**1.8**
25	-15.3	-5.8	-13.8	-3.6	-8.8	**0.04**
30	-21.4	-11.6	-15.7	-5.5	-10.4	-1.7
35	ND	ND	-18.2	-7.9	-12.5	-3.9
40	ND	ND	-23.1	-14.4	-14.7	-6.2

All values are kcal/mol. Favorable entropic contributions are highlighted in bold red font.

Table 2.3: Binding of tobramycin to ANT and variants in H_2O

Temperature (°C)	WT		T130K		D80Y	
	ΔH	TΔS	ΔH	TΔS	ΔH	TΔS
10	-5.6	**1.9**	-5.7	-1.1	-3.7	**3.8**
15	-8.7	-1.4	-8.3	-0.01	-4.9	**2.7**
20	-10.6	-2.8	-11.0	-2.7	-5.9	**1.7**
25	-17.5	-9.8	-14.2	-5.4	-9.0	-1.2
30	-21.8	-14.1	-20.0	-9.0	-11.1	-3.3
35	ND	ND	-25.8	-12.0	-18.0	-10.9
40	ND	ND	-22.6	-14.8	-22.9	-15.2

All values are kcal/mol. Favorable entropic contributions are highlighted in bold red font.

Table 2.4: Binding of tobramycin to ANT and variants in D_2O

Temperature (°C)	WT		T130K		D80Y	
	ΔH	TΔS	ΔH	TΔS	ΔH	TΔS
10	-5.6	**1.8**	-5.25	-3.8	-3.3	**4.2**
15	-6.6	**1.5**	-5.1	-3.7	-4.3	**3.3**
20	-9.5	-1.5	-8.3	0.3	-5.6	**2.3**
25	-11.5	-3.3	-11.9	-3.6	-6.8	**1.0**
30	-14.9	-6.5	-12.4	-3.9	-11.1	-3.5
35	ND	ND	-16.3	-7.9	-12.0	-4.0
40	ND	ND	-16.3	-7.8	-16.0	-7.8

All values are kcal/mol. Favorable entropic contributions are highlighted in bold red font.

However, at all temperatures studied, the favorable enthalpy overcame the unfavorable entropic contribution to favor ligand binding. Figure 2.3 shows the enthalpy of binding of neomycin and tobramycin to all three variants as a function of temperature in H_2O and D_2O. The data acquired with paromomycin and kanamycin A is shown in Figure 2.4. These data show that, in the range of temperature studied, ΔH decreases linearly with increasing temperature for binding of all four aminoglycosides to WT and T130K. The decrease in ΔH was not linear with D80Y indicating that the heat capacity change (ΔCp), unlike WT and T130K, is temperature dependent. Despite aminoglycoside specific variations, the rate of decrease in ΔH with increasing temperature was always faster in H_2O for WT and T130K in the temperature range tested. This was true for D80Y only at temperatures above ~20°C. Data acquired with neomycin and tobramycin, are shown in Figure 2.5 to highlight this point for WT and D80Y. T130K behaved similar to wild type, which was reported earlier *(14)*. Nevertheless, several titrations were repeated with T130K to reproduce the earlier data. The temperature dependence of enthalpy and ΔCp for binding of neomycin to all three variants is shown as a 3D plot in Figure 2.6.

Differences observed in binding enthalpies in H_2O and D_2O ($\Delta\Delta H = \Delta H_{H2O} - \Delta H_{D2O}$), as shown in Figure 2.7, enhances the distinction between D80Y and WT/T130K pair. Of the two thermostable variants, T130K behaves like the mesophilic WT, while D80Y shows different behavior. $\Delta\Delta H$ becomes more negative with increase in temperature in a linearly dependent manner and becomes positive at low temperature for both WT and T130K. In contrast, $\Delta\Delta H$ shows a nonlinear correlation with temperature and it remains always negative with D80Y (Figure 2.7). The only exception to this is binding of kanamycin to D80Y.

The temperature dependence of ΔCp for the formation of the binary D80Y—aminoglycoside complexes showed aminoglycoside specific variation, however it was always stronger in H_2O relative to D_2O. Figure 2.8 illustrates this for the formation of D80Y—neomycin and D80Y—tobramycin complexes. The change in ΔCp as a function of temperature ($\Delta\Delta Cp$) is determined from slopes of such plots and are shown in Table 2.5.

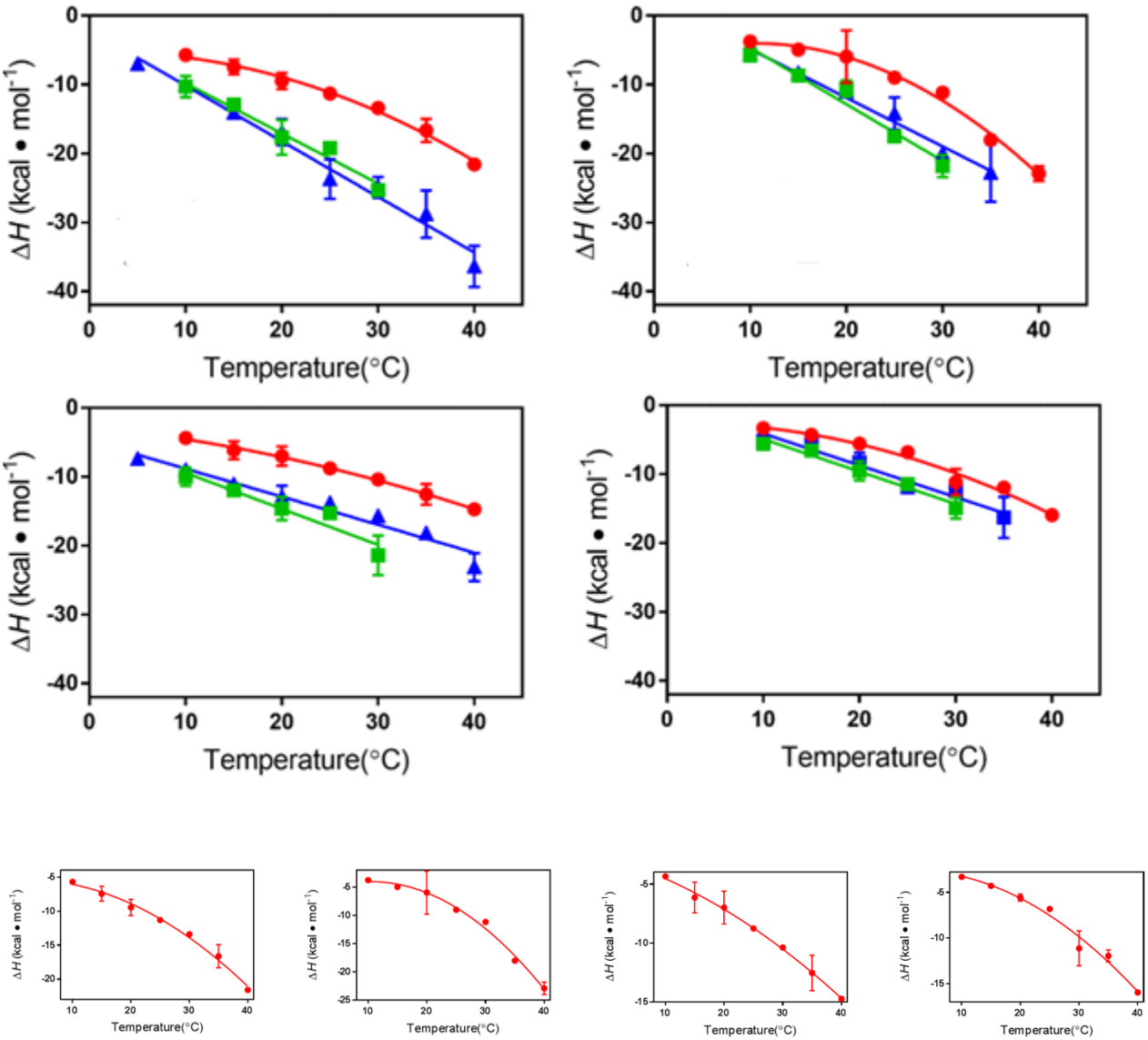

Figure 2.3: The binding enthalpy change as a function of temperature for neomycin and tobramycin. WT (green), T130K (blue) and D80Y (red). First row, neomycin (left) and tobramycin (right) binding in H_2O. Second row, neomycin (left) and tobramycin (right) binding in D_2O. Some of the error bars are smaller than the symbol size. Third row shows data for D80Y with an expanded Y axis, from left to right: D80Y-Neo- H_2O, D80Y-Neo- D_2O, D80Y-Tob- H_2O, D80Y-Tob- D_2O. Data for T130K is from *(14)*.

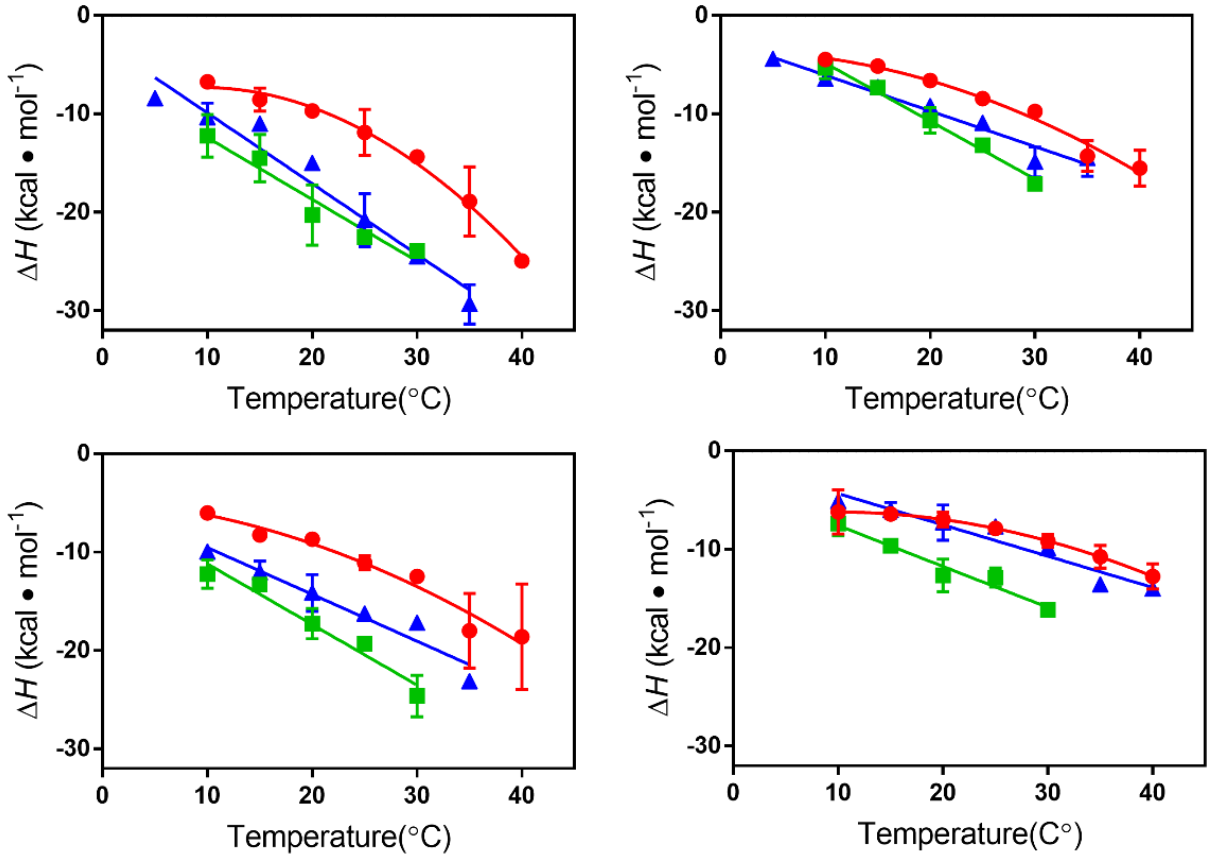

Figure 2.4: The binding enthalpy change as a function of temperature for paromomycin and kanamycin A. Binding of paromomycin (left panels) and kanamycin A (right panels) to WT (green), T130K (blue) and D80Y (red) in H_2O (top panels) and D_2O (bottom panels). Data for T130K is from *(14)*.

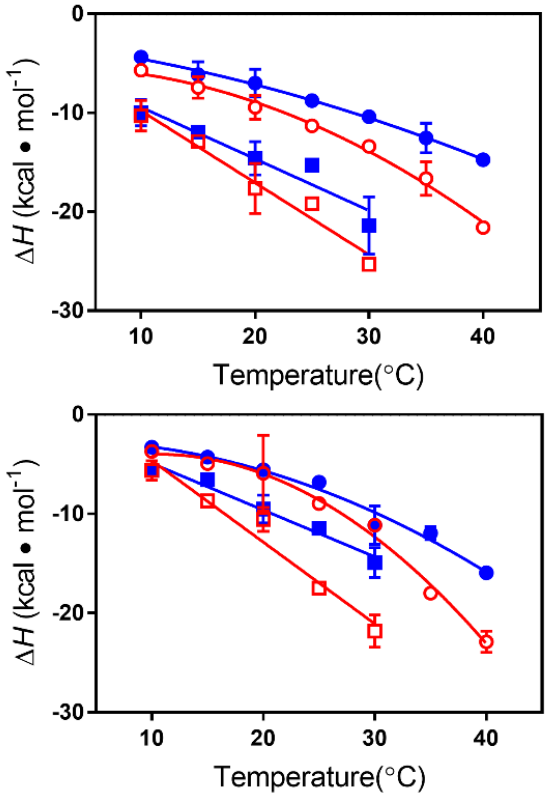

Figure 2.5: Comparison of binding enthalpies in different solvents. H_2O (open symbols) vs D_2O (filled symbols). Binding of neomycin (top) and tobramycin (bottom) to WT (squares) and D80Y (circles).

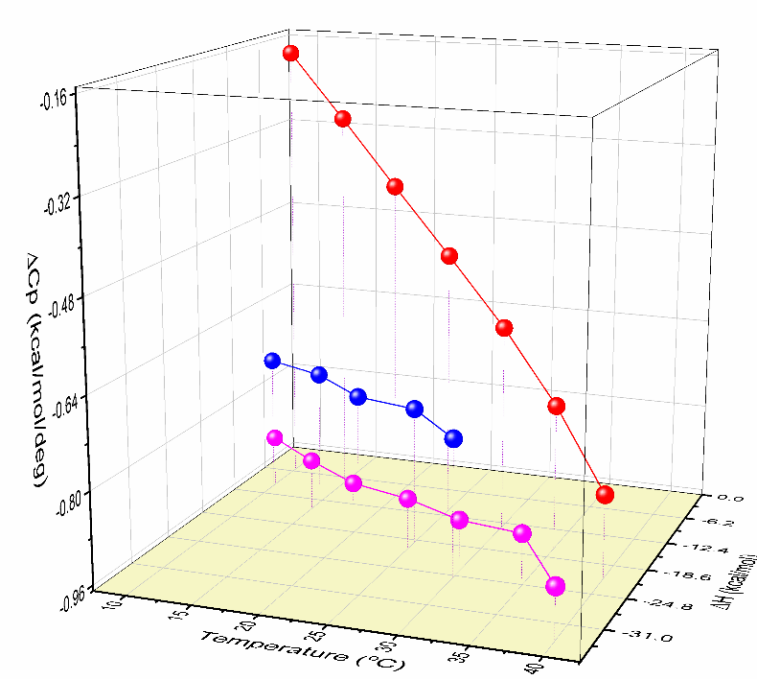

Figure 2.6: Binding of neomycin to all three enzymes. Vertical scale highlights temperature dependence of Δ*Cp* for D80Y (red). WT (blue) and T130K (purple) are also shown.

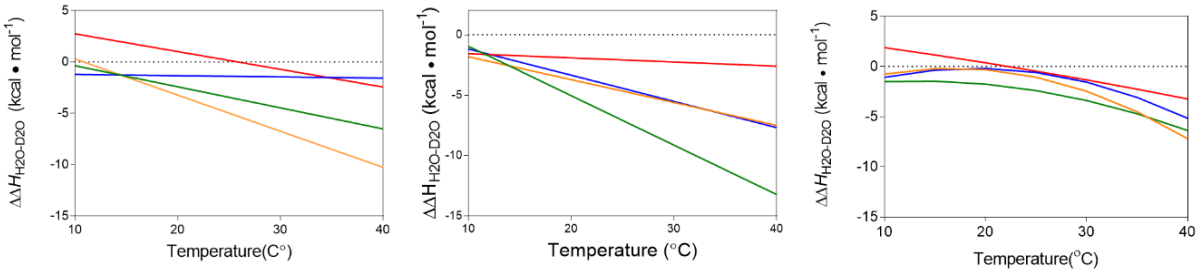

Figure 2.7: Temperature dependence of ΔΔ*H* for ANT variants. WT (left), T130K (middle) and D80Y (right). Neomycin (green), paromomycin (blue) tobramycin (orange) and kanamycin (red). Curves in D80Y plots are not representing any kind of fitting, they simply are connecting data points. Data for T130K is reprinted with permission from (Jing, X and Serpersu, E. H. (2014) *Biochemistry* **53**, 5544-5550). Copyright 2014 American Chemical Society.

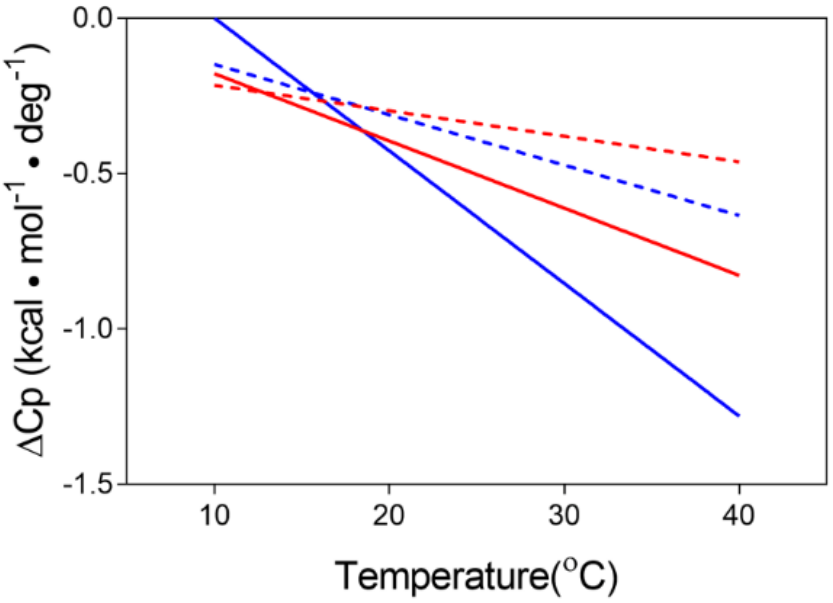

Figure 2.8: Change in heat capacity as a function of temperature. Binding of tobramycin (blue) and neomycin (red) to D80Y in H_2O (solid lines) and in D_2O (dashed lines).

Table 2.5: The change in ΔCp as a function of temperature and its aminoglycoside-dependent variation

	$\Delta\Delta Cp(H_2O)^a$ cal•mol^{-1}•deg^{-2}	$\Delta\Delta Cp(D_2O)^a$ cal•mol^{-1}•deg^{-2}
D80Y—Tobramycin	-42	-16
D80Y—Paromomycin	-37	-15
D80Y—Neomycin	-22	-8
D80Y—Kanamycin	-16	-14

[a]All R^2 values for curve fitting were >0.999.

Variation of ΔΔ*Cp* with different aminoglycosides was more significant in H_2O and showed a 2.6-fold difference between the lowest and highest values. In D_2O, apart from neomycin, ΔΔ*C*p was very similar with all three aminoglycosides (Table 2.5). In all cases, ΔΔ*Cp* was more negative in H_2O.

Differential temperature dependence of Δ*Cp* between H_2O and D_2O also indicates temperature dependent effects on transfer between these solvents. Δ*Cp* for transfer ($\Delta Cp_{tr} = \Delta Cp_{H2O} - \Delta Cp_{D2O}$) for the binary D80Y—aminoglycoside complexes are shown in Figure 2.9. ΔCp_{tr} for the transfer from D_2O to H_2O is negative above 20°C for all four aminoglycosides and becomes positive between 10°C and 20°C except for kanamycin for which ΔCp_{tr} is very small. There is no such variation for WT and T130K and ΔCp_{tr} is always negative with all aminoglycosides except for the binding of paromomycin to WT which is about zero (Table 2.6).

2.4.2 Monomer-dimer equilibrium is very similar for all three ANT variants

Analytical centrifugation studies showed that all three ANT4 variants exhibit a similar effect of temperature on monomer-dimer equilibrium over a temperature range studied (Figure 2.10). The increase in temperature results in a higher tendency towards dimerization with all. With the exception of small differences observed in the monomer-monomer association constants there were no differences between variants and the presence of salt increased the monomer-monomer affinity by about a factor of ten with all three variants *(14)*. No detectable temperature- dependent compaction or expansion was detected with all three variants.

2.5 Discussion

Differences in the temperature dependence of the binding enthalpy separated D80Y from the other thermostable variant T130K, which behaved like WT. Unlike WT and T130K, there was no linear correlation between the binding enthalpy and temperature with D80Y,

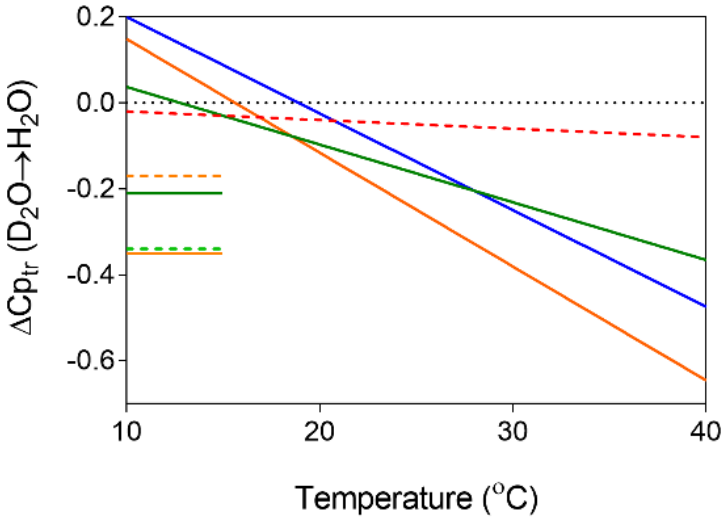

Figure 2.9: Temperature dependence of ΔCp_{tr} (ΔCp_{H2O} – ΔCp_{D2O}) for aminoglycoside binding. Binding of neomycin (green), paromomycin (blue), tobramycin (orange) and kanamycin (red) to D80Y. The constant ΔCp_{tr} for the binding of tobramycin (orange) and neomycin (green) to WT and T130K are shown for comparison as short lines.

Table 2.6: ΔCp_{tr} for WT and T130K

	$\Delta Cp(H_2O)$	$\Delta Cp(D_2O)$	ΔCp_{tr} (ΔCp_{H2O}- ΔCp_{D2O})
Neomycin–WT	-0.73 ± 0.07	-0.52 ± 0.09	-0.21 ± 0.09
Paramomycin–WT	-0.63 ± 0.08	-0.62 ± 0.08	-0.01 ± 0.08
Tobramycin–WT	-0.82 ± 0.1	-0.47 ± 0.05	-0.35 ± 0.05
Kanamycin–WT	-0.59 ± 0.03	-0.42 ± 0.05	-0.17 ± 0.05
Neomycin–T130K[a]	−0.81 ± 0.06	−0.47 ± 0.05	-0.34 ± 0.06
Paramomycin–T130K[a]	−0.67 ± 0.05	−0.41 ± 0.05	-0.26 ± 0.05
Tobramycin–T130K[a]	−0.55 ± 0.01	−0.39 ± 0.04	-0.16 ± 0.04
Kanamycin–T130K[a]	−0.35 ± 0.03	−0.29 ± 0.03	-0.06 ± 0.03

[a]Data from *(14, 15)*

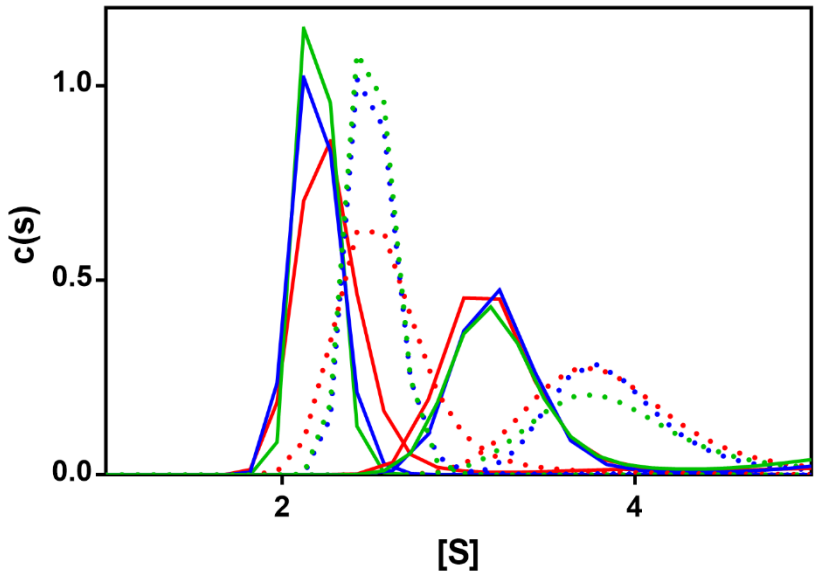

Figure 2.10: Temperature dependence of sedimentation coefficient for ANT variants. WT (green), T130K (blue) and D80Y (red). Curves from left to right represent data at 15°C, 20°C, 30°C and 40°C respectively.

which was indicative of temperature dependence of Δ*Cp*. In our earlier work, a hint of curvature with one aminoglycoside was detected but was not investigated further *(9)*. In this work, extended temperature range and the use of a couple of different aminoglycosides confirmed it and allowed that behavior to be investigated. The extent of curvature in Δ*H* vs temperature plots for the formation of D80Y─aminoglycoside complexes were different for each ligand and didn't seem to be correlated with any structural features of the ligand itself (Figure 2.1). Curvature in Δ*H* vs *T* plots of D80Y starts well below the Tm of D80Y (Figure 2.4) suggesting that unfolding coupled to binding *(19)* may not be the reason but two partially overlapping enthalpic processes with different negative Δ*Cp* may be at play instead. The binding enthalpy of all four aminoglycosides was always more favorable in H_2O at temperatures above 15°C with all three enzymes. At lower temperatures binding of some of the aminoglycosides was enthalpically more favored in D_2O with WT and T130K. Contrary to this, apart from kanamycin, ligand binding to D80Y at low temperatures was still enthalpically more favorable in H_2O. These observations suggest that, in D_2O, the bound state is stabilized at low temperature and unbound states are stabilized above 15-20°C with WT and T130K *(20)*. In the case of D80Y, there is no such temperature-dependent shift and always unbound states are stabilized relative to enzyme─aminoglycoside complexes.

It is not clear why kanamycin binding to D80Y is showing a different pattern than other aminoglycosides. However, we note that kanamycin is the only aminoglycoside within this set with an -OH group at the 2' site (Figure 2.1). We have earlier shown that the presence of $-NH_2$ versus -OH at the 2' site can have significant effect not only in thermodynamics but even determines substrate behavior. For example, kanamycin B is a substrate for the aminoglycoside *N3*-acetyltransferase-VIa (AAC-VIa) while no detectable activity was observed with kanamycin A *(21)*. Their enthalpies of binding to different aminoglycoside-modifying enzymes can be different as much as 6.9 kcal/mol *(22)*. The only difference between these two aminoglycosides is the presence of $-NH_2$ at the 2' site in kanamycin B and an -OH in kanamycin A (Figure 2.1).

Differences between the two thermostable variants were enhanced by the temperature dependence of $\Delta\Delta H$. While $\Delta\Delta H$ can be positive at low temperatures with WT and T130K, it is always, except kanamycin, negative with D80Y. Transfer of hydrophobic groups from D_2O to H_2O occurs with positive ΔH that becomes more negative with increasing temperature *(23)*. $\Delta\Delta H$ for WT and T130K are consistent with this. The same is true for D80Y only above ~20°C. Again, kanamycin is the exception with D80Y. Furthermore, a linear correlation is observed between $\Delta\Delta H$ and temperature with WT and T130K, which was nonlinear with D80Y (Figure 2.7).

The negative ΔCp_{tr} with all variants is also consistent with the transfer of hydrophobic groups from D_2O to H_2O *(23, 24)*. However, this is true for D80Y only above 20°C and, at lower temperatures, ΔCp_{tr} becomes positive (again, except for kanamycin) in an aminoglycoside-dependent manner. This is also consistent with the effect on the transfer of polar groups from D_2O to H_2O and, again, separates D80Y from WT and T130K. It is likely that protein dynamics and protein-solvent interactions have different temperature dependence for D80Y as compared to WT and T130K. These thermodynamic data are consistent with the differences in temperature dependence of global protein dynamics between D80Y and WT and T130K as determined by molecular dynamics simulations *(9)*.

Variable ΔCp_{tr} values for D80Y suggests that, at higher temperatures, the transfer of hydrophobic groups from D_2O to H_2O is impacting this parameter while at low temperatures (<15°C) the effect on polar groups becomes dominant for D80Y. Since $\Delta\Delta H$ remains always negative for D80Y, this observation suggests that the temperature dependence of $\Delta\Delta H$ alone cannot be attributed to the transfer of hydrophobic groups from D_2O to H_2O. These observations are consistent with multiple overlapping events affecting the behavior of D80Y in solution and temperature-dependent alteration of their dominance on thermodynamics of D80Y-aminoglycoside interactions. Earlier, it was shown by MD simulations that the second principle component is the most effective in the dynamics of D80Y. This is unlike WT and T130K where the first principle component was the most effective for both enzymes*(9)*. This was observed even though the motion of protein

appears to be similar in all three enzymes. Our data suggest that the thermodynamic parameter Δ*Cp* for ligand binding separated D80Y from WT/T130K pair.

Different Δ*Cp* values in H_2O and D_2O suggest contribution of solvent reorganization to binding is temperature dependent *(20)*. Solvent contribution to binding can also be shown by ΔΔ*H* vs Δ*Cp* plots *(20)*. Such a plot, representing data acquired at different temperatures, is shown in Figure 2.11 for WT and D80Y. Each of the four data points for a given temperature represent data acquired with a different aminoglycoside. For the WT, the correlation between ΔΔ*H* vs Δ*Cp* becomes stronger with increasing temperature similar to what was observed with T130K *(14)*. This is not the case with D80Y. As shown in Figure 2.11 the correlation is still weak even at higher temperatures. Figure 2.11 shows the same plot at 30°C for all three enzymes for comparison. A plot of correlation coefficient against temperature for all three variants is shown in Figure 2.12. These data show that the contribution of solvent rearrangement to Δ*Cp* increases with increasing temperature and becomes the major effector above 20°C for WT and T130K. Data acquired with D80Y show no such systematic change and even at 40°C the correlation is still weak. Data also suggest that such correlation may start to be established for D80Y at temperatures above 40°C. However, we did not test binding at higher temperatures because even a small degree of protein unfolding can make significant impact on the observed Δ*H* and cause curvature in Δ*H* vs temperature plots. Thus, rendering data analysis difficult if not impossible.

Another contrasting aspect of these data are shown in Figure 2.13 as the temperature dependence of the slopes determined from ΔΔ*H* vs Δ*Cp* plots. The slopes have unit of temperature in degrees and yields the offset temperature, the temperature difference to observe the same binding enthalpy in H_2O and D_2O *(20)*. A steady increase observed with WT and T130K is not visible with D80Y. These data are indicative of the fact that D80Y does not follow the pattern observed with WT and T130K. This is very likely to be a result of differential solvent-protein interactions and differences in global dynamics of these proteins.

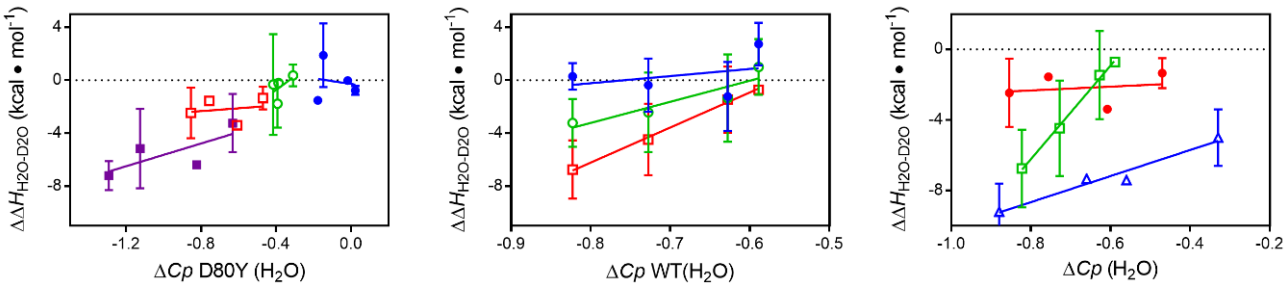

Figure 2.11: ΔΔ*H* versus Δ*Cp* at different temperatures. Data for 10°C (blue), 20°C (green), 30°C (red), and 40°C (purple) are shown for D80Y (left panel) and WT (middle panel). Each data point at a given temperature represents a different aminoglycoside. Data acquired at 30°C are replotted for all three enzymes for comparison (right panel), WT (green), T130K (blue), and D80Y (red). Data for T130K is from *(14)*.

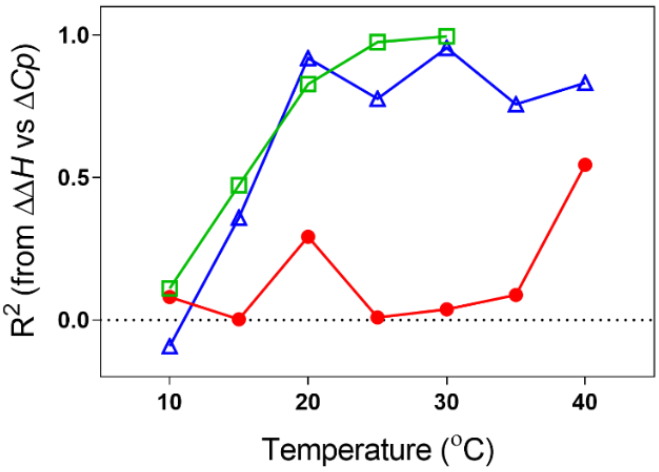

Figure 2.12: Temperature dependent variation of the correlation coefficient from least square fits of ΔΔ*H* versus Δ*Cp*. Data for WT (green), T130K (blue) and D80Y (red).

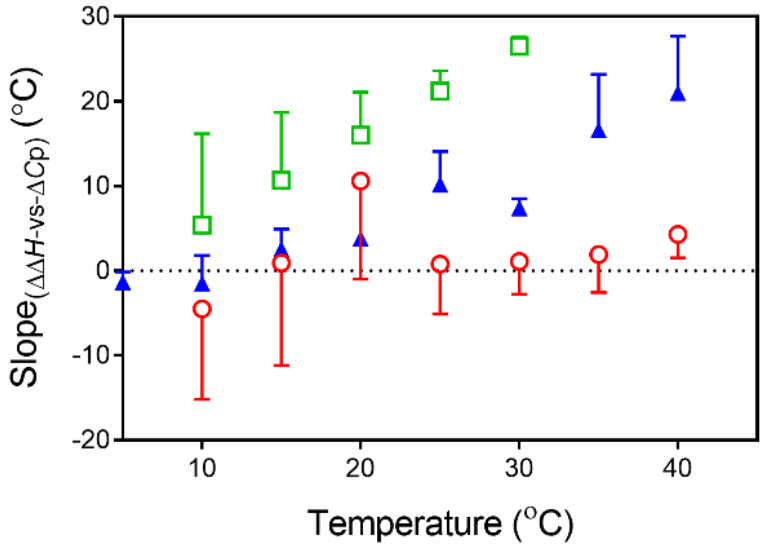

Figure 2.13: Slopes from ΔΔ*H* versus Δ*Cp* data. WT (green), T130K (blue) and D80Y (red).

Solvent reorganization and changes in low frequency vibrations of proteins are the major contributors of Δ*Cp (25)*. Data acquired with D80Y suggest unlike WT and T130K, that changes in the low frequency vibrational modes of the protein is the major source of the observed change in heat capacity. If the solvent contribution becomes more dominant at temperatures above 40°C, this will still separate D80Y from T130K.

Our thermodynamics studies show that T130K resembles WT, while D80Y is significantly different from them in terms of solvent reorganization upon ligand binding. We have also successfully obtained the crystal structures of the apo forms of all three ANT variants as well as the T130K-neomycin and WT-neomycin bound forms. Methodology on how these structures were obtained is explained in detail in chapter 4. Despite our effort, we were not able to obtain an aminoglycoside bound crystal structure of D80Y. All ANT variants bind to neomycin the tightest with D80Y binding to neomycin more than 25-fold weaker compared to others *(9)*. One reason that D80Y might bind to neomycin weaker compared to the other ANT variants can be due to a steric clash between the neomycin and Tyr 80 as suggested by our structural work (Figure 2.14). It is possible that we were not able to obtain a neomycin bound D80Y crystal structure due to its low binding affinity. Figure 2.15 shows that both in T130K-neomycin and WT-neomycin structures, neomycin is positioned in the same orientation, indicating that these enzymes bind to neomycin in the same fashion. The RMSD value for the superimposition of the apo forms of ANT variants is 0.4 Å while it is 0.3 Å for the neomycin bound forms of WT and T130K, indicating that these structures are highly similar to each other. Solvent arrangement in the ligand binding site is also very similar for the T130K-neomycin and WT-neomycin structures (Figure 2.15). On the other hand, the solvent arrangement at the active site is different for the T130K and D80Y when apo proteins are compared (Figure 2.16). T130K has more detectable solvent molecules at the active site compared to that of D80Y. Table 2.7 shows the solvent accessible area (SAA) and the molecular surface area calculations (MSA) of the ANT variants both in their apo and ligand bound forms, which were calculated using PyMol. In order to account for the differences in the volumes of the ANT variants which harbor different mutations, we have calculated the SSA/MSA ratio. The similarity in the structures enabled us to compare their SSA/MMA. SSA/MSA ratio is around 0.4 for all

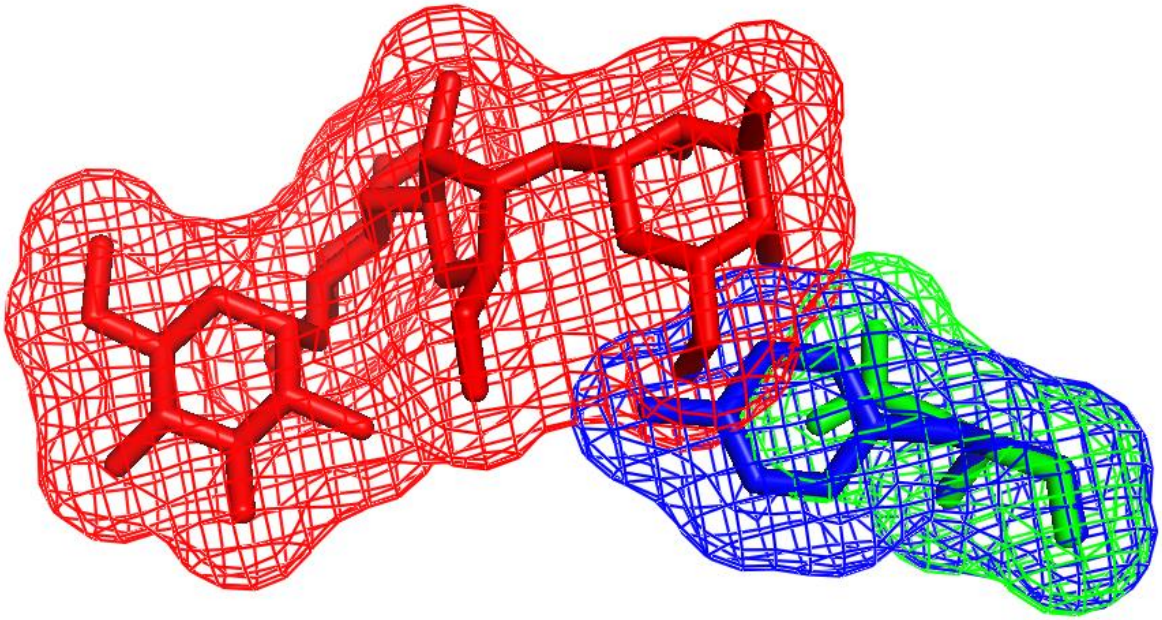

Figure 2.14: Steric clash between Tyr 80 and neomycin in the D80Y structure. Neomycin (red), Tyr 80 (blue), Asp 80 (green). The steric clash between Tyr 80 and neomycin in the D80Y structure explains the weaker affinity of D80Y towards neomycin compared to other ANT variants.

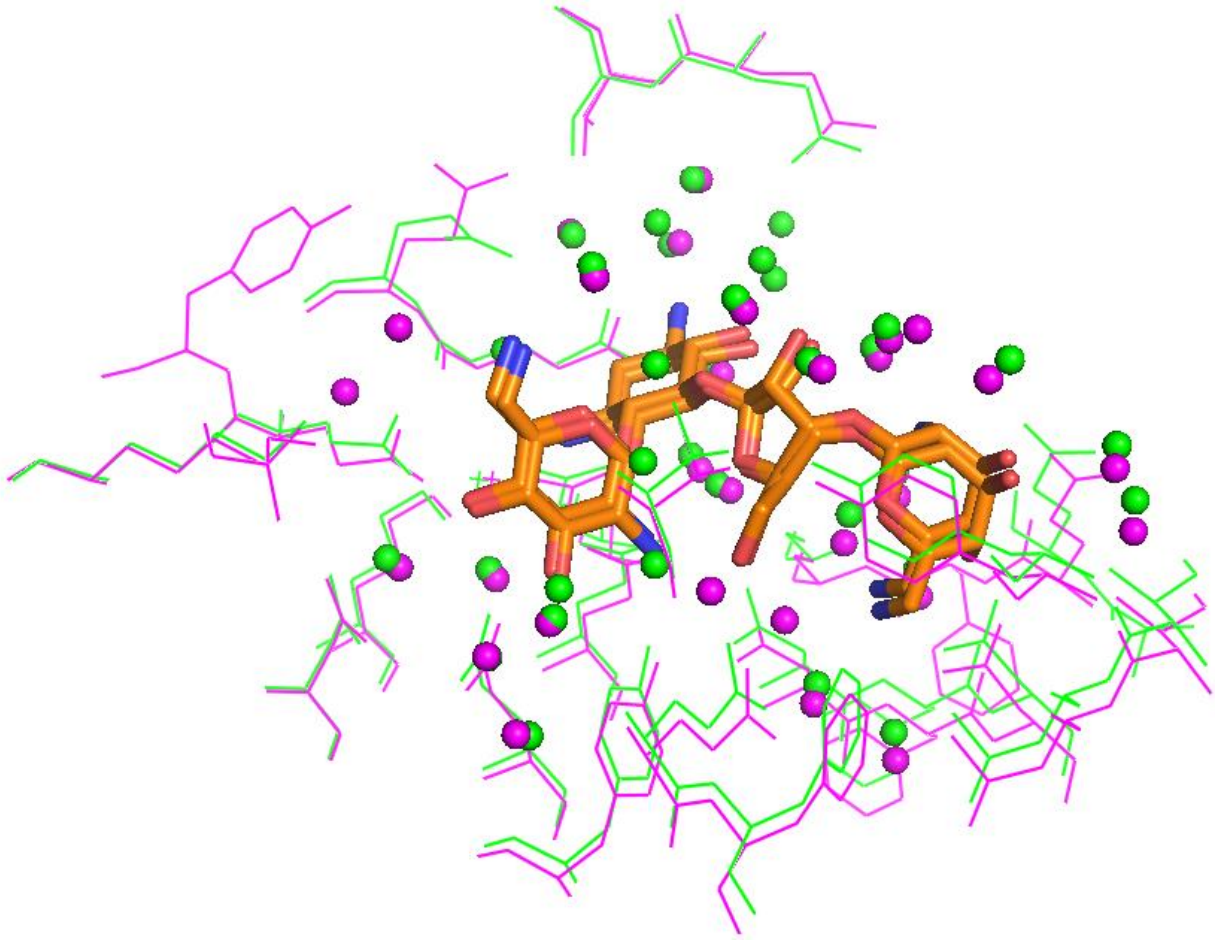

Figure 2.15: Ligand bound forms of WT and T130K have similar solvent patterns. Superimposition of the T130K-neomycin (magenta) and WT-neomycin (green) structures. Residues surrounding the neomycin within 6 Å are shown. The solvent molecules coming from the structures are shown as spheres. Neomycin molecules coming from both structures are shown in orange and neomycins are oriented in the same way.

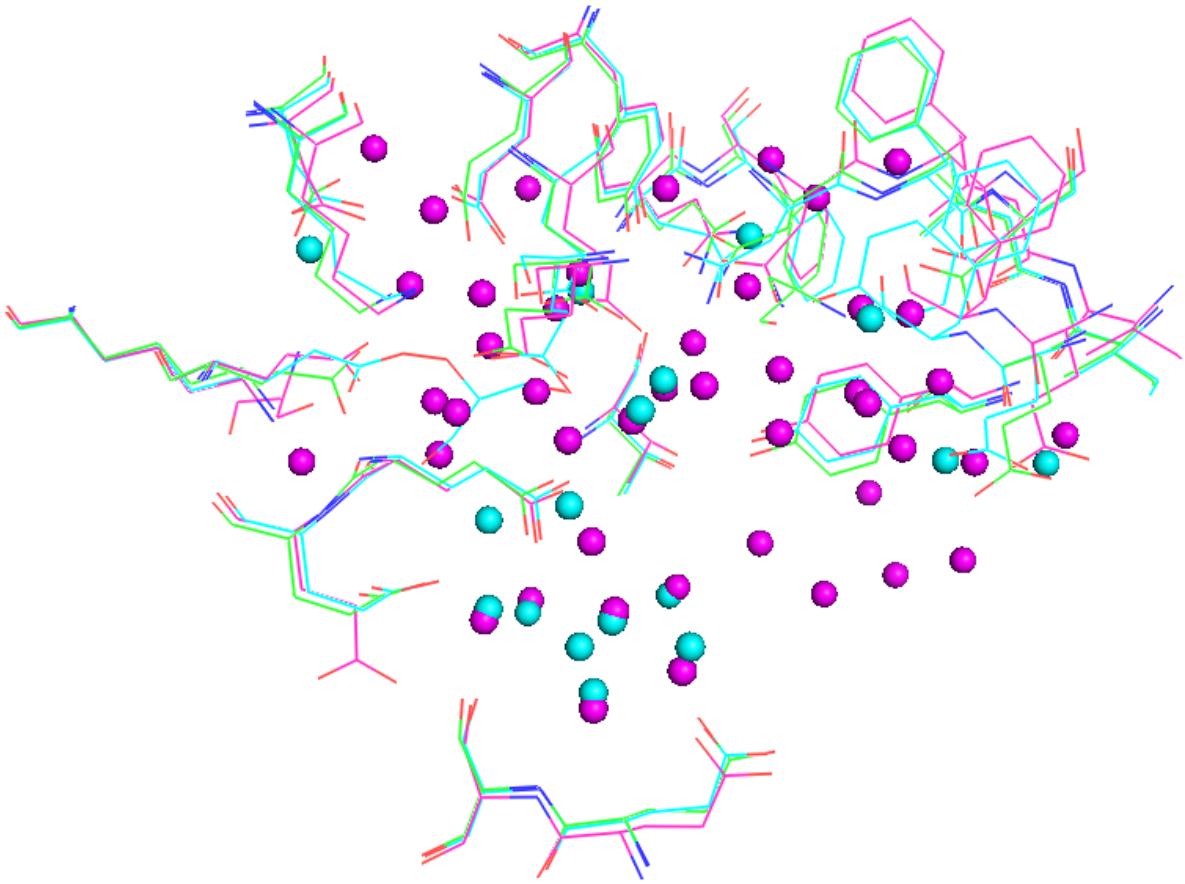

Figure 2.16: Solvent reorganization in the ligand binding site of D80Y is different than that of the T130K. Superimposition of the D80Y Apo and T130K Apo structures. Residues surrounding the active site are shown in cyan for D80Y and in magenta for T130K. WT-neomycin structure (green) is used in the superimposition to locate the ligand binding site. The solvent molecules coming from the T130K Apo structure are shown as magenta spheres while the solvent molecules coming from the D80Y Apo structure are shown as cyan spheres.

Table 2.7: Solvent accessible area (SAA) calculations of ANT structures

Structure	Molecular Surface Area (MSA)	Solvent Accessible Area (SAA)	SAA/MSA
WT Apo	52291.910	21964.994	0.42
T130K Apo	52374.090	21546.854	0.41
D80Y Apo	52682.633	22356.020	0.42
WT-Neomycin	54829.062	27746.559	0.51
T130K-Neomycin	55303.707	27884.092	0.50

MSA and SAA were calculated using PyMOL. The units are $Å^2$. WT, T130K and D80Y are all similar to each other in terms of solvent accessible area considering the entire protein structure both in apo and in the ligand bound forms.

apo ANT variants and increases to around 0.5 for all ligand bound forms of ANT variants since the ligand is also solvated (Table 2.7). This indicates that WT, T130K and D80Y are all similar to each other in terms of solvent accessible area considering the entire protein structure (Table 2.7). However, arrangement of water molecules in the ligand binding sites indicates that WT and T130K are highly similar to each other and significantly different from D80Y (Figures 2.15 and 2.16). Thus, crystal structures of ANT variants are consistent with differences in solvent effects observed in thermodynamics of ligand binding. Even though T130K shows thermostability, thermodynamics of ligand binding and solvent effects mirror that of WT. Thus, T130K may simply be a more heat stable variant of WT but does not carry thermophilic properties. These data are consistent with MD simulations that also highlighted differences in protein dynamics and its temperature dependence between D80Y and WT/T130K pair *(9)*.

We note that these data should not be interpreted as temperature dependence of Δ*Cp* as a unique property of thermophilic proteins. Such temperature dependence has been observed with DNA-ligand interactions *(26)*. The observed temperature dependence of Δ*Cp* for D80Y-aminoglycoside interactions suggests that two linked processes with different temperature dependence and negative Δ*Cp* values are involved. This was not observed with WT and T130K.

2.6 Conclusions

In this work, we showed that two thermostable variants of ANT, each with a single site mutation, may provide clues to distinguish thermophilic proteins from variants that have simply become thermostable by an additional stabilizing interaction such as addition of a disulfide bond or an ionic interaction but otherwise identical to mesophilic WT. Both T130 and D80 are away from the subunit-subunit interface and accessible to solvent *(27)*. Figure 2.17 shows a close-up view of the location of both residues. It is likely that substitution of lysine at 130 may allow an ionic interaction between this residue and Asp 127 or Glu130 or backbone oxygen of Ser90 that is in the proximity of T130 and increase the thermostability of this variant without affecting other properties significantly. D80Y,

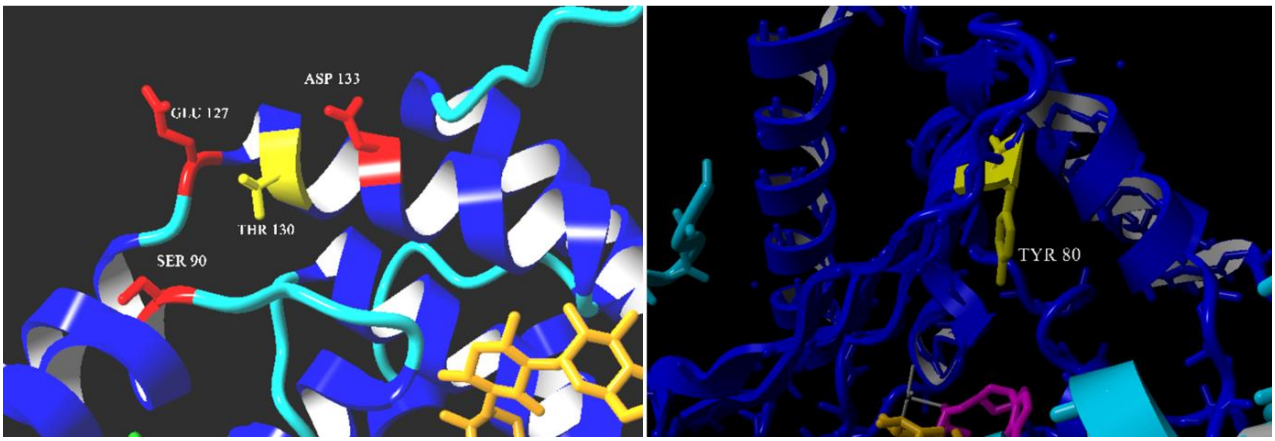

Figure 2.17: Close-up of protein structure around residues 130 and 80. Residues around 130 (left panel) and 80 (right panel) shown using the crystal structure of D80Y *(27)*.

on the other hand, doesn't appear to be positioned to engage in such a bond formation interaction. However, replacement of an ionic side chain with Tyr may potentially increase hydrophobic interactions leading to achieve thermostability. Thus, Y80 may be a node impacting protein dynamics and its interactions with solvent and ligands leading to thermophilic behavior.

Protein function in thermophilic environment may require more than just an increased Tm such as different protein dynamics and/or solvent-protein interactions or interactions with other molecules and ligands as such. Our earlier work showed significant differences in dynamic properties of apo-enzymes that separated D80Y from WT and T130K *(9)*. This work shows that thermodynamics of enzyme-ligand interactions also provide features that separates two thermostable variants from each other. We should note that the additivity of melting temperatures of T130K and D80Y as observed in the double mutant also suggests different mechanisms of achieving thermostability for these two variants *(9)*. Since thermodynamics of enzyme-ligand interactions of T130K is identical to WT, we believe that its Tm is increased by interactions of 130K with one of the candidate sites as described earlier without affecting other molecular properties of the WT. D80Y, on the other hand, have significantly different thermodynamics (and higher Tm than T130K), and therefore denoted as "thermophilic". There are currently accepted properties that are associated with thermophilic proteins such as deletion of loops at the surface, increased fraction of aliphatic hydrophobic side chains as well as charged residues and increased polar interactions *(3, 28)*. We note that replacement of D80 with Y is also against the current paradigm of thermophilic proteins having more polar interactions because an ionic side chain is replaced by a phenolic one. Thus, it appears that determinants of thermophilicity are broader and may not be easily determined by sequence of structural comparisons. General applicability of these results to other systems in one or another thermodynamic parameter of protein-ligand interactions remains to be seen.

2.7 References

1. Xiao, L.; Honig, B., Electrostatic contributions to the stability of hyperthermophilic proteins. *Journal of Molecular Biology* **1999,** *289* (5), 1435-1444.
2. Vinther, J. M.; Kristensen, S. M.; Led, J. J., Enhanced stability of a protein with increasing temperature. *Journal of the American Chemical Society* **2011,** *133* (2), 271-278.
3. Kumar, S.; Nussinov, R., How do thermophilic proteins deal with heat? *Cellular and Molecular Life Sciences* **2001,** *58* (9), 1216-1233.
4. Elcock, A. H., The stability of salt bridges at high temperatures: Implications for hyperthermophilic proteins. *Journal of Molecular Biology* **1998,** *284* (2), 489-502.
5. Stickle, D. F.; Presta, L. G.; Dill, K. A.; Rose, G. D., Hydrogen bonding in globular proteins. *Journal of Molecular Biology* **1992,** *226* (4), 1143-1159.
6. Gromiha, M. M.; Pathak, M. C.; Saraboji, K.; Ortlund, E. A.; Gaucher, E. A., Hydrophobic environment is a key factor for the stability of thermophilic proteins. *Proteins: Structure, Function and Bioinformatics* **2013,** *81* (4), 715-721.
7. Hollien, J.; Marqusee, S., Structural distribution of stability in a thermophilic enzyme. *Proceedings of the National Academy of Sciences USA* **1999,** *96* (24), 13674-13678.
8. Meinhold, L.; Clement, D.; Tehei, M.; Daniel, R.; Finney, J. L.; Smith, J. C., Protein dynamics and stability: The distribution of atomic fluctuations in thermophilic and mesophilic dihydrofolate reductase derived using elastic incoherent neutron scattering. *Biophysical Journal* **2008,** *94* (12), 4812-4818.
9. Jing, X.; Falcon, W. E.; Baudry, J.; Serpersu, E. H., Thermophilic enzyme or mesophilic enzyme with enhanced thermostability: can we draw a line? *The Journal of Physical Chemistry B* **2017,** *121* (29), 7086-7094.
10. Norris, A. L.; Ozen, C.; Serpersu, E. H., Thermodynamics and kinetics of association of antibiotics with the aminoglycoside acetyltransferase (3)-IIIb, a resistance causing enzyme. *Biochemistry* **2010,** *49* (19), 4027-4035.
11. Matsumura, M.; Katakura, Y.; Imanaka, T.; Aiba, S., Enzymatic and nucleotide sequence studies of a kanamycin inactivating enzyme encoded by a plasmid from

Thermophilic Bacilli in comparison with that encoded by plasmid PUB110. *Journal of Bacteriology* **1984,** *160* (1), 413-420.

12. Liao, H. H., Thermostable mutants of kanamycin nucleotidyltransferase are also more stable to proteinase K, urea, detergents and water miscible organic solvents. *Enzyme and Microbial Technology* **1993,** *15* (4), 286-292.

13. Jing, X. M.; Wright, E.; Bible, A. N.; Peterson, C. B.; Alexandre, G.; Bruce, B. D.; Serpersu, E. H., Thermodynamic characterization of a thermostable antibiotic resistance enzyme, the aminoglycoside nucleotidyitransferase (4'). *Biochemistry* **2012,** *51* (45), 9147-9155.

14. Jing, X. M.; Serpersu, E. H., Solvent reorganization plays a temperature dependent role in antibiotic selection by a thermostable aminoglycoside Nucleotidyltransferase-4'. *Biochemistry* **2014,** *53* (34), 5544-5550.

15. Jing, X. M.; Wright, E.; Bible, A. N.; Peterson, C. B.; Alexandre, G.; Bruce, B. D.; Serpersu, E. H., Thermodynamic characterization of a thermostable antibiotic resistance enzyme, the aminoglycoside nucleotidyltransferase (4') (vol 51, pg 9147, 2012). *Biochemistry* **2015,** *54* (32), 5120-5120.

16. Schuck, P., On the analysis of protein self association by sedimentation velocity analytical ultracentrifugation. *Analytical Biochemistry* **2003,** *320* (1), 104-124.

17. Laue, T. M.; Shah, B. D.; Ridgeway, T. M.; Pelletier, S. L., Analytical Ultracentrifugation in Biochemistry and Polymer Science. Harding, S. E., Rowe, A. J., and Horton, J. C., Ed. Royal Society of Chemistry: Cambridge, UK, 1992; pp 90-125.

18. Schuck, P., Size-distribution analysis of macromolecules by sedimentation velocity ultracentrifugation and Lamm equation modeling. *Biophysical Journal* **2000,** *78* (3), 1606-1619.

19. Spolar, R. S.; Record, M. T., Coupling of local folding to site-specific binding of proteins to DNA. *Science* **1994,** *263* (5148), 777-784.

20. Chervenak, M. C.; Toone, E. J., A Direct measure of the contribution of solvent reorganization to the enthalpy of ligand-binding. *Journal of the American Chemical Society* **1994,** *116* (23), 10533-10539.

21. Kumar, P.; Serpersu, E. H., Thermodynamics of an aminoglycoside modifying enzyme with low substrate promiscuity: The aminoglycoside N3 acetyltransferase-VIa. *Proteins: Structure, Function and Bioinformatics* **2017,** *85* (7), 1258-1265.

22. Serpersu, E. H.; Norris, A. L., Effect of protein dynamics and solvent in ligand recognition by promiscuous aminoglycoside modifying enzymes. *Advances in Carbohydrate Chemistry and Biochemistry, Vol 67*, 2012; Vol. 67, pp 221-248.

23. Kresheck, G. C.; Schneider, H.; Scheraga, H. A., Effect of D_2O on thermal stability of proteins. Thermodynamic parameters for transfer of model compounds from H_2O to D_2O. The *Journal of Physical Chemistry* **1965,** *69* (9), 3132-3144.

24. Lopez, M. M.; Makhatadze, G. I., Solvent isotope effect on thermodynamics of hydration. *Biophysical Chemistry* **1998,** *74* (2), 117-125.

25. Sturtevant, J. M., Heat capacity and entropy changes in processes involving proteins. *Proceedings of the National Academy of Sciences USA* **1977,** *74* (6), 2236-2240.

26. Liu, C. C.; Richard, A. J.; Datta, K.; LiCata, V. J., Prevalence of temperature-dependent heat capacity changes in protein-DNA interactions. *Biophysical Journal* **2008,** *94* (8), 3258-3265.

27. Pedersen, L. C.; Benning, M. M.; Holden, H. M., Structural investigation of the antibiotic and ATP-binding sites in kanamycin nucleotidyltransferase. *Biochemistry* **1995,** *34* (41), 13305-13311.

28. Szilagyi, A.; Zavodszky, P., Structural differences between mesophilic, moderately thermophilic and extremely thermophilic protein subunits: results of a comprehensive survey. *Structure* **2000,** *8* (5), 493-504.

3 STRUCTURAL STUDIES OF AMINOGLYCOSIDE *O*-NUCLEOTIDYLTRANSFERASE(4') VARIANTS ON THERMOSTABILITY AND THE IDENTIFICATION OF THE ACTIVE SITE RESIDUES

3.1 Abstract

The aminoglycoside nucleotidyltransferase (4') (ANT) variants do not show a difference in their global structure. Our structures have shown that the neomycin molecules are positioned the same way in the neomycin bound forms of both the T130K and the WT, which is in line with our previous observation that T130K resembles the WT in terms of ligand binding thermodynamics. T130K has an additional H-bond formed between the side chain of Lys 130 and the backbone oxygen of Ser 90, which suggests that T130K has achieved thermostability through the formation of an additional stabilizing interaction. Even though D80Y has the highest melting temperature (Tm), an additional stabilizing interaction did not seem likely to occur when we investigated the D80Y mutation site in apo D80Y structure, since Tyr 80 was too far away from the neighboring residues. Our previous studies had shown that D80Y is more dynamic than the T130K and WT. It is possible that, even though we were not able to observe additional interactions in D80Y by analyzing the crystal structure, these interactions are likely to occur in solution due to the dynamic nature of the D80Y. These observations further strengthen our statement that T130K is the thermostable variant due to an additional chemical interaction but otherwise mimics the behaviors of the WT, while D80Y displays thermophilic enzyme properties and uses different strategies from the T130K by establishing the Tyr 80 as a node in protein dynamics to confer thermal adaptation. Our structural work has also enabled us to identify Glu 145, Asp 50, Glu 52 and Glu 76, which are away from the T130K and D80Y mutation sites, as candidates for catalytic residues.

3.2 Introduction

Comparisons of the thermophilic and mesophilic enzyme homologues have shown that disulfide bridges, aromatic and hydrophobic interactions, hydrogen (H-) bonds and ion pairs can be seen more in thermophilic enzymes *(1-3)*. As explained in greater detail in Chapter 1 of this thesis, creation of a single additional hydrophobic interaction, ion pair, aromatic pair or anion pi interaction can increase the protein stability in a range of 1.3-9.5

kcal/mol *(4-9)*. Thus, these interactions are believed to result in the thermostability of the thermophilic enzymes by creating a more stable protein structure. In Chapter 2 of this thesis, we have shown that the T130K variant of the aminoglycoside nucleotidyltransferase (4') (ANT) resembles the WT in terms of ligand binding and enzyme dynamics, while the D80Y variant, which has the highest Tm, behaved very differently from them. These findings led us to further distinguish T130K from D80Y and claim D80Y as the variant with the thermophilic enzyme properties, while we referred to T130K as just a more thermostable version of the WT since it was mimicking the WT. In this chapter, we analyzed the X-ray crystal structures of ANT variants, which were obtained by us and our collaborators, to investigate if the thermophilic character of D80Y and the increased structural stability of T130K compared to WT could be explained due to the possible differences in their structures.

Before we obtained the X-ray crystal structures of ANT variants, only a 2.5 Å resolution structure of the D80Y variant in complex with the nonhydrolyzable ATP analogue (AMPCCPP) and kanamycin was available (PDB ID: 1KNY) *(10)*. We have obtained the apo form of all ANT variants as well as the ligand bound forms of WT and T130K at a resolution range of 1.65-2.5 Å. Our structures highly resemble the 1KNY structure (Figure 3.1). The root mean square deviation (RMSD) between the 1KNY (when depleted of its ligands) with apo T130K is 0.529 Å.

Investigating our ANT structures has enabled us to study the thermostability and the catalysis of ANT variants. ANT transfers an AMP group from Mg-ATP to the 4’-OH group of the aminoglycosides. ANT utilizes a Bi–Bi kinetic mechanism, in which aminoglycoside binds to the ANT before the Mg-ATP and adenylated neomycin is released the last *(11)*. We were able to obtain the apo, neomycin bound, neomycin and AMPCPP bound, as well as the product state (adenylated neomycin) structures of T130K, which enabled us to identify the residues in the active site of ANT (some of which perform catalysis) and their relation to T130K and D80Y mutations.

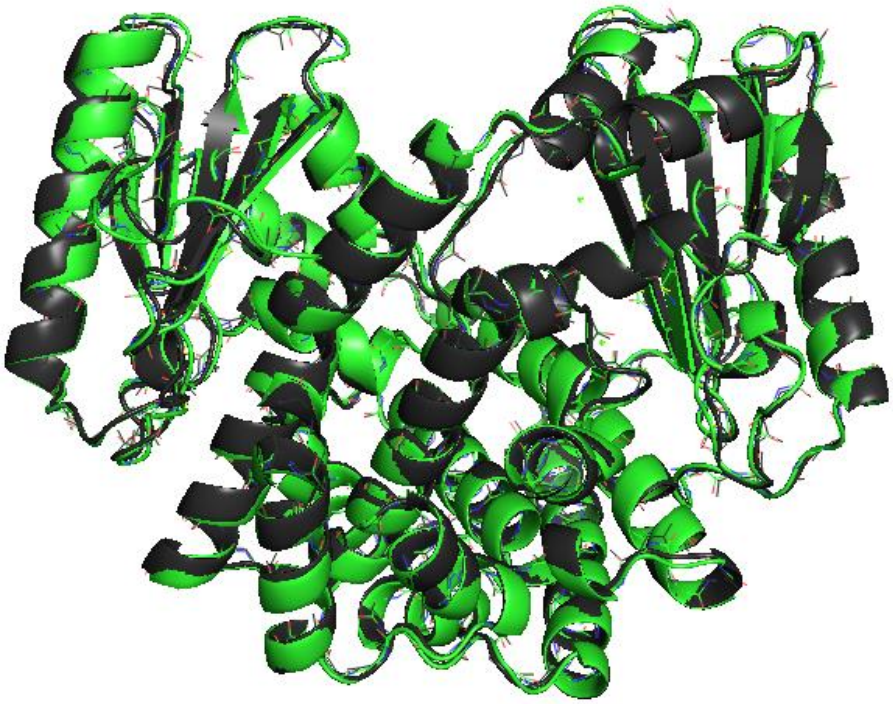

Figure 3.1: Our crystal structures are very similar with the previous ANT structure in the literature. Superimposition of apo T130K (green) with the previous ANT structure in literature (PDB ID: 1KNY) (black) *(10)*. The root mean square deviation (RMSD) between the 1KNY (when depleted of its ligands as shown in this figure) with apo T130K is 0.529 Å.

3.3 Materials and methods

All ANT variants mentioned in this chapter were purified as explained in Chapter 2. All the ANT crystals mentioned in this study were grown in hanging drop vapor diffusion method at 12 °C, using droplets containing 1:1 ratio of protein solution and mother liquor. The concentration of the ANT variants used for crystallization were 15 mg/ml. The crystallization conditions were: 16-18% PEG 8K, 0.1 M Tris pH 7.5-8.0, 0.1-0.2 M $MgCl_2$ for the apo ANT variants. Binary crystals were obtained by incubating the enzyme with 2-3 mM neomycin for 2 h at room temperature and then mixing with an equal amount of mother liquor. More detailed explanation of the methodology along with crystallography statistics can be found in Chapter 4 of this thesis.

3.4 Results

3.4.1 All three ANT variants have very similar structures

All three variants of ANT: WT, T130K and D80Y return an RMSD value of 0.4 Å when they are superimposed in their apo forms, indicating that there are no global structural differences among these variants (Figure 3.2). In the neomycin bound forms of WT and T130K, neomycin molecules are also oriented the same amongst the structures (Figure 3.3).

3.4.2 Structural investigation of thermostability on ANT variants

The distance between the side chain of Lys 130 and the backbone oxygen of Ser 90 in the T130K structure is only 2.6 Å, indicating that in the T130K structure, there is an additional H-bond created (Figure 3.4). Creation of such an additional H-bond is not likely to occur in the WT or the D80Y, since these variants have a Thr 130 whose hydroxyl group on its side chain is 5.5 Å away from the backbone oxygen of Ser 90. This makes it unlikely for them to engage in a H-bond since the maximum distance between the atoms

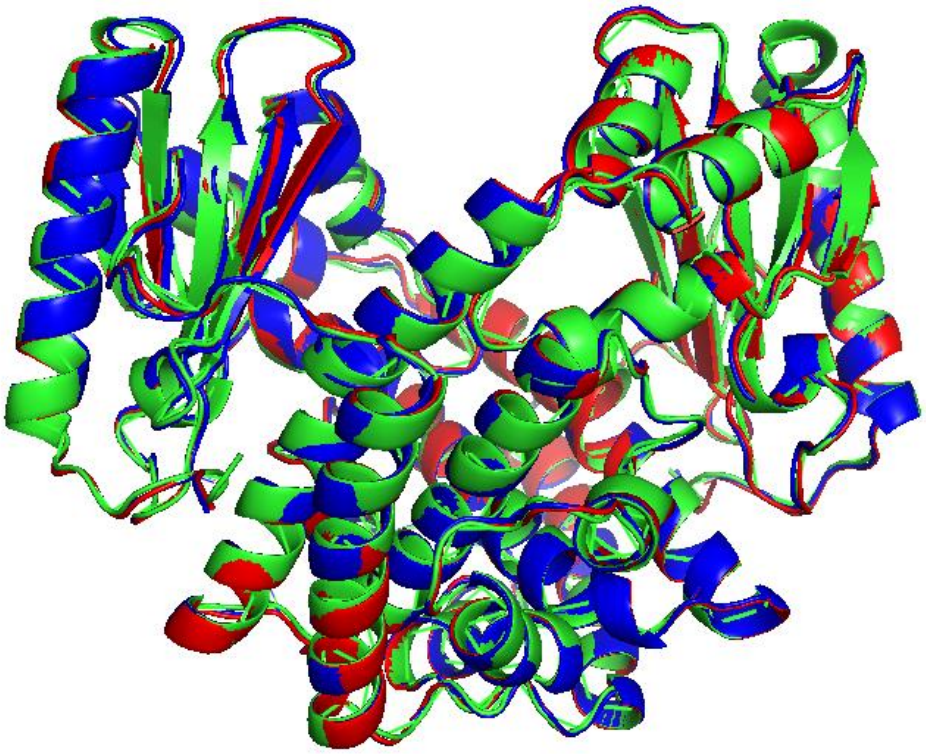

Figure 3.2: There are no global structural differences amongst the ANT variants. Superimposition of WT (blue), T130K (green) and D80Y (red) is 0.4 Å, indicating that there are not any global structural differences amongst the ANT variants.

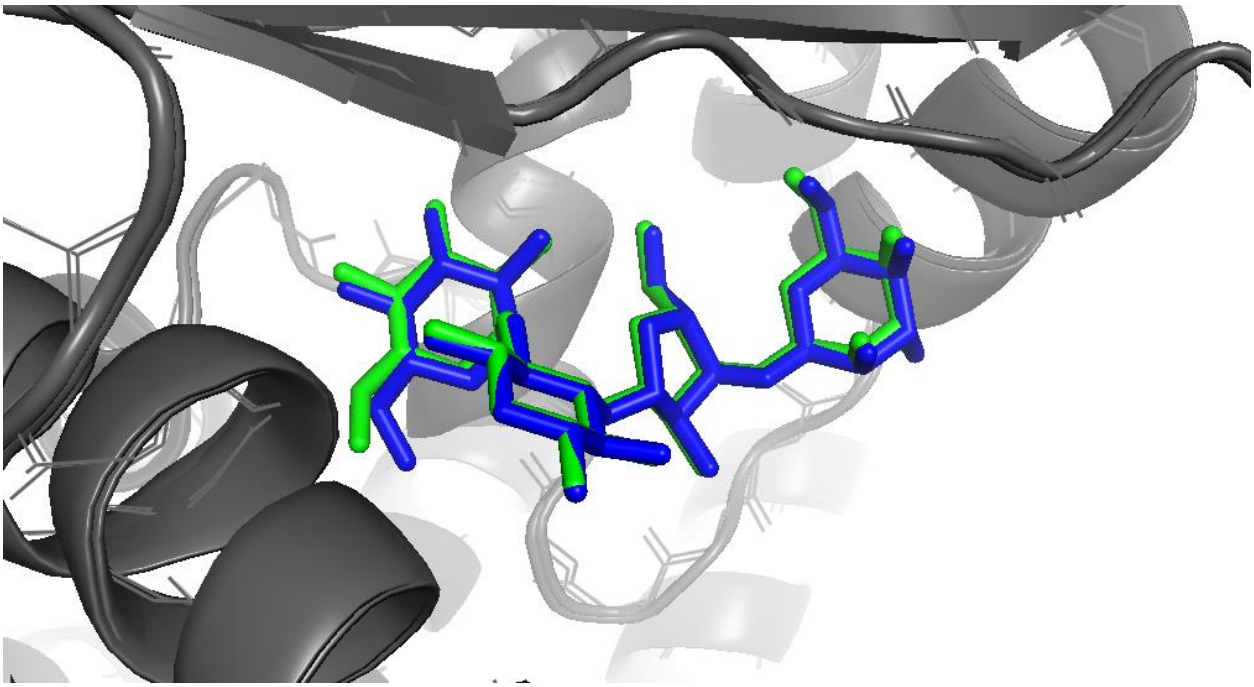

Figure 3.3: Both T130K and D80Y bind to neomycin in the same structural manner. Neomycin molecules are positioned the same way in the neomycin bound forms of both the T130K and the WT. Neomycin in the WT structure is shown in blue, while the neomycin in the T130K structure is shown in green. Neomycin bound forms of T130K and WT are superimposed and the enzymes are shown in gray in order to see the neomycin molecules more clearly.

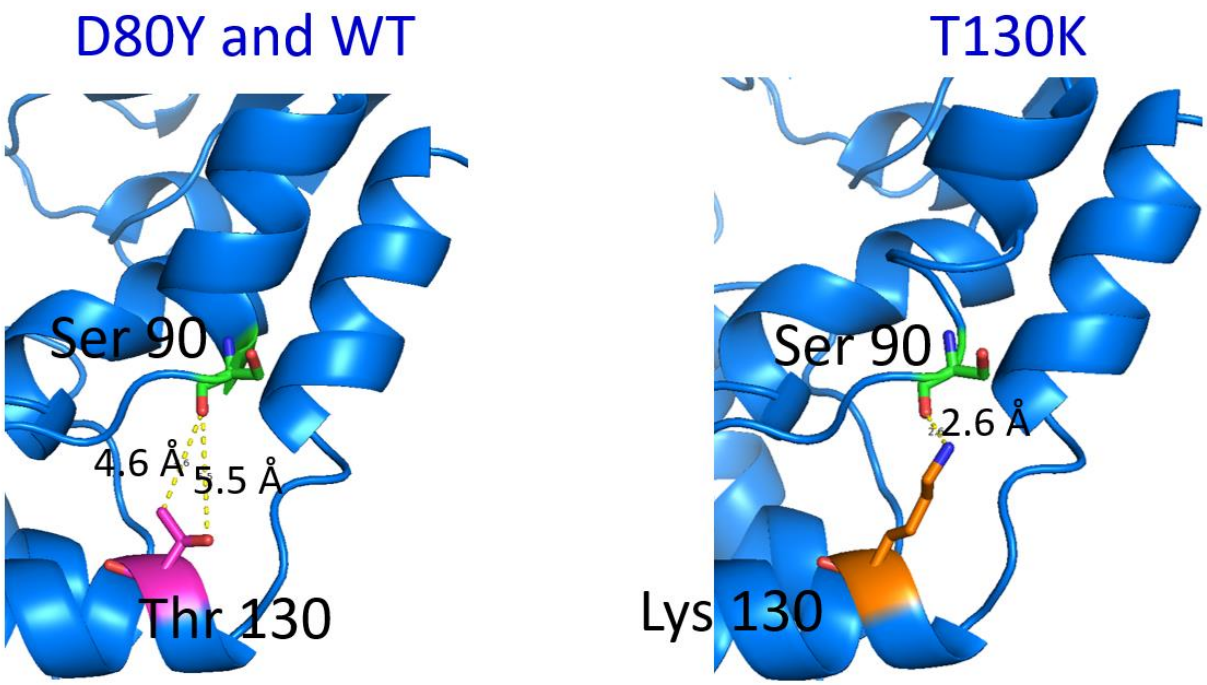

Figure 3.4: T130K achieved thermostability through the formation of an additional H-bond. The distance between the side chain of Lys 130 (orange) and the backbone oxygen of Ser 90 (green) in the T130K structure is only 2.6 Å, indicating that in the T130K structure, there is an additional H-bond created between these residues. Creation of such an additional H-bond is not likely to occur in the WT or the D80Y, since these variants have a Thr 130 (pink) whose hydroxyl group on its side chain is 5.5 Å away from the backbone oxygen of Ser 90, which makes it unlikely for them to engage in a H-bond. On the residues, oxygen atoms are shown in red and nitrogen atoms are shown in dark blue. Protein structures are shown in blue.

to create a H-bond is around 3.3 Å *(12)*. This observation shows that T130K achieved thermostability through the formation of a stabilizing interaction.

We also studied the structure of D80Y to see if there are any additional interactions that might explain its increased Tm. Tyr 80 is surrounded by residues like Tyr, Gln and Asn, which can in theory create chemical bonds like H-bonds or aromatic pair interactions with a tyrosine via their side chain. However, these residues are too far away from Tyr 80, which makes it very unlikely for them to create an additional bond within the D80Y mutation site (Figure 3.5). In T130K and WT, there is an Asp 80 instead of Tyr 80, which also does not seem to create a noncovalent bond with its surrounding residues, indicating that D80Y mutation does not abolish any previous interactions within the protein.

3.4.3 Identification of the residues in the ANT active site

Obtaining apo, neomycin bound, neomycin and AMPCPP bound and the product state (adenylated neomycin) forms of T130K enabled us to identify the residues in the ANT active site. We identified Glu 145, Asp 50, Glu 52 and Glu 76 as the residues which are in close proximity of the 4'-OH modification site of neomycin and the α-phosphate on the AMPCPP, which make them the likeliest candidates to perform catalysis. ANT is a homodimer enzyme. In the active site, Glu 145 is found on another subunit than the Asp 50, Glu 52 and Glu 76 (Figure 3.6). When we examined Glu 145, Asp 50, Glu 52 and Glu 76 on the apo forms of D80Y, WT and ANT, we saw that folding of all ANT variants around the active site is also the same (Figure 3.7).

3.5 Discussion

Apo forms of all three ANT variants share the same global structure, indicating that the T130K and D80Y mutations are not causing any changes in the global fold of the protein (Figure 3.1) that might affect their different degrees of thermostability. We were also able to obtain the neomycin bound forms of WT and T130K. Even though we also tried to obtain the neomycin bound form of D80Y, we were not successful. As explained in greater

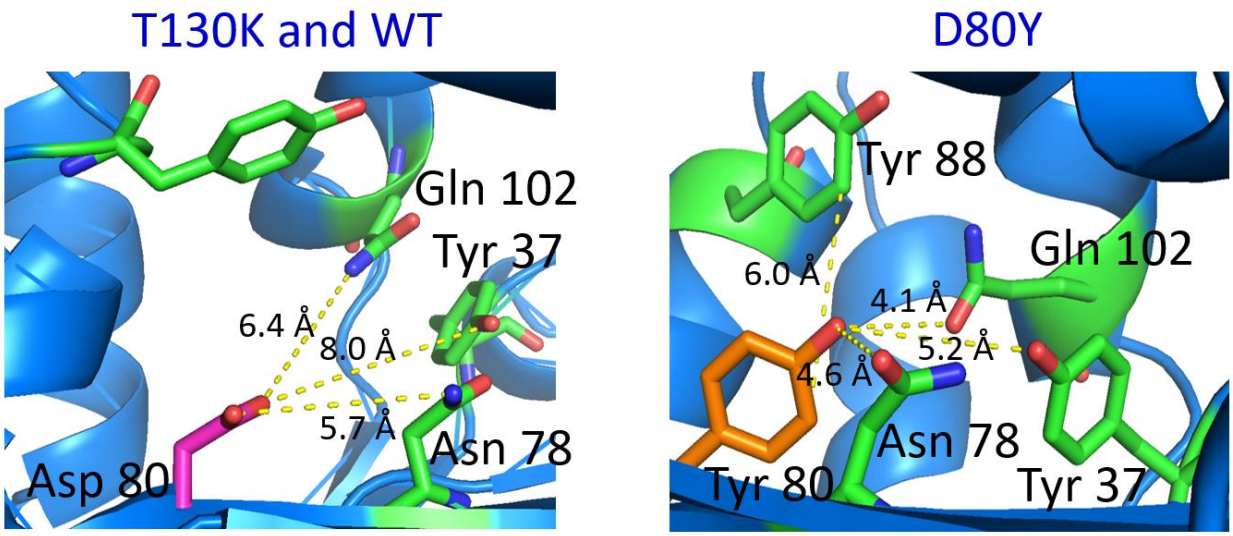

Figure 3.5: There are no obvious additional interactions in D80Y. Tyr 88, Gln 102, Tyr 37 and Asn 78 all shown in green are too far away from Tyr 80 (orange) to create an additional bond within D80Y. In T130K and WT, there is an Asp 80 (pink) instead of Tyr 80 which also does not seem to create a noncovalent bond with its surrounding residues, indicating that D80Y mutation does not abolish any previous interactions within the protein. On the residues, oxygen atoms are shown in red and nitrogen atoms are shown in dark blue. Protein structures are shown in blue.

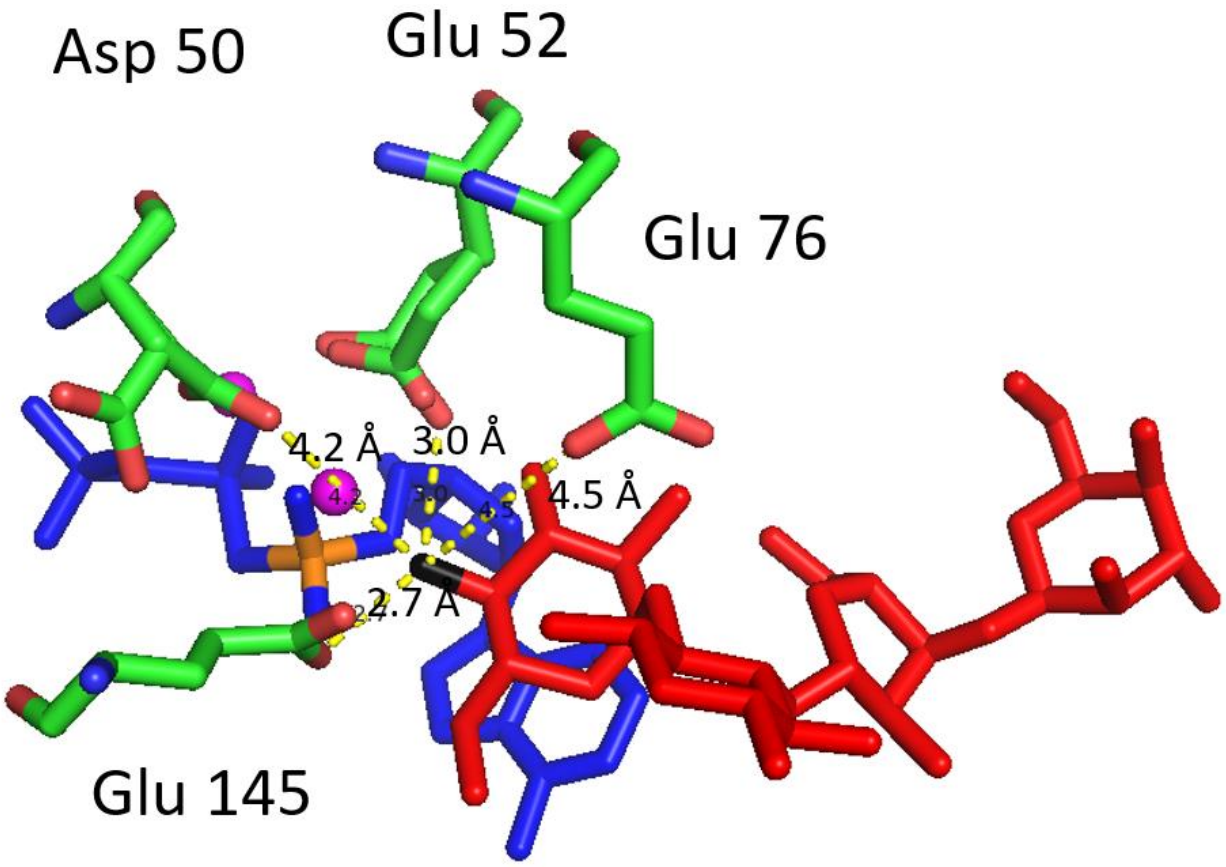

Figure 3.6: Identification of the residues found in the ANT active site. Glu 145, Asp 50, Glu 52 and Glu 76 are found in the active site of ANT and are the most likely candidates to perform catalysis. This image is prepared using the structure of T130K (green) bound to AMPCPP (dark blue) and neomycin (dark red). The distances of the side chains of the residues from the neomycin modification site (black) are shown. The distances of the side chains of the residues Glu 76, Glu 52, Glu 50 and Glu 145 from the α-phosphate (orange) are 7.5 Å, 3.8 Å, 5.0 Å and 4.1 Å, respectively. Glu 145 is found on a different subunit than the Asp 50, Glu 52 and Glu 76 in the dimeric T130K structure. On the residues, oxygen atoms are shown in red and nitrogen atoms shown in dark blue. Mg ions are shown in magenta as spheres.

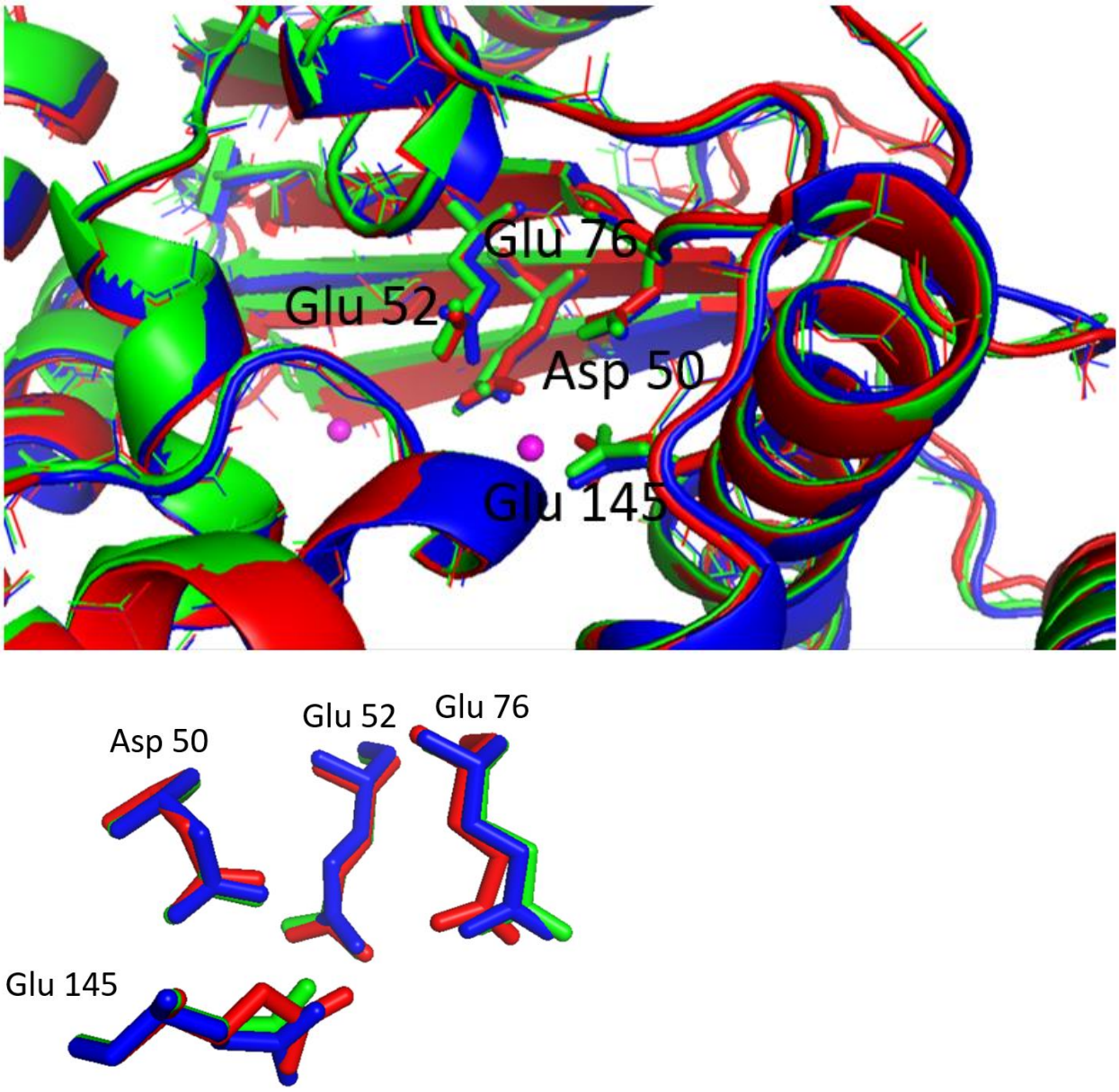

Figure 3.7: Folds of the ANT variants are also the same around the active site. Apo forms of WT (blue), T130K (green) and D80Y (red) superimposed. Folds of these proteins are the same around the active site residues. Mg ions are shown in magenta as spheres. Bottom panel shows the close-up view of just the residues whose side chains are also in very similar orientations.

detail in Chapter 2, when we superimposed the neomycin bound structures of WT or T130K with apo D80Y, we saw that in D80Y, Tyr 80 seems to be involved in a steric clash with neomycin, which might explain why we were not able to obtain a neomycin bound D80Y structure. Neomycin molecules are positioned the same way in the neomycin bound forms of both the T130K and the WT. This shows that in addition to T130K resembling the WT in terms of ligand binding thermodynamics *(13)*, these two variants also bind to neomycin in the same structural manner.

Since we did not observe any global structural differences amongst the ANT variants, we investigated if there are any local structural differences in the T130K and D80Y mutation sites that can explain their increased Tm. T130K has an additional H-bond formed between the side chain of Lys 130 and the backbone oxygen of Ser 90, which suggests that T130K has achieved thermostability through the formation of a stabilizing interaction. This H-bond seemed like it can potentially act as a hairpin bringing the alpha helices shown in Figure 3.4 together and thereby creating additional interactions that can further explain the increased Tm of T130K. However, when we compared these alpha helices in the T130K structure to that of the other two ANT variants, we did not see any obvious additional interactions. In this case, it seems like just one additional H-bond formation was responsible for the increased Tm of the T130K. However, one should keep in mind that X-ray structures are just a static image of the protein, where in reality proteins are dynamic and sample multiple conformations. Thus, it is possible that in some conformations of T130K, the H-bond formed between the side chain of Lys 130 and the backbone oxygen of Ser 90 can in fact be acting as a hairpin to create further additional interactions amongst the mentioned alpha helices.

Even though D80Y has the highest melting temperature (Tm), an additional stabilizing interaction did not seem likely to occur when we investigated the D80Y mutation site, since Tyr 80 was too far away from the neighboring residues (Figure 3.5). Our previous studies had shown that D80Y is more dynamic than the T130K and WT *(14)*. It is possible that, even though we were not able to observe additional interactions in D80Y mutation site by analyzing the crystal structure, these interactions are likely to occur in solution due

to the dynamic nature of the D80Y. These observations further strengthen our statement that, T130K is the thermostable variant due to an additional chemical interaction, but otherwise mimics the behaviors of the WT, while D80Y displays thermophilic enzyme properties and uses different strategies from the T130K by establishing Tyr 80 as a node in protein dynamics to confer thermal adaptation. Our studies have shown that, rather than the local structural differences in the D80Y mutation sites, the differences in its global features, such as dynamics and ligand binding thermodynamics, manifest the thermophilic behavior of D80Y *(13, 14)*. Global features of proteins conferring thermostability rather than the specific stabilizing structural interactions have also been observed in other systems *(15)*.

Obtaining apo, neomycin bound, neomycin and AMPCPP bound and the product state (adenylated neomycin) forms of T130K enabled us to identify the residues in the ANT active site. We identified Glu 145, Asp 50, Glu 52 and Glu 76 as the residues which are in the close proximity of the 4'-OH modification site of neomycin and the α-phosphate on the AMPCPP, which make them the likeliest candidates to perform catalysis (Figure 3.6). In fact, an earlier kinetics study, which also utilized the 1KNY structure, had stated that Glu145 contributes to catalysis by abstracting a proton from the 4'-OH modification site of neomycin via its carboxylic group on its side chain *(11)*. Glu 145 happens to be on a different subunit compared to the others in our ANT structures. Observing mostly acidic residues in the active sites of aminoglycoside modifying enzymes (AGMEs) is common *(16)*. Even though the specific activities of the ANT variants were very similar at their own optimum temperatures, compared to WT, T130K and D80Y were more active at high temperatures (52 °C and 57°C), while they were less active at lower temperatures such as 37 °C *(17)*. D80Y was more active than the T130K at high temperatures. The protein fold of the apo ANT variants around the active site are the same (Figure 3.7), indicating that the differences in their activities cannot be explained due to structural differences in their active sites. This is not surprising because T130K and D80Y mutation sites are away from the active site (Figure 3.8), and thus are not likely to impose any direct structural changes on the active site. In that case, Tyr 80, acting as a node for protein dynamics in the D80Y, can also be responsible for facilitating its activity not through directly stabilizing

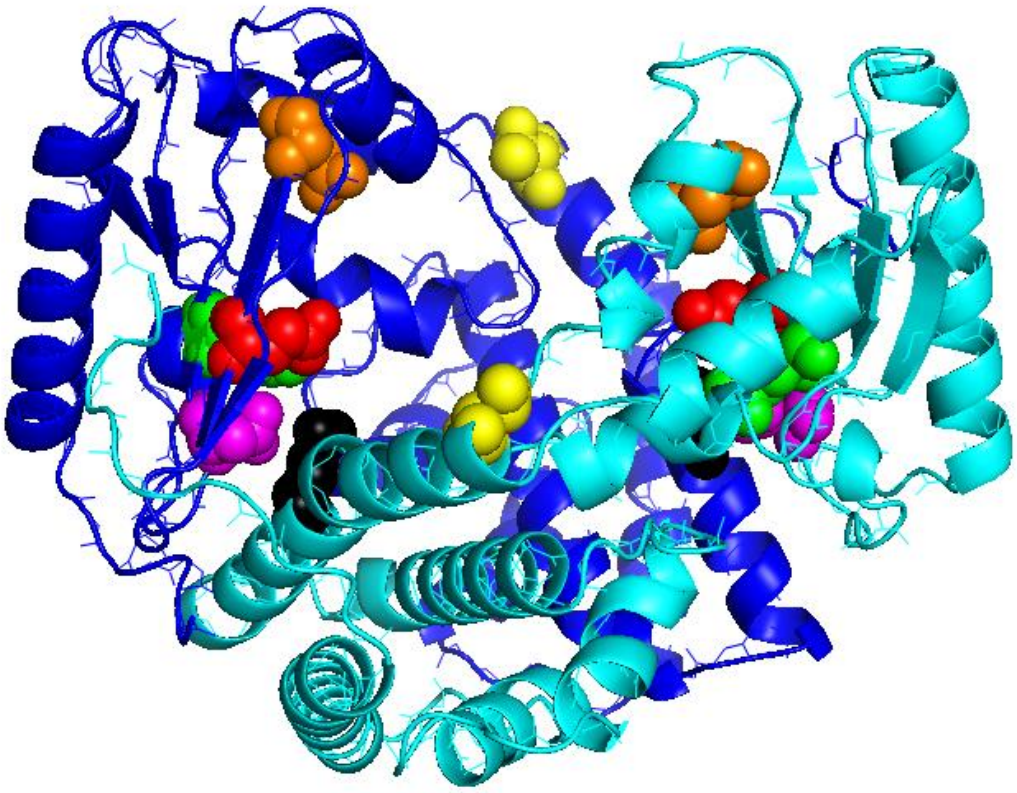

Figure 3.8: Active site residues highlighted on WT. Glu 76 (red), Glu 52 (green), Asp 50 (magenta) and Glu 145 (black) highlighted on the dimer WT apo protein whose subunits are shown in blue and cyan. Glu 145 is found on another subunit than the other active site residues. T130K mutation site (yellow), D80Y mutation site (orange) are both away from the active site residues.

structural interactions, but through global dynamics. Furthermore, the differences in ligand binding thermodynamics of D80Y compared to the other ANT variants can also play a role in its difference in catalytic activity. A detailed analysis as to which of these residues found in the active site (Glu 145, Asp 50, Glu 52 and Glu 76) actually perform the catalysis is explored in Chapter 4 of this thesis.

3.6 References

1. Elcock, A. H., The stability of salt bridges at high temperatures: implications for hyperthermophilic proteins. *Journal of Molecular Biology* **1998,** *284* (2), 489-502.
2. Gromiha, M. M.; Oobatake, M.; Sarai, A., Important amino acid properties for enhanced thermostability from mesophilic to thermophilic proteins. *Biophysical Chemistry* **1999,** *82* (1), 51-67.
3. Zhou, P.; Tian, F.; Lv, F.; Shang, Z., Geometric characteristics of hydrogen bonds involving sulfur atoms in proteins. *Proteins: Structure, Function, Bioinformatics* **2009,** *76* (1), 151-163.
4. Anderson, D. E.; Becktel, W. J.; Dahlquist, F. W., pH-induced denaturation of proteins: a single salt bridge contributes 3-5 kcal/mol to the free energy of folding of T4 lysozyme. *Biochemistry* **1990,** *29* (9), 2403-2408.
5. Kapoor, K.; Duff, M. R.; Upadhyay, A.; Bucci, J. C.; Saxton, A. M.; Hinde, R. J.; Howell, E. E.; Baudry, J., Highly dynamic anion–quadrupole networks in proteins. *Biochemistry* **2016,** *55* (43), 6056-6069.
6. Pace, C. N., Contribution of the hydrophobic effect to globular protein stability. *Journal of Molecular Biology* **1992,** *226* (1), 29-35.
7. Serrano, L.; Bycroft, M.; Fersht, A. R., Aromatic-aromatic interactions and protein stability: investigation by double mutant cycles. *Journal of Molecular Biology* **1991,** *218* (2), 465-475.
8. Shirley, B. A.; Stanssens, P.; Hahn, U.; Pace, C. N., Contribution of hydrogen bonding to the conformational stability of ribonuclease T1. *Biochemistry* **1992,** *31* (3), 725-732.
9. Zavodszky, M.; Chen, C. W.; Huang, J. K.; Zolkiewski, M.; Wen, L.; Krishnamoorthi, R., Disulfide bond effects on protein stability: Designed variants of Cucurbita maxima trypsin inhibitor-V. *Protein Science* **2001,** *10* (1), 149-160.
10. Pedersen, L. C.; Benning, M. M.; Holden, H. M., Structural investigation of the antibiotic and ATP-binding sites in kanamycin nucleotidyltransferase. *Biochemistry* **1995,** *34* (41), 13305-13311.

11. Chen-Goodspeed, M.; Vanhooke, J. L.; Holden, H. M.; Raushel, F. M., Kinetic mechanism of kanamycin nucleotidyltransferase from *Staphylococcus aureus*. *Bioorganic Chemistry* **1999,** *27* (5), 395-408.

12. McRee, D. E., *Practical protein crystallography*. Elsevier: 1999.

13. Kocaman, S.; Serpersu, E. H., The thermodynamics of ligand binding to the aminoglycoside O-nucleotidyltransferase(4') and variants yields clues about thermophilic properties. *Biochemistry* **2019,** *58* (12), 1579-1586.

14. Jing, X.; Evangelista Falcon, W.; Baudry, J.; Serpersu, E. H., Thermophilic enzyme or mesophilic enzyme with enhanced thermostability: can we draw a line? *The Journal of Physical Chemistry B* **2017,** *121* (29), 7086-7094.

15. Hollien, J.; Marqusee, S., Structural distribution of stability in a thermophilic enzyme. *Proceedings of the National Academy of Sciences* **1999,** *96* (24), 13674-13678.

16. Kaplan, E.; Guichou, J.F.; Chaloin, L.; Kunzelmann, S.; Leban, N.; Serpersu, E. H.; Lionne, C., Aminoglycoside binding and catalysis specificity of aminoglycoside 2 ″-phosphotransferase IVa: A thermodynamic, structural and kinetic study. *Biochimica et Biophysica Acta -General Subjects* **2016,** *1860* (4), 802-813.

17. Matsumura, M.; Aiba, S., Screening for thermostable mutant of kanamycin nucleotidyltransferase by the use of a transformation system for a thermophile, *Bacillus stearothermophilus*. *Journal of Biological Chemistry* **1985,** *260* (28), 15298-15303.

4 “CATCH AND RELEASE”: A NOVEL VARIATION OF THE ARCHETYPAL NUCLEOTIDYL TRANSFER REACTION

4.1 Abstract

Nucleotidyl transfer is an archetypal enzyme reaction central to DNA replication and repair, yet it is also used by antibiotic modifying enzymes to covalently inactivate antibiotics. The protein fold of the aminoglycoside nucleotidyl transferase 4' (ANT) shares significant structural similarity to the human DNA polymerase β catalytic domain, in addition to conservation of the arrangement of the canonical polymerase catalytic active site residues. Through structural characterization of ANT at various stages of the reaction coordinate, we show that although the underlying nucleotidyl transfer reaction mechanism is conserved with polymerases, a short low-barrier hydrogen bond is formed to facilitate tighter binding of the aminoglycoside substrate, which is then disrupted by the formation of the catalytically active complex. The need for ANT to release substrates post catalysis, rather than the requisite processivity of polymerases, leads to this novel variation of the nucleotidyl transfer reaction. These results shed important insights into this fundamental reaction mechanism, while revealing new strategies to combat antibiotic resistance.

4.2 Introduction

Nucleotide triphosphates (NTP) are ubiquitous enzyme substrates and cofactors in a myriad of biological processes. The most common enzyme mechanisms attack the gamma phosphate of the NTP, resulting in a nucleotide diphosphate and phosphate in phospho-transfer reactions, or attack the alpha phosphate resulting in a nucleotide monophosphate and pyrophosphate in nucleotidyl transfer reactions. The latter reaction is central to DNA/RNA synthesis and repair by polymerases, most of which have a conserved active site and catalytic mechanism despite some structural diversity among the family members *(1, 2)*. The reaction coordinate of nucleotidyl transfer in DNA polymerases has been studied in significant detail over many years now. These studies have demonstrated how polymerases use metal ions and active site carboxylate groups to deprotonate and activate a hydroxyl oxygen on the DNA primer terminus, which is subsequently followed by in-line attack of the α phosphate of the NTP, generating free pyrophosphate and a phosphodiester bond *(3-6)*. The catalytic metal is responsible for

lowering the pKa of the 3' OH primer terminus, whereas the second metal, the nucleotide binding metal, coordinates the pyrophosphate moiety of the nucleotide. These two metals are coordinated by three active site carboxylate groups (aspartic or glutamic acid) which are conserved among polymerases and proposed to serve as the catalytic base that receives the proton from the nucleotide primer terminus. Recent studies have also identified a third transient metal ion that plays a role in product release *(3, 4)*.

Antibiotic resistance enzymes, such as aminoglycoside modifying enzymes (AGMEs), have evolved to perform both phosphotransferase and nucleotidyl transfer reactions with the high energy bonds of NTPs to inactive antibiotics such as kanamycin and neomycin *(7)*. The adenylation or phosphorylation results in alteration of the requisite interactions between the antibiotics, and their target substrates, the bacterial ribosome *(8)*. The aminoglycoside nucleotidyl transferase 4' (ANT) is a promiscuous AGME that inactivates members from both of the two main structural classes of aminoglycoside antibiotics by transferring a nucleoside monophosphate group from ATP to the 4'-hydroxyl group of the antibiotic *(9-11)*. Based on initial studies, a two metal ion nucleotidyl transfer mechanism similar to polymerases was proposed as the structural homology between ANT and the catalytic domain of the human base-excision DNA repair polymerase, polymerase beta (Pol β), was identified *(12, 13)*. (Figure 4.1). Owing to the similarity of underlying nucleotidyl transfer reaction and structure with Pol β, the ANT active site carboxylate groups are arranged in a similar manner (Figure 4.1). Interestingly, in ANT Glu 76 coincides with the position of the Pol β catalytic base (Asp256), yet the homodimeric nature of ANT leads to the placement of an additional carboxylate group into the active site (Glu 145) from an adjacent monomer, and this residue had been initially proposed to be the catalytic base (Figure 4.1) *(9)*. However, in a mechanism suggested to encode substrate promiscuity in ANT, either Glu 76 or Glu 145 can act as the catalytic base *(14)*.

A complete understanding of the catalytic details of ANT is required to decipher the basis of antibiotic inactivation, as well as to aid in the design the next generation of aminoglycosides. Here, we determined the crystal structure of ANT in the binary

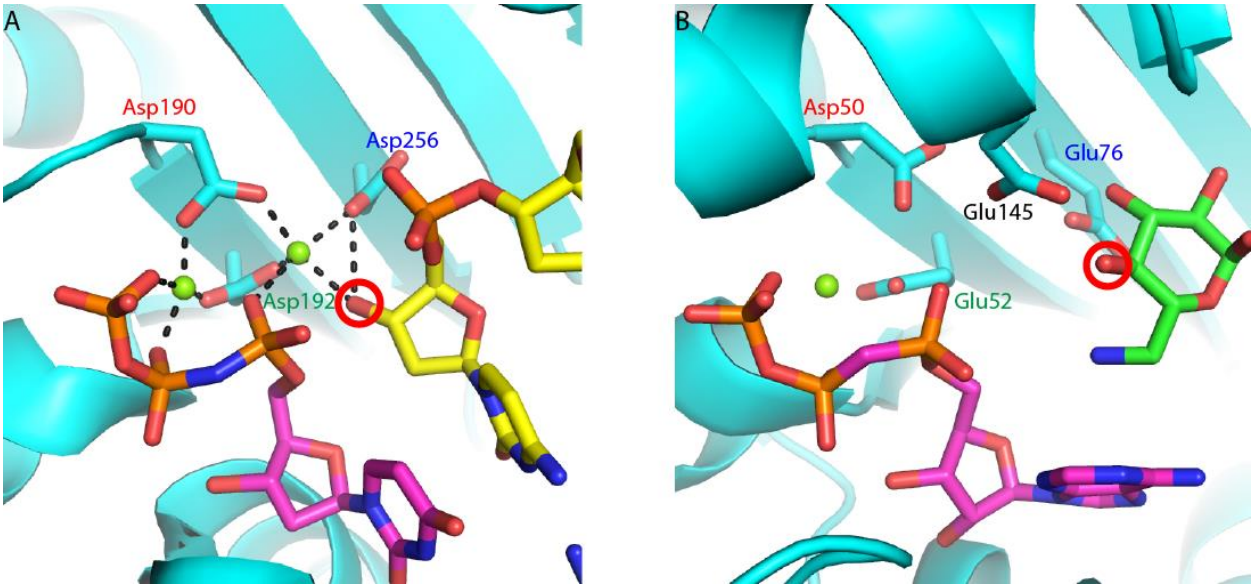

Figure 4.1: Conservation of nucleotidyl transfer active sites. A. Close-up view of the pol β ternary complex active site (PDB code 2FMS). B. Close-up view of the D80Y ANT 4' ternary complex active site (PDB code 1KNY). In Pol β the nucleotide binding metal is ligated with the β and γ phosphates of the NTP, as well as Asp 190 and Asp 192. The catalytic metal is coordinated by all three aspartate residues, including the catalytic base (Asp256) and the activated nucleophile hydroxyl from the carbohydrate moiety (Figure 4.1). In ANT Asp 50 and Glu 52 are homologous to Asp 190 and Asp 192 in Pol β. Conserved active site carboxylate groups of D80Y ANT 4' and pol β are shown and colored the same. The nucleophilic oxygen atom is circled. Hydrogen bonds in pol β are represented as black dashed lines.

(neomycin), ternary substrate (neomycin and AMPNP), and product complex (AMP-neomycin-pyrophosphate), thus permitting a complete picture of the reaction coordinate of this enzyme. Although the active site is essentially identical to a polymerase, novel adaptations are used in ANT-mediated antibiotic inactivation. Based on these structures and structures of an active site mutant, as well as enzyme kinetics and isothermal calorimetry (ITC) binding studies, we propose a novel nucleotidyl transfer mechanism in ANT. We show how modulation of a low barrier hydrogen bond (LBHB) *(15)* is used to achieve tight binding in the aminoglycoside bound state, while formation of the complete active complex results in disruption of the LBHB, thereby aiding in product release. The new insights into this reaction archetype not only lead to a better understanding of nucleotidyl transfer, but also sheds light on the strategies that can be used to evade the action of AGMEs.

4.3 Materials and methods

4.3.1 Protein expression and purification

All the ANT variants used in this study (WT, T130K and T130K/E52D) were cloned in a pGEX-4T-3 vector with a TEV (Tobacco Etch Virus) protease cleavage site at the C-terminus of the GST affinity tag. The proteins were expressed in BL21 RIL *E. coli* cells and grown in Terrific Broth media at 37 °C and transferred to 21 °C after induction with 1 mM IPTG. The cells were grown for 16 hours, harvested, resuspended in lysis buffer (1× PBS buffer, 1 mM DTT and 0.1% Triton) and lysed by sonication. The cell lysate was clarified with centrifugation and the supernatant was then incubated with Glutathione Sepharose 4B resin for 2-3 hours before being loaded into a column. The column was washed with wash buffer (1× PBS buffer, 1 mM DTT) before TEV protease was added. The protein-loaded GST resin was incubated with TEV protease for 16 hours at 4 °C. The cleaved protein was collected in the flow through and treated with the HiTrap Ni^{2+} chelating HP column to remove the TEV protease. The flow through was collected and dialyzed in 50 mM Tris pH 8.0, 100 mM NaCl and 5 mM EDTA to remove imidazole and any nucleotide contaminants. The dialyzed protein was further purified with a Superdex

75 10/300 column (GE healthcare Life Sciences) equilibrated in 50 mM Tris pH 8.0 and 100 mM NaCl. The purity of the enzymes was evaluated by SDS PAGE subsequent to being flash-frozen using liquid nitrogen and stored at -80 °C.

4.3.2 Crystallization and X-ray data collection

All the ANT crystals mentioned in the study were grown in hanging drop vapor diffusion method at 12 °C, using droplets containing 1:1 ratio of protein solution and mother liquor. WT, T130K and T130K/E52D enzymes were used at the concentration of 15 mg/ml in 50 mM Tris pH 8.0 and 100 mM NaCl buffer for crystallization. The crystals were cryoprotected using respective mother liquor with 30% glycerol prior to mounting and flash freezing in liquid nitrogen. Binary crystals were obtained by incubating the enzyme with 2-3 mM neomycin for 2 h at room temperature and mixed with an equal amount of precipitant (16-17% PEG 8K, 0.1 M Tris pH 7-8, 0.1-0.2 M $MgCl_2$). For the preparation of the non-hydrolyzable ternary complex crystals of ANT-Neo-AMPCPP, the enzyme (15 mg/ml in 50 mM Tris pH 8.0 and 100 mM NaCl buffer) was incubated with 2 mM neomycin and 4 mM AMPCPP for 2 hours at room temperature and mixed with the precipitant solution (12% PEG 8K, 0.1 M Tris pH 8.0, 0.1-0.2 M $MgCl_2$). For the ternary complex crystals of ANT-adenylated Neo-PP, the enzyme was dialyzed in 50 mM Tris pH 8.0 and 100 mM NaCl buffer containing 10 mM $CaCl_2$ before setting up crystallization trays. The Ca-dialyzed enzyme was then crystallized in 9-10% PEG 5K MME, 0.1 M Tris pH 7.5-8.0, 0.1-0.2 M $CaCl_2$. The crystals were transferred to a cryo-solution containing 9-10% PEG 5K MME, 0.1 M Tris pH 7.5-8.0, 10 mM $MgCl_2$ and 30% glycerol for 45 min. This resulted in the formation of ternary product complex with pyrophosphate. The reaction was stopped by freezing the crystals in liquid nitrogen prior to data collection. All the binary and ternary complex crystals were collected at 100K at different beamlines (23ID-D, 23ID-B, 21ID-F) at the Advanced Photon source (APS) using a Pilatus 3-6 M detector, Eiger 16M and Rayonix MX300 detectors, respectively. Diffraction data were processed with XDS *(22)* or HKL-3000 *(23)* or MOSFLM *(24)* and scaled with SCALA or AIMLESS from the CCP4 suite *(25)*. Space groups, cell parameters, and data collection statistics are shown.

4.3.3 Structure determination and refinement

The structures were solved by molecular replacement with PHASER *(26)* using PDB:1KNY as the template. Model building and refinement were carried out with COOT *(27)* and Phenix-Refine *(28)*. Model analysis was done with MolProbity *(29)* and figures were prepared with Pymol. Atomic coordinates and the structure factors for all complexes have been deposited in the Protein Data Bank (PDB) (Tables 4.1 and 4.2). Crystallographic refinement statistics are listed in Tables 4.1 and 4.2.

4.3.4 Enzyme kinetics

ANT enzymes (T130K, T130K/E52D) were checked for activity using the EnzCheck Pyrophosphate assay kit (Thermofisher Scientific). Clear polypropylene 96-well plates were used for the assays. The assay was performed in triplicates in a final volume of 100 µl in 50 mM Tris pH 8.0, 100 mM NaCl and 4 mM $MgCl_2$ buffer. The reaction was monitored for pyrophosphate production at 360 nm using a Spectramax® i3 Platform plate reader (Molecular Devices) using the Softmax Pro 6.4 software. 1 µM of enzyme and 10 µM of neomycin were used. The mixture was incubated with constant shaking for 10 min at 25°C and the reaction was initiated by adding ATP. ATP dependence was measured by varying its concentration from 0.5 µM to 5 mM. No-enzyme and no-ATP controls were performed. The reaction rates were typically calculated over the first 5 min and the data were accessed and plotted using OriginPro 2019. *Km* and *Vmax* were determined using the Michaelis-Menten equation.

4.3.5 Binding studies

All ITC experiments were performed at 25°C using the Microcal VP-ITC (Microcal Inc, USA) with cell volumes of 2 ml. All solutions were degassed prior to the experiments. 13-40 µM of ANT enzymes (T130K and T130K/E52D) were dialyzed in 50 mM MOPS pH 8.0, 100 mM NaCl and with or without 4 mM $MgCl_2$ buffer and titrated against 0.3 mM of

Table 4.1: Data collection and refinement statistics of wild type and T130K ANT

	WT Neomycin	T130K Neomycin	T130K Neomycin-AMPCPP	T130K product state (adenylated neomycin)
Resolution range[1]	50.0-1.65 (1.71 to 1.65)	51.07-1.90 (1.94 to 1.90)	45.42-2.00 (2.05 to 2.00)	38.58-2.50 (2.60 to 2.50)
Space group	$P2_12_12_1$	$P2_12_12_1$	$P2_12_12_1$	$P2_1$
Unit cell				
a, b, c (Å)	57.25, 97.65, 101.08	59.00, 97.71, 101.97	59.21, 98.03, 102.38	85.51, 59.25, 102.04
α, β, γ (°)	90, 90, 90	90, 90, 90	90, 90, 90	90, 94.80, 90
Unique reflections	68631	45570	40016	30831
Multiplicity[1]	4.3 (4.0)	6.5 (6.0)	4.9 (4.6)	3.8 (3.2)
Completeness (%)	99.2 (99.8)	97.0 (93.7)	97.8 (95.7)	86.6 (81.9)
Mean I/sigma(I)	24.2 (1.8)	18.5 (4.4)	11.4 (2.7)	12.2 (5.1)
Wilson B-factor	22.2	24.64	27.76	25.13
R-merge	0.048 (0.481)	0.056 (0.374)	0.082 (0.602)	0.077 (0.224)
Reflections used in refinement	68569	45531	39968	30831
Reflections used for R-free	1989	2334	1984	1499
R-work	0.173 (0.237)	0.170 (0.203)	0.197 (0.264)	0.173 (0.223)
R-free	0.198 (0.265)	0.210 (0.243)	0.229 (0.284)	0.230 (0.305)
Number of non-hydrogen atoms				
macromolecules	4166	4204	4129	8110
ligands	85	87	150	428
solvent	557508	387	368	217
RMS(bonds)	0.006	0.012	0.006	0.004
RMS(angles)	1.14	1.41	1.14	0.98
Ramachandran favored (%)	97.4	98.40	97.60	96.40
Ramachandran allowed (%)	2.4	1.60	2.40	3.50
Ramachandran outliers (%)	0.2	0.00	0.00	0.10
Clashscore	3.4	4.50	4.89	4.19

Table 4.1 Continued

Average B-factor				
macromolecules	25.83	26.42	30.61	29.12
ligands	31.22	39.94	36.28	35.29
solvent	37.63	34.85	36.11	25.80
PDB Code		6NMK	6NML	6NMM

Numbers in parentheses represent values in the highest resolution shell.

Table 4.2: Data collection and refinement statistics of T130K/E52D double mutant

	Neomycin	Neomycin-AMPCPP	Product state (adenylated neomycin)
Resolution range[1]	49.22-2.30 (2.38 to 2.30)	48.98 to 2.30 (2.38 to 2.30)	49.65 to 2.20 (2.27 to 2.20)
Space group	$P2_12_12_1$	$P2_12_12_1$	$P2_12_12_1$
Unit cell			
a, b, c (Å)	58.70, 98.45, 101.82	58.71, 97.95, 100.70	59.75, 99.30, 101.49
α, β, γ (°)	90, 90, 90	90, 90, 90	90, 90, 90
Unique reflections	26344	25660	30558
Multiplicity[1]	5.2 (5.0)	3.5 (3.4)	6.8 (6.8)
Completeness (%)	98.4 (98.6)	97.3 (95.2)	97.6 (94.6)
Mean I/sigma(I)	5.5 (5.0)	5.8 (2.0)	8.8 (3.9)
Wilson B-factor	34.69	25.98	24.65
R-merge	0.162 (0.644)	0.140 (0.575)	0.124 (0.440)
Reflections used in refinement	26263	25620	30512
Reflections used for R-free	1427	1396	1549
R-work	0.196 (0.284)	0.180 (0.245)	0.194 (0.239)
R-free	0.235 (0.344)	0.221 (0.313)	0.224 (0.292)
Number of non-hydrogen atoms			
macromolecules	4167	4098	4060
ligands	85	150	150
solvent	143	199	228
RMS(bonds)	0.005	0.010	0.007
RMS(angles)	1.10	1.38	1.25
Ramachandran favored (%)	96.60	97.01	95.20
Ramachandran allowed (%)	3.40	2.99	4.60
Ramachandran outliers (%)	0.00	0.00	0.20
Clashscore	6.93	8.17	4.61
Average B-factor			
macromolecules	40.58	31.10	29.52
ligands	60.88	29.93	24.53
solvent	40.34	31.95	32.55
PDB Code	6PO4	6PO6	6PO8

neomycin. For the set of experiments with AMPCPP, both the enzyme and neomycin were premixed with 0.5 mM AMPCPP and degassed prior to the titration. The titration data were fitted to a single set of identical sites model using MicroCal ORIGIN software supplied with the instrument. Base-line correction, peak integration and binding parameters (number of binding sites (n), binding constant (Ka), change in binding enthalpy (ΔH) and change in binding entropy (ΔS)) were obtained using the ORIGIN software.

4.4 Results

4.4.1 Crystallographic snapshots of wild-type ANT catalysis

A total of seven structures of ANT were determined with resolutions ranging between 1.90 and 2.50 Å (Tables 4.1 and 4.2) in a thermally stable T130K mutant background, with the exception of a binary neomycin complex that was determined in a wild-type enzyme to ensure aminoglycoside binding is not perturbed by this mutation (Figure 4.2). The T130K mutation is on the surface of ANT and over ~21 Å from the enzyme active site. Earlier studies showed that the thermodynamics of ligand binding and solvent effects *(16, 17)*, as well as protein dynamics *(18)* of wild-type ANT and its T130K variant are identical.

The previously determined structure of a D80Y ANT mutant was determined in the presence of kanamycin, whereas neomycin was used in our studies. The binding site of neomycin in the wild-type ANT crystal structure is identical to the T130K mutant complex and occurs within a pocket that is lined with negatively charged hydrogen bonding groups that form salt-bridges with the positively charged aminoglycoside (Figure 4.2). The primed ring of neomycin is placed directly into the active site composed of three carboxylate groups in a manner identical to the canonical DNA polymerase active site, yet it differs from the orientation of the kanamycin 4' hydroxyl found in the earlier studies of an active site D80Y mutant of ANT *(12)*. We note that D80Y variant has significantly different thermodynamics of ligand binding, solvent effects, and protein dynamics relative

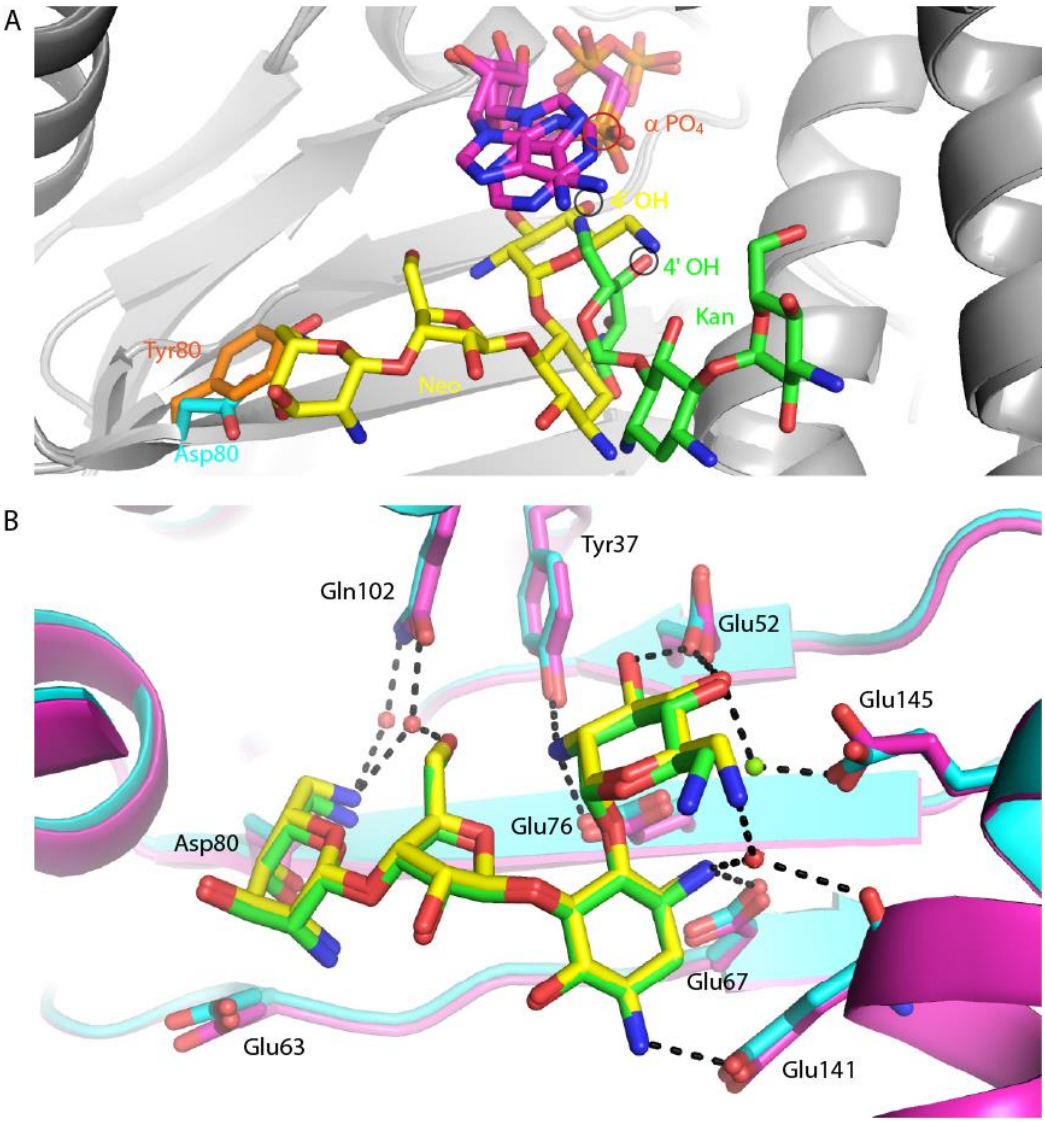

Figure 4.2: Comparison of ANT mutant structures. A. Superposition of D80Y ANT and the T130K ANT ternary complexes. The D80Y ANT mutant is shown with kanamycin (green carbon atoms) and AMPNPP (magenta carbon atoms). The T130K ANT mutant is shown with neomycin (yellow carbon atoms) and AMPCPP (magenta carbon atoms). The 4' hydroxyl, the site of adenylation, is circled in black, and the alpha phosphate is circled in red. B. Superposition of wild-type ANT (magenta carbon atoms) bound to neomycin (green carbon atoms) with T130K ANT (cyan carbon atoms) bound to neomycin (yellow carbon atoms). Hydrogen bonds to the T130K-neomycin complex are shown as black dashed lines.

to WT and T130K variants of ANT *(16-18)*. In the T130K mutant background, the position of the 4' hydroxyl of neomycin, the site of adenylation, overlaps with the position of the 3' OH of the DNA primer terminus of Pol β and is in a better position for attack of the α phosphate of the nucleotide than in the kanamycin complex of the D80Y ANT mutant (Figure 4.2). The neomycin complex is crystallized in the presence of high concentrations of Mg(II) (100-200 mM), and a Mg ion (termed Mg(II)-A) is present and coordinated by three water molecules, Glu 76, Glu 145 and the 4' OH of neomycin (Figure 4.3). One of the active site carboxylate groups (Glu 52) forms a short 2.4 Å hydrogen bond with the 3' hydroxyl of neomycin (shown as red dotted lines in Figure 4.3 panel A). The rather short distance between heavy atoms suggests this hydrogen bond is a low-barrier hydrogen bond (LBHB), where matched pKa values of heavy atoms leads to resonance stabilization and additional ~5-10 kcal more energy versus a canonical hydrogen bond *(15)*. LBHBs have recently been shown to be involved in enhancing catalysis in other AGMEs *(19, 20)*.

Upon formation of a non-hydrolyzable ternary complex (neomycin/AMPCPP) the catalytic Mg(II) and nucleotide binding Mg(II) are found coordinated to the 4' OH and the β and γ phosphates respectively (Figure 4.3). The catalytic Mg(II) is coordinated by Glu 145, Asp 50, Glu 52 and the 4' OH of the neomycin, which is likely in a deprotonated form, as the distance from the catalytic Mg(II) is 2.1 Å. Glu 52 also ligates the nucleotide binding Mg(II), thus forming a bidentate hydrogen bond with both metals. The engagement of the two metal ions by Glu 52 causes the LBHB to the 3' OH to be lost, with the electronegativity of the carboxylate group drawn to the two positively charged metal ions, rather than the aminoglycoside. The adenine ring of the nucleotide stacks directly above the prime ring of neomycin where it forms Van Der Waals interactions that likely compensate for the loss of the LBHB upon engagement of the two Mg ions by Glu 52.

Soaking of ANT ternary crystals, prevented the turnover of the substrate in the presence of calcium at the active site, while in buffer with magnesium, permitted the capture of the post catalysis adenylated neomycin product as well as the pyrophosphate leaving group (Figure 4.3). The catalytic metal and the metal-pyrophosphate were still present in the active site. Rather than forming an LBHB with the ligand, Glu52 completely engages

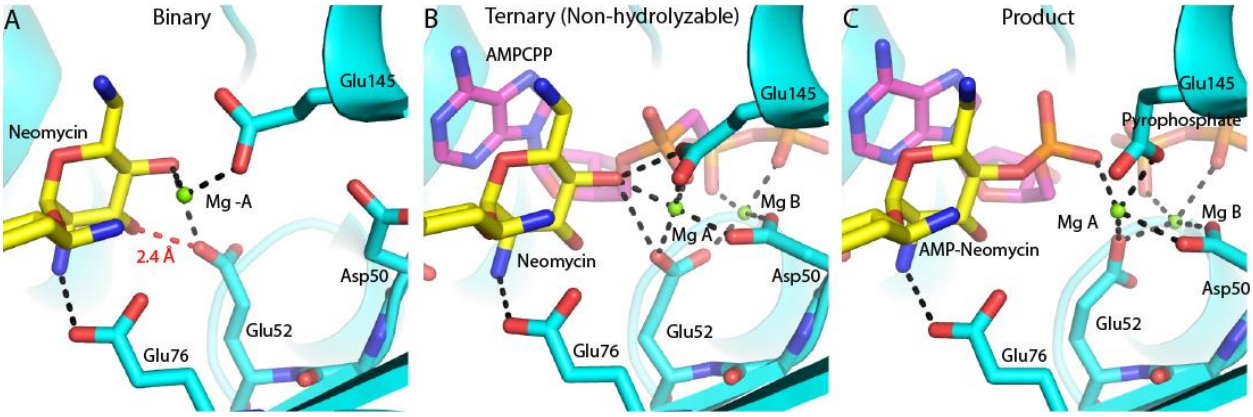

Figure 4.3: Crystallographic snapshots of the T130K ANT reaction coordinate. A. The T130K ANT neomycin complex active site. The short hydrogen bond to the neomycin 3' OH is represented as a red dashed line. B. The ternary (neomycin-AMPCPP) ANT active site. C. The product state (adenylated neomycin) ANT active site.

the catalytic Mg ion as well as Glu 145. Only a single hydrogen bond to Glu 76 remains formed with the adenylated primed ring of neomycin. The product-mediated reorganization of the hydrogen bonding network, including loss of the LBHB, likely leads to a significantly weaker interaction energy with the product state, thus aiding in product release. Indeed, in this crystal form multiple rounds of catalysis occurred within the confines of the crystal, which is evident by an additional adenylated AMP located adjacent to the active site (Figure 4.4).

4.4.2 Crystallographic snapshots of T130K/E52D mutants

To test the proposed role of the short hydrogen bond in ANT catalysis the crystal structures of a T130K/E52D double mutant were determined in a binary neomycin form, a ternary neomycin-AMPCPP form and a product state (adenylated neomycin-pyrophosphate). As expected, the LBHB is absent in the T130K/E52D binary complex (Figure 4.5), rather a longer and weaker 3.2 A canonical hydrogen bond is formed. Upon formation of the non-hydrolyzable ternary complex, the geometry of the active site is identical to the wild-type enzyme, demonstrating the transient role of the LBHB in ligand recognition, rather than catalysis (Figure 4.5). Just as the T130K enzyme, the T130K/E52D mutant was able to form product in the crystal, and the organization of the active site and products are similar to the wild-type enzyme (Figure 4.5), with the exception of Asp52 forming a bifurcated hydrogen bond to the both metals.

4.4.3 The LBHB in kinetics and thermodynamics of ANT

To support our structural interpretation of ANT catalysis, ITC based dissociation constants (K_d) and steady state kinetic rate constants were determined for T130K and T130K/E52D mutants (Table 4.3, Figure 4.6, and Figure 4.7). Consistent with the loss of the LBHB, the T130K/E52D mutant binds neomycin 2.5-fold weaker (equivalent to 2.3 kcal of energy) than wild-type, although this is in stark discrepancy to the proposed energetic

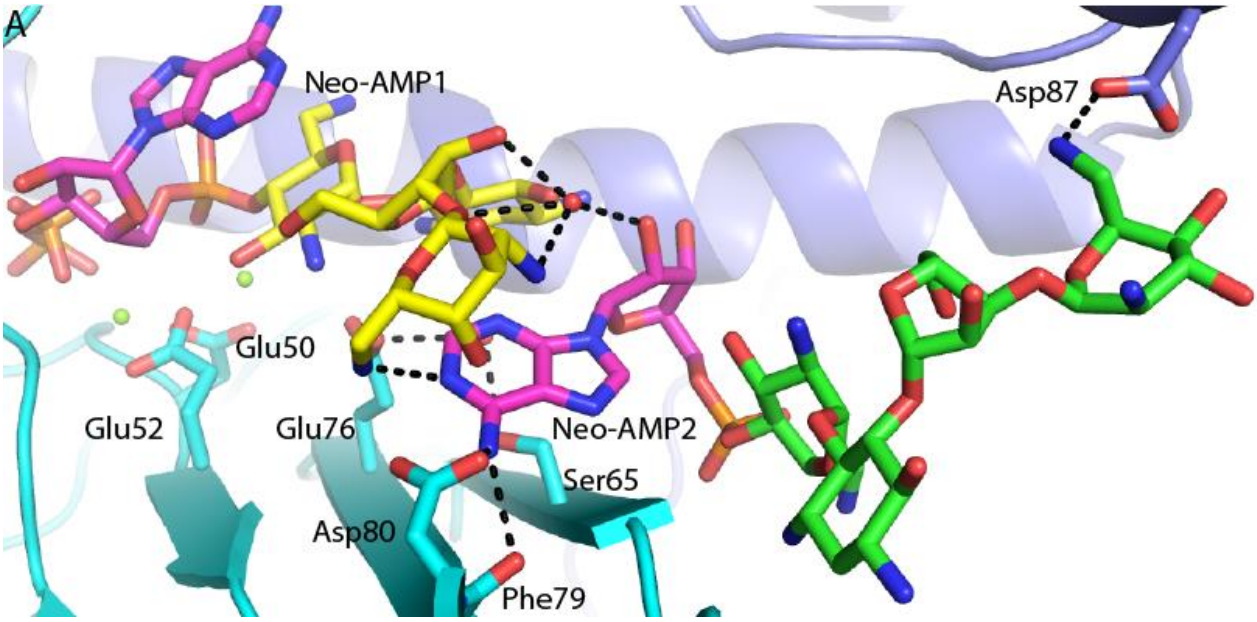

Figure 4.4: Additional adenylated neomycin in ANT structure. The second adenylated neomycin product (Neo-AMP2) binds directly to the adenylated neomycin in the active site (Neo-AMP1) and both monomers of ANT. Hydrogen bonds are represented as black dashed lines.

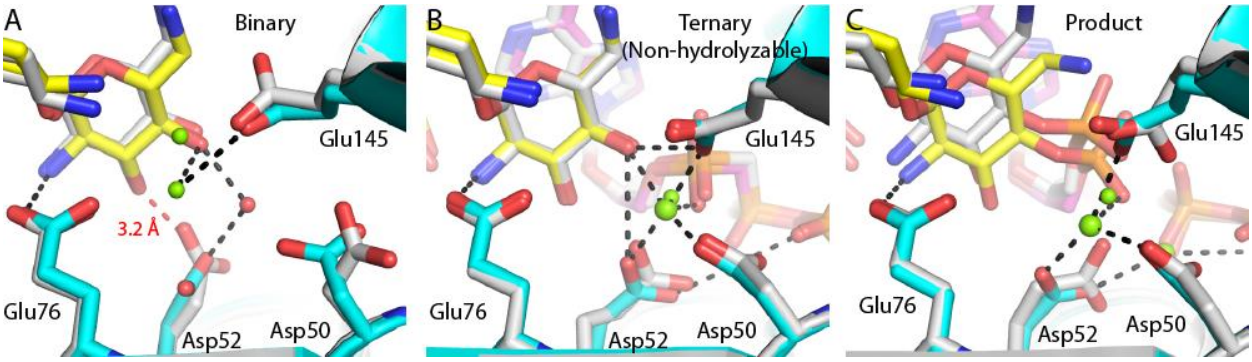

Figure 4.5: Crystallographic snapshots of the T130K/E52D ANT reaction coordinate. A. Superposition of the T130K/E52D ANT neomycin bound active site with the T130K ANT neomycin complex. The 3.2 Å hydrogen bond to the neomycin 3' OH is represented as a red dashed line. B. Superposition of the T130K/E52D ANT ternary complex (neomycin-AMPCPP) active site with the T130K ANT ternary complex. C. Superposition of the T130K/E52D ANT product state (adenylated neomycin) active site with T130K ANT product complex. The T130K/E52D ANT is shown with cyan ribbon representation with yellow carbon atoms for neomycin. T130K ANT is shown with all gray carbon atoms.

Table 4.3: Kinetics and binding of ANT

Enzyme	Ligand	N	K_d (μM)
T130K	Neomycin	0.9 ± 0.01	0.34 ± 0.03
T130K (No Mg(II))	Neomycin	1.0 ± 0.01	0.066 ± 0.01
T130K/E52D	Neomycin	0.8 ± 0.01	0.87 ± 0.08
T130K/E52D (No Mg(II))	Neomycin	1.0 ± 0.02	0.296 ± 0.10
T130K/AMPCPP	Neomycin	0.7 ± 0.004	0.13 ± 0.02
T130K/E52D/AMPCPP	Neomycin	0.7 ± 0.001	0.12 ± 0.03
Enzyme	ATP K_m (μM)	V_{max} (nmol min^{-1})	k_{cat} (s^{-1})
T130K	283.81 ± 67.05	113.27 ± 11	18.87 ± 1.84
T130K/E52D	171.19 ± 32.48	87.67 ± 6.0	14.61 ± 1.01

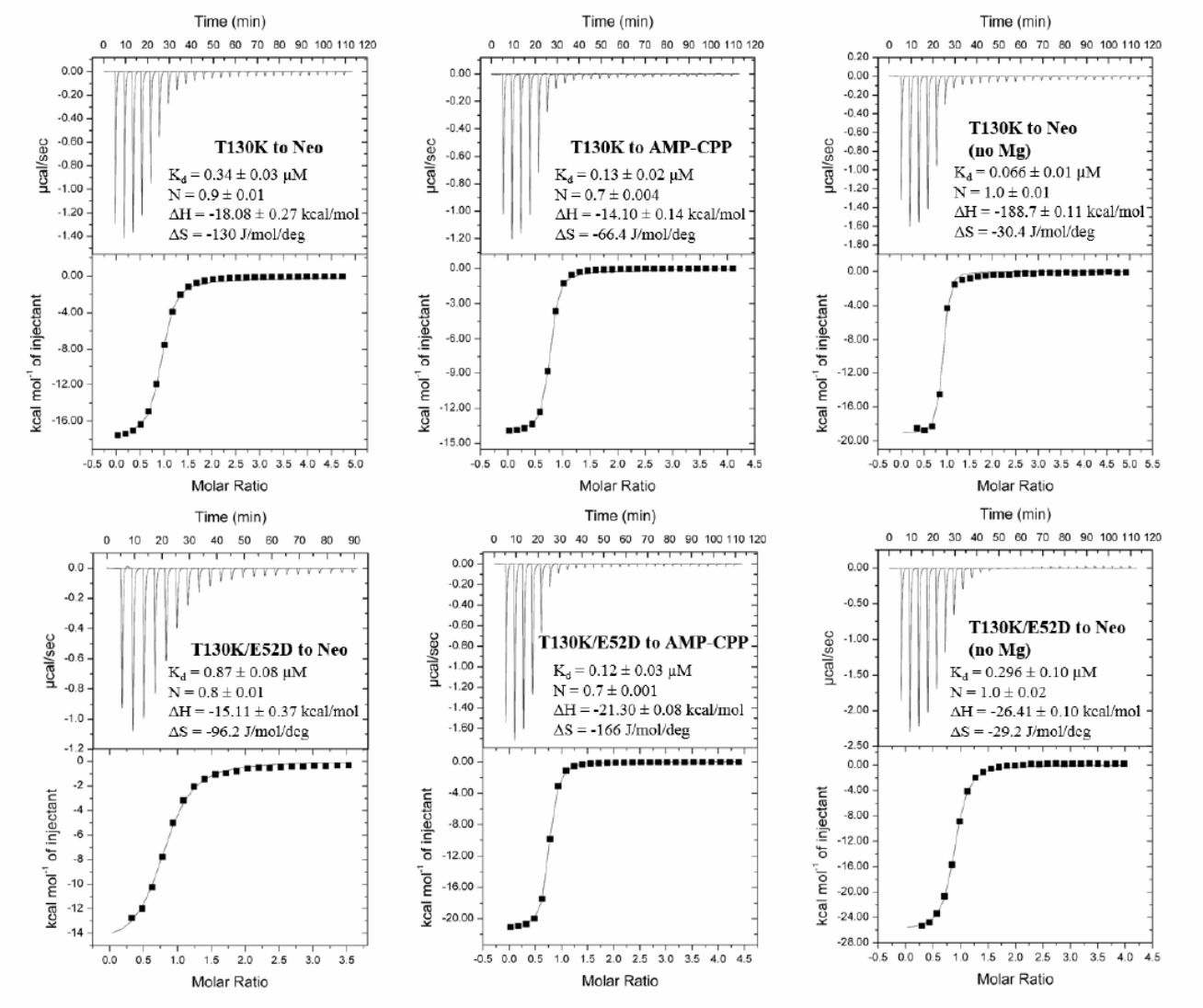

Figure 4.6: ITC based dissociation constants (K_d) for T130K and T130K/E52D ANT.

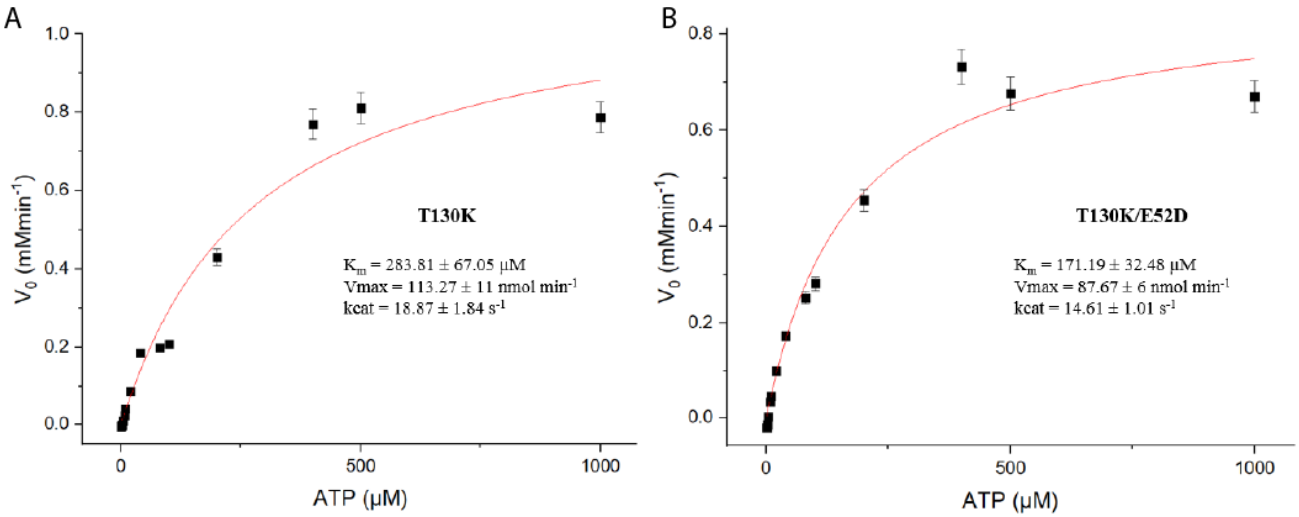

Figure 4.7: Kinetics of T130 and T130K/E52D ANT. A. Steady state kinetics for T130K ANT were determined for the adenylation of neomycin in the presence of increasing amounts of ATP. B. Steady state kinetics for T130K/E52D ANT were determined for the adenylation of neomycin in the presence of increasing amounts of ATP.

enhancement of LBHBs. ANT is crystallized in the presence of high amounts of divalent metal ions (100-200 mM Ca(II) or Mg(II)), and Mg(II) is found in the neomycin complex (Mg(II)-A) active site where it is coordinated by Glu52, the residue forming the LBHB with the neomycin. The 100-200 mM Mg(II) in the crystallization conditions is far higher than the typically free cellular Mg(II) concentration of <1.0 mM. Indeed, the K_d for neomycin binding in the absence of Mg(II) is 13 times tighter than in the presence (5 mM), which suggests the strength of the LBHB is modulated in response to the magnesium in the binding site (Table 4.3). Moreover, in the absence of Mg(II), the T130K/E52D mutant binds to neomycin five-fold weaker than the wild-type enzyme, equivalent to 3.6 kcal of energy. ITC titrations of the apo protein with Mg(II) failed to produce measurable heats of injection, which suggests the Mg(II) in the neomycin complex are due to crystallization conditions and the K_d values measured are in the absence of Mg ions. In direct support of the lack of engagement of the neomycin by residue 52 in the ternary complex, the K_d values for neomycin binding in the presence of AMPCPP are identical to one another in the T130K and T130K/E52D mutants (Table 4.3). Interestingly, the K_d for binding to this state is only two-fold weaker than the formation of the binary aminoglycoside complex. It is likely that the loss of the LBHB from the binary neomycin complex is compensated by the stacking interaction between the adenine ring and the prime ring of neomycin in the ternary non-catalytic complex.

These observations are further supported by the steady-state kinetic assays, where the k_{cat} is essentially identical between T130K/E52D and the T130K ANT enzymes (Table 4.3 and Figure 4.7). Thus, again re-enforcing the role of the LBHB strictly in the pre-catalytic state, before the metal bound ternary complex active site is assembled.

4.5 Discussion

This unique variation of nucleotidyl transfer reaction found in ANT demonstrates how this reaction archetype can be evolutionary tuned to function in a variety of biological processes beyond nucleic acid synthesis. In AGMEs, the evolutionary force on an ancient polymerase was the ability to recognize a class of antibiotics, perform chemistry and

release the modified product. This is in stark contrast to the requisite processivity of the canonical DNA polymerase NT reaction, which undergoes thousands of rounds of NT without release of the DNA template *(21)*. The LBHB of ANT plays a novel role in this variant of the NT reaction where it allows trace amount of antibiotics to be tightly bound pre-catalysis, while the loss of the LBHB serves as a signal for product release post a single round of catalysis. The LBHB modulates the free energy of the enzyme substrate complexes during the reaction coordinate where it is present in only the pre-catalytic binary drug complex, where tight, specific recognition of bacteriostatic antibiotics would be most important. Upon formation of the catalytically relevant ternary complex with nucleotide triphosphate and cations, the LBHB to the aminoglycoside is lost, with the catalytic carboxylate groups engaging both of the canonical NT Mg ions. The Mg ions in ANT play a unique role in the reaction, where the catalytic Mg(II) functions not only in activating the NT nucleophile, but also in modulating the free energy of the reaction coordinate. Concomitant with the loss of the LBHB in the formation of the ternary state, the K_d is two-fold weaker although no chemistry has taken place. Once NT occurs, only one of the three hydrogen bonds remain formed to the modified primed ring of the aminoglycoside, which serves to further reduce the energy of the protein drug product complex, from that of the LBHB-containing starting state. Thus, the modulation of this short hydrogen bond serves as a thermodynamic signal that mediates the “catch and release” of the antibiotic substrates.

4.6 Acknowledgements

We would like to thank our collaborators Dr Matt Cuneo, Dr Brinda Selvaraj and Maria Trifas, together we obtained all the ANT crystal structures mentioned in this thesis. They have especially provided their valuable insights on understanding the kinetic mechanism of ANT and contributed greatly in writing this chapter which will soon be submitted for publication.

4.7 References

1. Yamtich, J.; Sweasy, J. B., DNA polymerase family X: function, structure, and cellular roles. *Biochimica et Biophysica Acta* **2010,** *1804* (5), 1136-1150.
2. Yang, W., Portraits of a Y-family DNA polymerase. *FEBS Letters* **2005,** *579* (4), 868-872.
3. Freudenthal, B. D.; Beard, W. A.; Shock, D. D.; Wilson, S. H., Observing a DNA polymerase choose right from wrong. *Cell* **2013,** *154* (1), 157-168.
4. Jamsen, J. A.; Beard, W. A.; Pedersen, L. C.; Shock, D. D.; Moon, A. F.; Krahn, J. M.; Bebenek, K.; Kunkel, T. A.; Wilson, S. H., Time-lapse crystallography snapshots of a double-strand break repair polymerase in action. *Nature Communications* **2017,** *8* (1), 253.
5. Nakamura, T.; Zhao, Y.; Yamagata, Y.; Hua, Y. J.; Yang, W., Watching DNA polymerase eta make a phosphodiester bond. *Nature* **2012,** *487* (7406), 196-201.
6. Freudenthal, B. D.; Beard, W. A.; Wilson, S. H., New structural snapshots provide molecular insights into the mechanism of high fidelity DNA synthesis. *DNA Repair (Amst)* **2015,** *32*, 3-9.
7. Wright, G. D., Aminoglycoside-modifying enzymes. *Current Opinion in Microbiology* **1999,** *2* (5), 499-503.
8. Taber, H. W.; Mueller, J. P.; Miller, P. F.; Arrow, A. S., Bacterial uptake of aminoglycoside antibiotics. *Microbiology Reviews* **1987,** *51* (4), 439-457.
9. Chen-Goodspeed, M.; Vanhooke, J. L.; Holden, H. M.; Raushel, F. M., Kinetic mechanism of kanamycin nucleotidyltransferase from *Staphylococcus aureus*. *Bioorganic Chemistry* **1999,** *27* (5), 395-408.
10. Le Goffic, F.; Baca, B.; Soussy, C. J.; Dublanchet, A.; Duval, J., [ANT(4')I: a new aminoglycoside nucleotidyltransferase found in "*Staphylococcus aureus*" (author's transl)]. *Annales de Microbiolgie (Paris)* **1976,** *127* (3), 391-399.
11. Le Goffic, F.; Martel, A.; Capmau, M. L.; Baca, B.; Goebel, P.; Chardon, H.; Soussy, C. J.; Duval, J.; Bouanchaud, D. H., New plasmid-mediated nucleotidylation of aminoglycoside antibiotics in *Staphlococcus aureus*. *Antimicrobial Agents and Chemotherapy* **1976,** *10* (2), 258-264.

12. Pedersen, L. C.; Benning, M. M.; Holden, H. M., Structural investigation of the antibiotic and ATP-binding sites in kanamycin nucleotidyltransferase. *Biochemistry* **1995,** *34* (41), 13305-13311.

13. Sakon, J.; Liao, H. H.; Kanikula, A. M.; Benning, M. M.; Rayment, I.; Holden, H. M., Molecular structure of kanamycin nucleotidyltransferase determined to 3.0-A resolution. *Biochemistry* **1993,** *32* (45), 11977-11984.

14. Matesanz, R.; Diaz, J. F.; Corzana, F.; Santana, A. G.; Bastida, A.; Asensio, J. L., Multiple keys for a single lock: the unusual structural plasticity of the nucleotidyltransferase (4′)/kanamycin complex. *Chemistry–A European Journal* **2012,** *18* (10), 2875-2889.

15. Cleland, W. W.; Frey, P. A.; Gerlt, J. A., The low barrier hydrogen bond in enzymatic catalysis. *The Journal of Biological Chemistry* **1998,** *273* (40), 25529-25532.

16. Jing, X.; Serpersu, E. H., Solvent reorganization plays a temperature-dependent role in antibiotic selection by a thermostable aminoglycoside nucleotidyltransferase-4'. *Biochemistry* **2014,** *53* (34), 5544-5550.

17. Kocaman, S.; Serpersu, E. H., The thermodynamics of ligand binding to the aminoglycoside O-nucleotidyltransferase(4') and variants yields clues about thermophilic properties. *Biochemistry* **2019,** *58* (12), 1579-1586.

18. Jing, X.; Evangelista Falcon, W.; Baudry, J.; Serpersu, E. H., Thermophilic enzyme or mesophilic enzyme with enhanced thermostability: can we draw a line? *The Journal of Physical Chemistry B* **2017,** *121* (29), 7086-7094.

19. Kumar, P.; Agarwal, P. K.; Brett Waddell, M.; Mittag, T.; Serpersu, E. H.; Cuneo, M. J., Low barrier and canonical hydrogen bonds modulate activity and specificity of a catalytic triad. *Angewandte Chemie International Edition in English* **2019**.

20. Kumar, P.; Serpersu, E. H.; Cuneo, M. J., A low barrier hydrogen bond mediates antibiotic resistance in a noncanonical catalytic triad. *Science Advances* **2018,** *4* (4), eaas8667.

21. Von Hippel, P. H.; Fairfield, F. R.; Dolejsi, M. K., On the processivity of polymerases. *Annals of the New York Academy of Sciences* **1994,** *726*, 118-31.

22. Kabsch, W., Xds. *Acta Crystallographica D Biological Crystallography* **2010,** *66* (Pt 2), 125-132.

23. Minor, W.; Cymborowski, M.; Otwinowski, Z.; Chruszcz, M., HKL-3000: the integration of data reduction and structure solution from diffraction images to an initial model in minutes. *Acta Crystallogaphicar D Biological Crystallography* **2006,** *62* (Pt 8), 859-866.

24. Battye, T. G.; Kontogiannis, L.; Johnson, O.; Powell, H. R.; Leslie, A. G., iMOSFLM: a new graphical interface for diffraction image processing with MOSFLM. *Acta Crystallography D Biological Crystallography* **2011,** *67* (Pt 4), 271-281.

25. Potterton, L.; Agirre, J.; Ballard, C.; Cowtan, K.; Dodson, E.; Evans, P. R.; Jenkins, H. T.; Keegan, R.; Krissinel, E.; Stevenson, K.; Lebedev, A.; McNicholas, S. J.; Nicholls, R. A.; Noble, M.; Pannu, N. S.; Roth, C.; Sheldrick, G.; Skubak, P.; Turkenburg, J.; Uski, V.; von Delft, F.; Waterman, D.; Wilson, K.; Winn, M.; Wojdyr, M., CCP4i2: the new graphical user interface to the CCP4 program suite. *Acta Crystallography D Structural Biology* **2018,** *74* (Pt 2), 68-84.

26. Bunkoczi, G.; Echols, N.; McCoy, A. J.; Oeffner, R. D.; Adams, P. D.; Read, R. J., Phaser.MRage: automated molecular replacement. *Acta Crystallography D Biological Crystallography* **2013,** *69* (Pt 11), 2276-2286.

27. Emsley, P.; Lohkamp, B.; Scott, W. G.; Cowtan, K., Features and development of Coot. *Acta Crystallography D Biololgical Crystallography* **2010,** *66* (Pt 4), 486-501.

28. Afonine, P. V.; Grosse-Kunstleve, R. W.; Echols, N.; Headd, J. J.; Moriarty, N. W.; Mustyakimov, M.; Terwilliger, T. C.; Urzhumtsev, A.; Zwart, P. H.; Adams, P. D., Towards automated crystallographic structure refinement with phenix.refine. *Acta Crystallography D Biological Crystallography* **2012,** *68* (Pt 4), 352-367.

29. Chen, V. B.; Arendall, W. B., 3rd; Headd, J. J.; Keedy, D. A.; Immormino, R. M.; Kapral, G. J.; Murray, L. W.; Richardson, J. S.; Richardson, D. C., MolProbity: all-atom structure validation for macromolecular crystallography. *Acta Crystallography D Biological Crystallography* **2010,** *66* (Pt 1), 12-21.

5 CONCLUSIONS AND FUTURE DIRECTIONS

5.1 Conclusions

In this thesis we worked with three variants of aminoglycoside nucleotidyltransferase(4') (ANT) to study enzyme thermostability and catalysis. Wild type (WT) ANT was originally isolated from the mesophilic *Staphylococcus aureus (1)*. Thermostable versions of WT ANT named as T130K and D80Y were created via direct evolution *(2)*. Previously our lab has shown that the melting temperature (Tm) of WT is (40.9±0.5ºC), T130K is (49.1±0.6 ºC) and D80Y is (56.2±0.2 ºC) *(3)*. The Tm, activity at high temperatures and the resistance against denaturants increase in the order of WT, T130K and D80Y, indicating that D80Y is more thermostable than T130K *(2, 4)*. Both T130K and D80Y differ from the WT by a single amino acid mutation. Most studies compared mesophilic/thermophilic homologues, which can differ from each other up to 60% in their sequence, in order to study the molecular features that govern enzyme thermostability *(5)*. It is not easy to tell if the difference in the molecular features of the homologues are actually related to thermostability or to some other function of the protein when the sequences vary. Thus, using ANT variants is an excellent system to study the molecular features that govern enzyme thermostability, since just one mutation can create a huge difference in their thermostabilities. This avoids the bias seen in enzyme homologues.

In this thesis we first compared the ligand binding thermodynamics of the ANT variants. We observed that T130K resembles the mesophilic WT in terms of ligand binding thermodynamics, while the D80Y significantly differs from them. We have performed our thermodynamics analysis using four ligands; neomycin and paromomycin, as the members of the neomycin family, and kanamycin and tobramycin, as the members of the kanamycin family of aminoglycosides. We have performed the ligand binding experiments over a temperature range of 10-40°C, both in H_2O and D_2O, to study the effect of solvent on ligand binding and how it might be related to enzyme thermostability. For all three ANT variants, in all cases, the binding enthalpy were always negative resulting in an overall negative ΔG. Except for the entropy of binding of kanamycin and tobramycin to WT and neomycin to T130K at 10°C, the entropy values for the T130K and WT were always unfavorable. D80Y, on the other hand, displayed favorable entropic contributions

up to 25°C. The thermodynamic parameters of ligand binding were solvent, aminoglycoside, temperature and enzyme dependent. The binding enthalpy became more favorable, while the entropic contribution became more unfavorable for all ANT variants as the temperature increased.

For binding of all four aminoglycosides to WT and T130K, in the temperature range that we studied, Δ*H* decreased linearly with increasing temperature. However, this decrease in Δ*H* was polynomial with D80Y indicating that the heat capacity change (Δ*Cp*), unlike WT and T130K, was temperature dependent. Furthermore, the rate of decrease in Δ*H* with increasing temperature was always faster in H_2O for WT and T130K in the temperature range tested, while this was true for D80Y only at temperatures above ~20°C.

The analysis of the observed differences in binding enthalpies in H_2O and D_2O ($\Delta\Delta H = \Delta H_{H2O} - \Delta H_{D2O}$), further highlighted the difference between the D80Y and WT/T130K pair. For both WT and T130K, while the ΔΔ*H* values were positive at lower temperatures, these values became increasingly negative in a linear fashion as the temperature increased. For D80Y, except for the curious case of kanamycin, the ΔΔ*H* values were always negative, following a polynomial fashion.

For D80Y, ΔCp_{tr} for the transfer from D_2O to H_2O ($\Delta Cp_{tr} = \Delta Cp_{H2O} - \Delta Cp_{D2O}$) was negative above 20°C for all four aminoglycosides and became positive between 10°C and 20°C, except for kanamycin for which ΔCp_{tr} was very small. There was no such variation for WT and T130K since their ΔCp_{tr} values were a negative constant value in all cases, independent of the temperature. Positive ΔCp_{tr} values are consistent with the transfer of polar groups from D_2O to H_2O, while negative values are consistent with the transfer of hydrophobic groups from D_2O to H_2O.

Our analytical centrifugation studies showed that all three ANT4 variants exhibit a similar effect of temperature on monomer-dimer equilibrium over the temperature range studied. The increase in temperature resulted in a higher tendency towards dimerization with all.

This observation states that the differences in the ligand thermodynamics of ANT variants is not due to a difference in their monomer-dimer equilibrium.

The two contributors of Δ*Cp* are the solvent effect and protein dynamics. Our ΔΔ*H* versus Δ*Cp* plots have shown that, for WT and T130K, solvent effect was the major factor contributing to Δ*Cp*, while for D80Y such a correlation between the Δ*Cp* and solvent effect was weak. The slopes obtained from the ΔΔ*H* versus Δ*Cp* plots return a unit of temperature in degrees and is referred to as the offset temperature (T_{off}), which is the temperature difference to observe the same binding enthalpy in H_2O and D_2O *(6)*. While a steady increase was observed with the T_{off} of WT and T130K, a change in the T_{off} of D80Y was not visible. This led us to conclude that, if solvent effect is not the major contributor of the Δ*Cp* for D80Y, then it is very likely that protein dynamics would be the major contributor of Δ*Cp* for D80Y. In fact, we had previously shown that D80Y is more dynamic compared to T130K and WT, and that the second principal component was dominating the dynamics of D80Y, unlike the case of the WT and T130K in which the first principle component was driving the protein dynamics *(3)*.

Taken together, our ligand binding thermodynamics studies of the ANT variants have shown that T130K highly resembles the mesophilic WT, while D80Y behaves differently from them *(7)*. This led us to further distinguish T130K from D80Y. In nature, thermophilic variants are known to behave differently than their mesophilic homologues, simply because they are subjected to a harsher environment and need to come up with strategies to accommodate their environment *(8)*. Thus, we decided to refer to T130K as the thermostable variant since it is just a structurally more stable variant of the WT and mimics the behaviors of the WT. On the other hand, we decided to refer to D80Y as the thermophilic variant, since it behaves very differently from the other ANT variants in order to achieve thermal adaptation.

Next, in this thesis we obtained the X-ray structures of the ANT variants in order to explore whether the differences in their ligand binding thermodynamics and thermostabilities can be explained by the possible differences in their structures. All our ANT structures were

crystallized as dimers, in which we saw that the T130K and D80Y mutation sites are away from both the dimer interface and the active site and are exposed to solvent. We observed that there are no global structural differences in the apo (nonligand bound) forms of ANT variants. However, when we examined the T130K mutation site, we saw that there is an additional H-bond formed between the side chain of Lys 130 and the backbone oxygen of Ser 90, which explains the increased melting temperature (Tm) of the T130K compared to WT. Interestingly, even though D80Y has the highest Tm, when we investigated the D80Y mutation site, Tyr 80 seemed to be too far away from its surrounding residues to be engaged in a direct stabilizing interaction as opposed to T130K. However, keeping in mind the dynamic nature of D80Y, it is possible that in the solution form, D80Y might also be creating additional interactions. Furthermore, we also observed that T130K and WT both bind to neomycin in the same structural manner and that the solvent reorganization in the ligand binding sites of T130K-neomycin and WT-neomycin structures are similar to each other, while they are different when we compare the apo structures of D80Y and T130K. The analysis of our structures in terms of solvent reorganization further supports our ligand binding thermodynamics studies that, T130K resembles the WT, while D80Y displays different behavior. Also, analyzing the T130K and D80Y mutation sites for additional structural interactions has shown that, while in the T130K variant, there was an additional H-bond formed to increase the Tm, such an obvious additional interaction was not identified in the D80Y mutation site. This observation also further supports our statement that, T130K is just a structurally more stable version of the WT but behaves like the WT, while D80Y displays thermophilic behavior through Tyr 80 serving as a node to influence global properties such as the ligand binding thermodynamics and the protein dynamics of the D80Y. We also have another ANT variant which is the double mutant named as T130KD80Y with a Tm of 62.6±0.1 ºC. The additivity in the Tm of the double mutant suggests that the T130K and the D80Y mutants achieve thermostability through different strategies, and in fact, our studies support this statement.

Our previous studies had shown that the dissociation constants (Kd) for the binding of all ANT variants to kanamycin were very similar to each other, while D80Y was bound to neomycin more than twenty times weaker than WT and T130K. We were also not able to

obtain a neomycin bound structure of D80Y probably due to its weak binding to neomycin. However, when we superimposed the neomycin bound forms of WT and T130K with the apo D80Y, we saw that Tyr 80 was in a steric clash with the neomycin, which gives a structural explanation as to why the D80Y binds to neomycin much weaker compared to WT and T130K.

Obtaining the apo, neomycin bound, neomycin and AMPCPP bound and the product state (adenylated neomycin) forms of T130K has enabled us to identify the residues in the ANT active site. We identified Glu 145, Asp 50, Glu 52 and Glu 76 as the residues which are in the proximity of the 4'-OH modification site of neomycin and the α-phosphate on the AMPCPP, which make them the likeliest candidates to perform catalysis. The fold of the ANT variants in the active site were also similar, indicating that the differences in their activities cannot be explained by the structural differences in their active sites. This was expected because the T130K and D80Y mutation sites are away from the active sites, thus are not likely to impose any direct structural differences in the active site.

Investigating these different structures of T130K has also enabled us to understand its catalytic mechanism where it transfers an AMP group from Mg-ATP to the 4'OH group of the aminoglycosides. ANT and DNA polymerases are similar in the sense that they all catalyze reactions in which they transfer nucleotide groups. Our research has shown that the protein fold of ANT is similar to that of the human DNA polymerase β catalytic domain and the active sites of both of these enzymes contain residues with carboxylic groups. Two magnesium ions play a role in both the binding of the aminoglycoside to ANT and in the catalysis. A low barrier hydrogen bond (LBHB) is formed between the Glu 52 and the 3'-OH group of neomycin which is 2.4 Å long. Formation of this LBHB enables the ANT to bind to neomycin tightly. Upon the binding of the AMPCPP and the formation of the tertiary complex, the LBHB is broken and Glu 52 forms a bidentate interaction with the two Mg(II) ions, eventually leading to product release after the catalysis. We suggest that Glu 145 is the catalytic base. Presence of this LBHB differentiates ANT from DNA polymerases. ANT mediates a novel "catch and release" nucleotidyl transfer reaction via

this LBHB, which enables the modified antibiotic to be released, unlike the processivity of the DNA polymerases in which the nucleotide chain keeps growing.

5.2 Future directions

5.2.1 Further testing the stabilizing interactions in the T130K mutation site

Our structural analysis of the T130K variant has shown that, in the T130K mutation site, the side chain of Lys 130 is in the proximity of the backbone oxygen of the Ser 90 enabling them to create an additional H-bond. As future directions, we would like to create the T130R variant of ANT. Substituting the Lys with another basic residue, such as the Arg, would allow us to further study the role of a positive charge in the mutation site and how it increases structural stability. We would also like to obtain the structure of the T130R variant and its Tm to see if it behaves like the T130K variant. If so, we would also further like to study the ligand binding thermodynamics of the T130R variant and see if it is similar to that of the T130K. This study would allow us to further investigate the thermostable variants (which are structurally more stable than the mesophilic WT but mimics the WT enzyme behavior) and their properties which can help us distinguish the true thermophilic enzyme variants from the thermostable variants.

5.2.2 Further investigations on how ANT variants interact with the solvent

We have shown through our ligand binding studies that, unlike the WT and the T130K, the solvent effect is not the major contributor of the Δ*Cp* for D80Y. This led us to decide to further investigate the solvation pattern of the ANT variants. In Chapter 2 of this thesis, through our structural analysis, we have shown that the solvent accessible area of all three ANT variants are very similar both in their apo and ligand bound forms. We also know from our previous studies that D80Y is more dynamic than the WT *(3)* and that Tyr 80 is acting as a node which affects the ligand binding thermodynamics and the protein dynamics of the D80Y variant and thereby facilitates thermophilic enzyme behavior *(7)*.

Next, we would like to explore if the solvation patterns of the ANT variants are different. We would like to perform a H/D exchange experiment and use NMR to detect the solvent exchange pattern. Firstly, we will label the ANT variants with ^{15}N during protein expression and detect solvent exposure pattern through acquiring a $^{1}H-^{15}N$ correlation spectra by utilizing the solvent exposed amide (SEA) HSQC technique *(9)*. We would like to study the solvent exposure of the ANT variants at different temperatures to understand the link between the solvent exposure and the thermal adaptation for these enzymes. We expect the solvation pattern, that is the parts of the protein undergoing solvent exchange, of the D80Y to be different than that of the others. The changes in the solvation pattern of the D80Y at different time points and temperatures can give us further insight on how Try 80 acts as a node in protein dynamics. With this approach, we can identify the residues that are in the network of the Try 80, which may collectively facilitate the thermophilic behavior of the D80Y. We have shown for D80Y that ΔCp_{tr} is ligand dependent, and unlike the WT and T130K it is also temperature dependent. Thus, we would also like to study the solvation pattern of the ANT variants when they are bound to different ligands. This would allow us to further understand if and how binding of different ligands to the enzyme affect its solvation pattern. If no solvent exchange is observed, that would mean that the enzyme has a protection layer against the solvent. The stronger hydration shell is known to protect the thermophilic proteins from the penetration of water, resulting in a more stable structure compared to their homologues *(10)*. Thus, we would expect the D80Y to go under less solvent exchange compared to the WT and T130K.

5.2.3 Obtaining neutron crystal structures and performing computational studies to further study the kinetics and the thermostability of ANT

Earlier, we performed a 100 ns molecular dynamics (MD) simulations on the apo forms of three ANT variants using the previously available crystal structure of ANT (PDB ID: 1KNY) *(11)*. From this study we learned that D80Y is more dynamic than the WT and the T130K and that the second principal component was dominating the dynamics of D80Y, unlike the case of the WT and T130K in which the first principle component was driving the protein dynamics *(3)*. In this thesis, we have obtained the X-ray crystal structures for

the apo forms of all ANT variants and the neomycin bound structures for the T130K and WT. Next, we would like to study the protein dynamics of the neomycin bound ANT variants and see if and how they differ from each other. In this study, we will build the neomycin in to the apo D80Y structure that we already have, in order to study the dynamics of the neomycin bound D80Y. We have shown that the ligand binding thermodynamics of D80Y is different than the other two variants and that the solvent affect was not the major contributor to its Δ*Cp*, which meant that protein dynamics could be the major contributor *(7)*. Thus, conducting MD simulations at different temperatures with our ligand bound ANT structures could further help us understand how the dynamics of these enzymes change in their ligand bound forms and how it can be related to thermal adaptation.

In this thesis, we have proposed that a LBHB has formed between Glu 52 and neomycin through a magnesium ion, which enables the enzyme to bind tightly to the neomycin. We also proposed that, upon the binding of the cofactor ATP, this LBHB is broken due to the formation of the activation complex. Next, we would like to obtain the neutron structures since neutron crystallography is able to detect hydrogen atoms which would enable us to study the LBHB bond formation in greater detail *(12)*. So far, we have studied the catalytic mechanism of ANT by obtaining and analyzing the X-ray crystal structures. However, the dynamic nature of enzymes also contributes to their catalysis. Next, we would also like to perform MD and QM/MM simulations to further study the catalysis of ANT.

5.3 References

1. Matsumura, M.; Katakura, Y.; Imanaka, T.; Aiba, S., Enzymatic and nucleotide sequence studies of a kanamycin-inactivating enzyme encoded by a plasmid from thermophilic bacilli in comparison with that encoded by plasmid pUB110. *Journal of Bacteriology* **1984,** *160* (1), 413-420.
2. Matsumura, M.; Aiba, S., Screening for thermostable mutant of kanamycin nucleotidyltransferase by the use of a transformation system for a thermophile, *Bacillus stearothermophilus*. *Journal of Biological Chemistry* **1985,** *260* (28), 15298-15303.
3. Jing, X.; Evangelista Falcon, W.; Baudry, J.; Serpersu, E. H., Thermophilic enzyme or mesophilic enzyme with enhanced thermostability: can we draw a line? *The Journal of Physical Chemistry B* **2017,** *121* (29), 7086-7094.
4. Liao, H. H., Thermostable mutants of kanamycin nucleotidyltransferase are also more stable to proteinase K, urea, detergents, and water-miscible organic solvents. *Enzyme Microbial Technology* **1993,** *15* (4), 286-292.
5. Davies, G. J.; Gamblin, S. J.; Littlechild, J. A.; Watson, H. C., The structure of a thermally stable 3-phosphoglycerate kinase and a comparison with its mesophilic equivalent. *Proteins: Structure, Function, Bioinformatics* **1993,** *15* (3), 283-289.
6. Chervenak, M. C.; Toone, E. J., A Direct measure of the contribution of solvent reorganization to the enthalpy of ligand binding. *Journal of the American Chemical Society* **1994,** *116* (23), 10533-10539.
7. Kocaman, S.; Serpersu, E. H., The thermodynamics of ligand binding to the aminoglycoside O-nucleotidyltransferase(4') and variants yields clues about thermophilic properties. *Biochemistry* **2019,** *58* (12), 1579-1586.
8. Vieille, C.; Zeikus, G. J., Hyperthermophilic enzymes: sources, uses, and molecular mechanisms for thermostability. *Microbiology Molecular Biology Review* **2001,** *65* (1), 1-43.
9. Norris, A. L.; Nickels, J.; Sokolov, A. P.; Serpersu, E. H., Protein dynamics are influenced by the order of ligand binding to an antibiotic resistance enzyme. *Biochemistry* **2013,** *53* (1), 30-38.

10. Sterpone, F.; Bertonati, C.; Briganti, G.; Melchionna, S., Key role of proximal water in regulating thermostable proteins. *The Journal of Physical Chemistry B* **2008,** *113* (1), 131-137.
11. Pedersen, L. C.; Benning, M. M.; Holden, H. M., Structural investigation of the antibiotic and ATP-binding sites in kanamycin nucleotidyltransferase. *Biochemistry* **1995,** *34* (41), 13305-13311.
12. Kumar, P.; Serpersu, E. H.; Cuneo, M. J., A low barrier hydrogen bond mediates antibiotic resistance in a noncanonical catalytic triad. *Science Advances* **2018,** *4* (4), eaas8667.

VITA

Seda Kocaman was born in Ankara, Turkey on the 25th of December, 1992. Seda graduated from TED Ankara College Private High School in 2010. She then obtained her Bachelor of Science degree in Molecular Biology and Genetics from Bilkent University in 2014. As a part of her undergraduate research experience, Seda did an internship in CECAD Aging Research Center in Cologne, Germany as an Erasmus Scholar in the summer of 2012. Seda joined The University of Tennessee (UTK) at Knoxville in 2014 to obtain her PhD degree in Biochemistry & Cellular and Molecular Biology. As Seda worked on obtaining her PhD degree, she also obtained her Master of Science degree in Statistics through the Intercollegiate Graduate Statistics Program (IGSP) of UTK. Seda has been serving as a member of the Biophysical Society Membership Committee since July 1, 2018 and her appointment will continue till June 30, 2021. After obtaining her PhD degree, Seda will continue her scientific career as a postdoctoral research scientist at the National Institutes of Health. In the long run, Seda wishes to continue her scientific career and research in social settings with traveling opportunities.